



**A University of Sussex DPhil thesis**

Available online via Sussex Research Online:

<http://sro.sussex.ac.uk/>

This thesis is protected by copyright which belongs to the author.

This thesis cannot be reproduced or quoted extensively from without first obtaining permission in writing from the Author

The content must not be changed in any way or sold commercially in any format or medium without the formal permission of the Author

When referring to this work, full bibliographic details including the author, title, awarding institution and date of the thesis must be given

Please visit Sussex Research Online for more information and further details

**INVESTIGATION OF CANCER CELL  
IDENTIFICATION IN SUSPENSION BY  
BIOIMPEDANCE SPECTROSCOPY**

A DISSERTATION  
SUBMITTED TO THE UNIVERSITY OF SUSSEX  
IN PARTIAL FULFILLMENT OF THE REQUIREMENTS  
FOR THE DEGREE OF MASTER OF PHILOSOPHY

Fan Zheng

April, 2012

I hereby declare that I wrote the content of this thesis and, except where acknowledged, it is my own work. The research described in this thesis was performed by myself, except part of biological assays, which include the cell culture and cell viability measurements. Due to the lack of access to biological laboratories and devices, these assays were conducted with support from Wei Duan, who was studying in School of Life Sciences.

The chamber used for impedance measurement in this thesis was designed and provided by Guofeng Qiao. Thus, the cross-section profile and 3-D view of the chamber (Figure 3.4 in the thesis) were Guofeng Qiao's work and his thesis was referred in this thesis. The two analytic models including 'Pauly-Schwan' theory and 'Hanai-Asami-Koizumi' theory were two classical models (Pauly, Packer et al., 1960; Hanai and Sekine, 1986) for physical analysis of the cell suspension system and were described in 'Bioimpedance Analysis for the Characterization of Breast Cancer Cells in Suspension' of which I am a co-author. The content of section 4.2.1, which described the analytic methodology in my thesis, is based on those analytic models, thus there is an overlap with the description in the paper. The references of the published paper and thesis have been added in this thesis.

**Signature:** \_\_\_\_\_

## Abstract

Bioimpedance has been of great significance for its applications in exploring the electrical properties of biological materials. It has been widely applied in cancer detection of tissues. However, studies at the tissue level have not achieved a consensus over the changes of impedance parameters due to the complex structure and heterogeneity of tissue. Moreover, the relationship of biological changes and their corresponding electrical changes is still unclear. Impedance research at the cellular level will help to establish the relationship between biological and electrical properties of cancer cells, which will ultimately promote the development of cancer detection.

In this thesis an application of impedance spectroscopy for cancer cell identification in suspension was proposed and investigated. Two breast cell lines, MCF-10A and MCF-7 representing normal cells and cancer cells respectively were investigated in suspension by impedance spectroscopy. In order to choose a suitable method for cell suspension measurement, a comparison of two-electrode and four-electrode measurements was carried out before the investigation of cell suspensions. Electrode polarization, which is the major problem of two-electrode measurement, was studied in order to interpret the results of the two-electrode measurement.

The results indicated both impedance and its parameters were significantly different between MCF-10A and MCF-7. To further analyse the electrical parameters in the two cell lines, an electrical circuit model and a physical model were adopted in this study. The impedance parameters involved were analysed and compared between two cell lines. Furthermore, the biological difference between the two cell lines was explored with biological assays. Based on the electrical and biological changes, the relationship between electrical parameters and biological features of normal cells and cancer cells was analysed and the possible biological factors influencing the electrical properties of cell will be discussed in this thesis.

# Acknowledgement

This work would not have been possible without the support from the Biomedical Engineering Group at the University of Sussex. There are many people involved to support the creation of this work.

First of all, I would like to thank my supervisor Dr. Wang for his support and assistance during my study at the University of Sussex. I want to thank him for his guidance and support throughout this research, and the time and the patience in reading this thesis. Also I want to thank my second supervisor, Dr. Constantino Carlos Reyes-Aldasoro for his kind support in the preparation of my viva. Although it was only a short period of supervision, I learned a lot from the communication with him.

I wish to appreciate the Cell Imaging Group leader, Dr. Guofeng Qiao for his support in my study and research in the past one and half years. Without his pertinent advice about my study and assistance in the execution of research, it would not have been possible to finish in 1.5 years. I would like to thank my colleague, Wei Duan, who contributed a lot in the biological experiments of the study. I also want to acknowledge my group colleague Xiaolin Zhang for her support in Matlab programming. I would like to acknowledge Dr. Julian R. Thorpe for his guidance in electron microscope observation of cell samples and Nevis Beqo for his previous work on Labview, which significantly facilitated my experiments.

Also I would like to thank Prof. Xiaoyun Xu and Dr. Lionel Ripley for serving on my oral defense committee, and reviewing this thesis. Their help and useful comments were greatly appreciated.

I would like to show my appreciation to my friends in China and the U.K. Life became easier with your kind encouragements. Although the result turned out to be different

from my original intention, I have learned a lot from the past 1.5 years and all of these experiences will definitely become priceless treasure in my life.

And finally, I want to thank my family for their permanent love to me and all the sacrifices they made to support my dream. Without all they have done for me, I would not have been able to finish this work.

# Contents

<b>Abstract</b> .....	iii
<b>Acknowledgement</b> .....	iv
<b>Contents</b> .....	vi
<b>List of Publications</b> .....	ix
<b>List of Figures</b> .....	x
<b>List of Tables</b> .....	xii
<b>List of Acronyms</b> .....	xiii
<b>List of Symbols</b> .....	xiv
<b>Chapter 1 INTRODUCTION</b> .....	1
1.1 Overview of bioimpedance .....	1
1.2 Objectives and goals.....	2
1.3 Structure of the thesis .....	3
<b>Chapter 2 BIOLOGICAL AND DIELECTRIC BACKGROUND OF CELL SUSPENSION AND CANCER CELLS</b> .....	5
2.1 Introduction .....	5
2.2 Cell structure and its biological properties .....	5
2.2.1 Cell membrane .....	6
2.2.2 Cytoplasm .....	8
2.3 Impedance basics.....	9
2.4 Dielectric properties of biological cells.....	10
2.5 Electrical model for cells and cell suspension.....	12
2.6 Introduction of cancer and its biological properties .....	17
2.6.1 Cancer and cell cycle.....	17
2.6.2 Features of cancer cells .....	19
2.6.3 Cell components changes in carcinogenesis.....	20
2.6.4 Biological methods for cancer research .....	22
2.6.5 Impedance measurement for cancer research.....	24
<b>Chapter 3 IMPEDANCE MEASUREMENT OF SALINE SOLUTION</b> .....	26
3.1 Introduction .....	26
3.2 Principles of two-electrode and four-electrode measurements.....	27
3.3 Electrode polarization.....	28

---

3.3.1	Electrode polarization and its effects in bioimpedance measurement.....	28
3.3.2	Methods to reduce the effect of electrode polarization .....	29
3.4	Objective of this study.....	31
3.5	Material and method.....	32
3.5.1	Preparation of the electrolyte .....	32
3.5.2	Instrumentation setup .....	32
3.5.3	Measurement and data analysis .....	34
3.6	Result and Discussion .....	36
3.6.1	System calibration.....	36
3.6.2	Electrical polarization.....	37
3.6.4	Comparison of two-electrode and four-electrode measurement.....	44
3.7	Summary .....	48
<b>Chapter 4 DIFFERENTIATION OF CANCER CELLS FROM NORMAL CELLS BY BIOIMPEDANCE SPECTROSCOPY .....</b>		<b>49</b>
4.1	Introduction .....	49
4.2	Background of study .....	50
4.2.1	Dielectric properties of cell suspensions .....	50
4.3	Objectives of this study .....	57
4.4	Materials and Methods .....	57
4.4.1	Cell culture .....	57
4.4.2	Cell suspension preparation and viability measurement .....	58
4.4.3	Volume fraction measurement.....	58
4.5	Impedance measurement system .....	59
4.5.1	Data analysis .....	59
4.6	Result and discussion .....	62
4.6.1	System errors.....	62
4.6.2	Environmental parameters control and their effects on measurement results .....	63
4.6.3	Impedance of cell suspension.....	65
4.6.4	Electric equivalent model.....	67
4.6.5	Results from the physical model .....	69
4.6.6	Applications of two models.....	72
4.7	Summary .....	74

---

<b>Chapter 5</b>	<b>RELATIONSHIP BETWEEN ELECTRICAL AND BIOLOGICAL PROPERTIES OF CELLS</b>	75
5.1	Introduction	75
5.1.1	Changes of the electrical parameters in normal cells and cancer cells	75
5.2	Objectives of this study	77
5.3	Material and method	78
5.3.1	Transmission electron microscopy (TEM) observation of cells	78
5.4	Results and discussion	79
5.4.1	Biological feature analysis from electrode microscopy	79
5.4.2	Relationship between electrical properties and biological properties of cells	82
5.5	Summary	86
<b>Chapter 6</b>	<b>LIMITATIONS, CONCLUSION AND FUTURE WORK</b>	87
6.1	Limitations	87
6.2	Conclusions	88
6.3	Future work	89

## List of Publications

### Conference papers:

W Zhang, N Huber, F Zheng, N Beqo, W Wang. Modelling the Stainless Steel Electrode for EIT System of Saline Tank, in Proceedings of 12<sup>th</sup> International Conference in Electrical Impedance Tomography (EIT 2011), May 4-6, 2011, Bath, UK, 81-84.

F Zheng, G Qiao, X Zhang, C Chatwin and W Wang . A comparison of two-and four-electrode bioimpedance measurements in electrolytes of different conductivity for measurement of cell suspension condition, in Proceedings of 13<sup>th</sup> International Conference in Electrical Impedance Tomography (EIT 2012), May 23-25, 2012, Tianjin, China. Accepted.

### Journal paper:

Qiao, G.; Wang, W.; Duan, W.; Zheng, F.; Sinclair, A.J.; Chatwin, C.R. (2012). "Bioimpedance analysis for the characterization of breast cancer cells in suspension," Biomedical Engineering, IEEE Transactions on , 59 (8): 2321-2329.

---

## List of Figures

Figure 2.1 The fluid-mosaic model of a cell membrane .....	7
Figure 2.2 Simulated dispersion regions of relative permittivity and conductivity .....	12
Figure 2.3 Three-component circuit model of the cell.....	13
Figure 2.4 Electrical models for cell suspension. ....	14
Figure 2.5 Current route and impedance behaviour of cell suspension at different frequencies .....	15
Figure 2.6 The cell cycle. ....	19
Figure 3.1 The principle of the two-electrode (A) and four-electrode (B) impedance method.....	27
Figure 3.2 Electrical circuit model for electrode polarization.....	32
Figure 3.3 Illustration of the system components.....	33
Figure 3.4 Illustration of the adopted chamber in the measurement.....	34
Figure 3.5 Impedance results of pure resistance.....	37
Figure 3.6 Part of fitting results of the saline solution with the electrical circuit model. ....	40
Figure 3.7 Comparison between the measured resistivity derived from the fitted $R_s$ value and the theoretical resistivity measured using the two-electrode measurement method .....	41
Figure 3.8 Variation of parameter $\beta$ with the changes of saline conductivity .....	43
Figure 3.9 Comparison between the measured resistivity derived from fitted $R_s$ value and the resistivity measured using the four-electrode measurement method .....	44
Figure 3.10 Comparison of frequency ranges of two-electrode and four-electrode measurements in conductivity of 0.65 mS/cm .....	45
Figure 3.11 Comparison of frequency ranges of two-electrode and four-electrode measurements in conductivity of 8.79 mS/cm .....	46

---

Figure 4.1 Accuracy performance of the measurement system.....	63
Figure 4.2 The resistance of MCF-10A and MCF-7 cell suspensions.....	66
Figure 4.3 The reactance of MCF-10A and MCF-7 cell suspensions.....	66
Figure 4.4 Fitting result of MCF-7 cell suspension with equivalent circuit model.....	68
Figure 4.5 Fitting result of MCF-10A cell suspension with equivalent circuit model. .	69
Figure 4.6 Physical model fitting of MCF-10A cells.....	70
Figure 4.7 Physical model fitting of MCF-7 cells. ....	70
Figure 5.1 Transmission electron micrograph of MCF-10A.....	81
Figure 5.2 Transmission electron micrographs of MCF-7 .....	82

## List of Tables

Table 2.1 Comparison of cancer cell and normal cell.....	20
Table 2.2 Relationship between the biological changes and parameters calculated in tissue .....	25
Table 3.1 Effect of electrode polarization on electrolyte of different conductivity .....	38
Table 3.2 The fitting results of parameters involved in equivalent circuit model .....	40
Table 4.1 Viability of cells before and after impedance measurement .....	64
Table 4.2 Volume fraction of cell suspension and diameter of cells .....	65
Table 4.3 Electrical parameters of cell suspensions from equivalent circuit model.....	69
Table 4.4 Fitting result of electrical parameters of cell suspension .....	69
Table 4.5 Other electrical parameters of cells derived from physical model .....	71
Table 5.1 Electrical parameters comparison of MCF-10A and MCF-7 in this study ...	77

# List of Acronyms

- EIT - Electrical Impedance Tomography
- CT - Computational Tomography
- MRI - Magnetic Resonance Imaging
- ECM - Extracellular Matrix
- CPA - Constant Phase Angle
- BNC connector - Bayonet Neill Concelman connector
- PC - Personal Computer
- DAQ - Data Acquisition
- MSE - Mean Squared Error
- EP - Electrode Polarization
- P-S theory - Pauly-Schwan theory
- H-A-K theory - Hanai-Asami-Koizumi theory
- LOC - Lab-on-chip
- PBS - Phosphate Buffered Saline
- TEM - Transmission Electron Microscopy
- AFM - Atomic Force Microscopy
- ADP - Adenosine Diphosphate
- ATP - Adenosine Triphosphate
- NAD - Nicotinamide Adenine Dinucleotide

# List of Symbols

$R$  - Resistance

$C$  - Capacitance

$R_e$  - Extracellular resistance

$R_i$  - Intracellular resistance

$C_m$  - Membrane capacitance

$Z$  - Impedance

$X$  - Reactance

$f$  - Frequency

$\omega$  - Radical frequency

$f_c$  - Characteristic frequency

$R_{ct}$  - Charge transfer resistance

$Z_{CPA}$  - Impedance of constant phase angle

$R_s$  - Resistance of saline

$C_{dl}$  - Capacitance of the double layer

$\sigma$  - Conductivity

$\rho$  - Resistivity

$\epsilon_r$  - Relative permittivity

$\tau$  - Relaxation time

$p$  - Volume fraction

$r$  - Radius

$d$  - Diameter

$\sigma_i$  - Intracellular conductivity

## ***Chapter 1***

---

### ***INTRODUCTION***

#### **1.1 Overview of bioimpedance**

Impedance is the ratio of the voltage to the current in an alternating current (AC) or direct current (DC) circuit. Bioimpedance is the impedance of biological material, which describes the ability of a living organism, such as tissues and cells, to impede electric current flow (Grimnes and Martinsen, 2008). As one of the key characteristics of human tissues and cells, bioimpedance was first investigated at the beginning of the 20th century. The earliest work on bioimpedance measurements can be traced back to the 1910s, where the low and high frequency conductivity of erythrocytes was measured (Hober, 1910; Coster, Chilcott et al., 1996).

For decades, scientists have been working on the early detection and treatment of cancer. Remarkable progress has been achieved on cancer detection and treatment. However, the five-year survival for certain cancers such as liver, pancreatic, and lung remains very low (6%–16%) (Jemal, Bray et al., 2011). Moreover, most of the cancer cases are detected in their mid or late stage (Haque, Schottinger et al., 2009), which leads to a low survival rate with current treatments. Nowadays the commonly used cancer detection techniques in clinic include Computational Tomography (CT), Magnetic Resonance Imaging (MRI) and Ultrasound. The most reliable means to confirm cancer is biopsy which requires removal of the tissue in the region of interest.

In recent years the application of bioimpedance for cancer detection has become an attractive research topic. This application can be traced back to the 1920s when Frick

and Morse found significant difference of capacitance between malignant breast tumours and normal tissues (Fricke and Morse, 1926). Bioimpedance shows great advantages over CT, MRI and Ultrasound in cancer detection. First, bioimpedance is a non-invasive, harmless and pain-free technique compared to CT, MRI and Ultrasound. Second, bioimpedance is relatively highly sensitive with respect to small changes occurring inside malignant tissues, which potentially allows for the detection of tumours in their early stage. Finally, bioimpedance techniques are able to realize real-time detection when compared to other clinical used techniques. All those advantages make bioimpedance technique a promising method on early detection of cancer.

Many studies have been carried out in cancer detection at the tissue level by bioimpedance based techniques (Surowiec, Stuchly et al., 1988; Morimoto, Kimura et al., 1993; Jossinet, 1996). However, due to the application of different methods for measurements, the complex structure and heterogeneity of the tissue and variation of the different tissues, no standard has been achieved on how to differentiate cancer from the surrounding normal tissue. In addition, there is no agreement on the changes of impedance parameters in different cancer tissues. Moreover, the relationship of electrical properties and corresponding biological changes of tissues is still unclear. It is known that both the morphology and the components of the cell experience subtle changes in the process of carcinoma transformation at the cell level. The electrical properties of the cell are dependent on its physiological state. This fact has indicated the investigation at the cell level is likely to provide the direct information on the relationship between the biological properties and electrical properties of cells, which is of vital importance to the early detection of cancer by an impedance based technique.

## **1.2 Objectives and goals**

This study will focus on applying impedance spectroscopy to cancer identification from the cellular level. Both normal cell suspensions and cancer cell suspensions will be measured by impedance spectroscopy; and the electrical parameters of normal cells and

cancer cells will be further analysed and compared to verify the feasibility of identification of cancer cells by impedance spectroscopy. In order to yield accurate results, both two-electrode and four-electrode measurements will be adopted and compared in this study. Electrode polarization, a major problem in two-electrode measurement, will be analysed for accurate interpretation of the results.

Based on these results, this study attempts to establish the relationship between the biological properties of cells and their impedance response. The electrical properties derived from theoretical models will be correlated with the physiological changes of cancer cells and normal cells derived from related biological assays. Through the analysis of the relationship between cell impedance response and biological functions of cells and pathological properties by bioimpedance spectroscopy, it is hoped to provide basic information for the application of the bioimpedance spectroscopy as a clinical technique for cancer detection and also provide a different view to the understanding of carcinogenesis development from the electrophysiological point of views.

### **1.3 Structure of the thesis**

Chapter 2 aims to provide a biological and electrical background to the cell and cell suspensions. A detailed introduction to cancer cells will be provided from the biological perspective and a comparison of normal cells and cancer cells will be discussed at a sub-cellular level. Reviews on impedance detection in cancer research will also be provided at the end of Chapter 2.

Chapter 3 will focus on the investigation and comparison of two different methods for impedance measurements. At the beginning of Chapter 3, a brief literature review on electrode polarization will be delivered due to its potent effect on two-electrode measurements. The impedance measurement of electrolytes with different conductivities by two-electrode and four-electrode techniques will be reported. The effects of electrode polarization on the result will be investigated in detail in this chapter. At the end of this

chapter, two-electrode and four-electrode measurements will be compared in order to choose the more suitable method for further investigation on cell suspensions.

Chapter 4 will mainly focus on the identification of cancer cells by impedance spectroscopy using a four-electrode technique. The background of the electrical model and physical model and different means to explore the electrical properties of cells will be described at the beginning of this chapter. Suspensions of normal cells and cancer cells have been investigated with impedance spectroscopy in a controlled testing environment. Two analytical methods will be applied to analyse the results. Detailed information on the electrical parameters extracted from the two models will be given and compared in this chapter.

The last chapter will focus on the interpretation of the results from Chapter 4 from the biological perspective. The research into the electrical parameters of cancer will be summarized for both tissue level and cell level, which is the main task of this study. Biological assays have been employed to compare cancer cells and normal cells. Detailed analysis of the electrical parameters and biological properties will be provided at the end of this chapter. The thesis provides a conclusion derived from this study and also describes possible directions for further investigation.

## ***Chapter 2***

# ***BIOLOGICAL AND DIELECTRIC BACKGROUND OF CELL SUSPENSION AND CANCER CELLS***

### **2.1 Introduction**

The cell is the lowest level of structure capable of performing all kinds of activities in organisms. It is hard for one to investigate the relationship between electrical properties of cells without a knowledge and understanding of the biological background of the cell. Therefore, in this chapter, the content will begin with an introduction to the biological background of cells. Following this, the dielectric properties of cells are reviewed and electrical and theoretical models of cells will be discussed and used to understand the basic principles involved in this study. In addition, the biological background of a cancer cell and its features are compared to those of a normal cell. Finally, a brief summary of the impedance research into cancer is given to back up this study.

### **2.2 Cell structure and its biological properties**

Cells are highly organized structures. All of the functional units of a cell, but also the cell itself, are separated by membranes from the surrounding medium (Alberts, Bray et al., 2007). Cells can be divided into two major categories, prokaryotic and eukaryotic cells, which are different in both the cell structure and many biological properties. Since both of the cell lines adopted in our study are breast cells, which are one kind of eukaryotic cell, we will only focus on eukaryotic cell in the thesis.

Cells consist of a lipid bilayer membrane surrounding an intracellular fluid containing numerous organelles, including nucleus, mitochondrion, ribosomes, endoplasmic

reticulum, lysosomes, etc. As to the tissues, there are various proteins and non-protein substances, metabolites, ions that might affect cellular function in extracellular space.

### **2.2.1 Cell membrane**

Cell membrane is the most significant portion of the cell as it separates each cell from the surrounding world. It is about 4-10nm in thickness. According to the widely accepted 'fluid mosaic model' proposed by S.J. Singer and G.L. Nicolson (Singer and Nicolson, 1972), the biological membranes are composed of long fatty chains with a charged head group (mainly charged phosphates) and many proteins that are connected to the liquid layer in different ways (Figure 2.1). Energy minimization forces lipids in water to arrange into membranes, where the hydrophilic head groups face the water while the hydrophobic tails are inside the membrane. This is the basic structural building block of the cellular membrane, constructed so that the cell may survive in an aqueous environment while maintaining the independent intracellular cytoplasm. In the membrane, cholesterol molecules interspersed in the layer provide some rigidity, but most cellular stability is achieved through a network of proteins both intracellular cytoskeleton and the proteins in extracellular matrix.

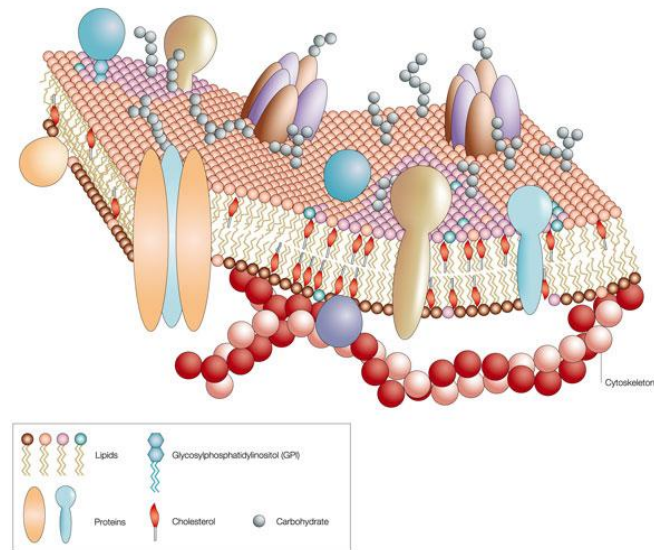


Figure 2.1 The fluid-mosaic model of a cell membrane (Pietzsch, 2004). Cell membrane is a complicated structure which includes phospholipids, proteins, cholesterol *et al.* The lipid bilayers form the basis of the membranes and cholesterol could regulate the fluidity of the membrane. Various proteins play a significant role in the functions of cell membrane, such as ion transport and signal transduction.

The protective function of a cell mostly depends on the permeability of membranes. There are three independent mechanisms for the transport of materials from extracellular space, including free diffusion, facilitated diffusion, and active transport. Small nonpolar (hydrophobic) molecules like gases can penetrate the membrane without great hindrance. While as to the charged ions like  $\text{Na}^+$ ,  $\text{K}^+$  or  $\text{Cl}^-$  even though they are small, the permeability decreases with the size and hydrophobicity of the molecules and approaches zero. Ionic channels are especially important for the electrical properties of the membrane, since they allow the ionic flow across a highly isolating barrier. These channels can be always open leak channels (i.e.  $\text{K}^+$  channel) or they can be either open or closed. The activation of such a channel can be due to ligand binding or a physical stimulus like pressure, temperature or a change of the electrical potential difference across the membrane (Pliquett, 2008). Since the cell membrane is selectively permeable to sodium and potassium and some other ions, a different concentration of those ions

will build up on either side of the membrane, which leads to a relatively higher positive charge on the outer membrane surface than the inner membrane surface. Therefore an electrical potential across the membrane is formed (Charman, 1996). The movements of charged ions and electrons across the membrane are restricted. They can go through the membrane from the specialized ion channels and membrane spanning protein semiconductors respectively (Aidley and Stanfield, 1996).

### 2.2.2 Cytoplasm

The cytoplasm is a highly complicated system, which contains not only large amounts of salts, proteins and nucleic acids but also many organelles that are of great significance for the cell function, including the nucleus, mitochondria, the endoplasmatic reticulum and the Golgi apparatus etc. Most of the internal organelles of the cell are surrounded by membrane structures.

The nucleus is the largest cellular organelle in animal cells that is membrane-enclosed. The chromosomes inside the nucleus contain most of the genetic information. Those chromosomes are composed of multiple long linear DNA molecules and a large variety of proteins, such as histones. The function of the nucleus is to maintain the integrity of these genes and to control the activities of the cell by regulating gene expression. The nucleus is, therefore, the control centre of the cell.

Mitochondria are the 'power factory' for the cells. They are responsible for the support of adenosine triphosphate (ATP) for the normal cell function by respiratory reaction. The specialized proteins and enzymes involved in oxidative phosphorylation are located on the inner mitochondrial membrane and form a molecular respiratory chain. This electron transport chain passes electrons donated by several important electron donors through a series of intermediate compounds to molecular oxygen, which becomes reduced to water. In the process adenosine diphosphate (ADP) is converted into ATP. Electrical properties of cells are closely related to mitochondria.

The cytoskeleton is another important structure for cell function and provides the cell with shape and structure. It consists of three types of structural protein filaments, which are actin filaments, microtubules, and intermediate filaments, that may be distinguished by their diameter and their chemical properties. The cohesive meshwork constructed by protein filaments allows movement of the cell, shaping of the cellular membrane, and intracellular transport of different substances.

The cytoplasm can be regarded as a highly conducting solution due to the high content of ions and other charged proteins. Therefore cytoplasm is considered to function as a resistance in most cases.

### 2.3 Impedance basics

As stated in Chapter 1, impedance is the ratio of the voltage to the current in alternating current (AC) and direct current (DC) circuits. It can be expressed in the form of a complex number, including the real part ( $R$ ) and imaginary part ( $X$ ) components. Both the real part and imaginary part of impedance are functions of frequency. The impedance can be defined as:

$$Z(\omega) = R(\omega) + jX(\omega) \quad (2.1)$$

where  $R$  and  $X$  stand for resistance and reactance respectively and  $\omega$  is the angular frequency.

Both the impedance and its components are related to the electrical properties of samples and their geometry. Besides, the resistivity,  $\rho$ , and conductivity,  $\sigma$ , are commonly utilized in the impedance study. Those variables are dependent only on the electrical properties of samples. The relationships between these variables are given by equations 2.2 and 2.3.

$$R(\omega) = \frac{\rho(\omega) \times L}{S} \quad (2.2)$$

$$\sigma(\omega) = \frac{1}{\rho(\omega)} \quad (2.3)$$

where  $L$  and  $S$  are the length and cross-sectional area of the samples measured.

The capacitive reactance of a capacitor  $X$  at angular frequency  $\omega$  is given by:

$$X = \frac{1}{j\omega C} \quad (2.4)$$

#### 2.4 Dielectric properties of biological cells

Electrical properties of biological materials are always an area of interest due to an increasing awareness of the related physiological status elicited by the electrical properties of biological materials. Therefore, the measurements of the electrical properties of biological materials hold a pre-eminent position in several areas of physiology and biophysics. The dielectric properties of biological materials are always an area of intense interest. Impedance techniques have been used to study the dielectric properties of tissues and cell suspensions (Schwan, 1957; Dijkstra, Brown et al., 1993), also extending from cell membrane to the ultrastructures inside the cell (Oncley, 1940; Pethig and Kell, 1987). Today such studies are an area of intensive interest and are leading to practical and commercial applications, such as bacterial monitoring in the food industry (Spreekens and Stekelenburg, 1986; Varshney and Li, 2008).

When a material is exposed to an electric field, its response to the applied electric field can be described by its conductivity ( $\sigma$ ) and permittivity ( $\epsilon$ ), which is also applied to biological systems like tissues and cell suspensions. The conductivity gives a measure of the ability of cells to conduct, whereas the permittivity gives a measure of the ability to permit storage of electric energy (Grimnes and Martinsen, 2008). Permittivity is often

expressed as the relative permittivity  $\epsilon_r$  (dimensionless), which is a dielectric constant and defined as the permittivity relative to that of vacuum. The bulk properties of material can be expressed by conductivity or permittivity. They are often expressed as complex number, which are shown in equation 2.5 and 2.6.

$$\epsilon^* = \epsilon_r^* \epsilon_0 \quad (2.5)$$

Where  $\epsilon^*$  is the permittivity of material,  $\epsilon_r^*$  is the relative permittivity of material,  $\epsilon_0$  is the permittivity of vacuum, which equals to  $8.854 \times 10^{-12} F/m$ .

$$\sigma^* = \sigma' + j\sigma'' \quad (2.6)$$

where  $\sigma'$  is the real component of conductivity and  $\sigma''$  is the imaginary component of conductivity.

As to biological materials, the permittivity and conductivity are frequency dependent. The permittivity will fall and conductivity will increase with the increase of frequency. There will be three dispersions corresponding to the changes of the dielectric properties of biological material with the frequency. The dispersion is the momentary delay in the dielectric constant of a material, which is usually caused by the phase shift in molecular polarization with respect to a changing electric field in a dielectric medium. The  $\alpha$ -dispersion occurs at low frequencies (10 Hz – 10 kHz) and is mainly affected by lateral movement of ions attached to the cell surface. Since at low frequency the cell membrane impedes the current route in cell suspension, the impedance at low frequencies can provide the information about the cell volume fraction (Pliquett, Frense et al., 2010). At high frequencies (10 kHz–10 MHz), the current can pass through the cytoplasm while membranes are electrically shorted. The impedance decreases due to the accessibility of the cytoplasm as a current path, which forms the  $\beta$ -dispersion. The  $\beta$ -dispersion is associated with polarisation of cell membranes, proteins, and other macromolecules. At high frequencies (>10 MHz), the  $\gamma$ -dispersion is found to be related

to water molecules (Figure 2.2). Sometimes a transitive dispersion between  $\alpha$ - and  $\gamma$ -dispersion is introduced, which is named as  $\delta$ -dispersion. The  $\alpha$ - and  $\beta$ -dispersion regions are more interesting in medical applications, since most differences between pathological and normal tissue occur in this range.

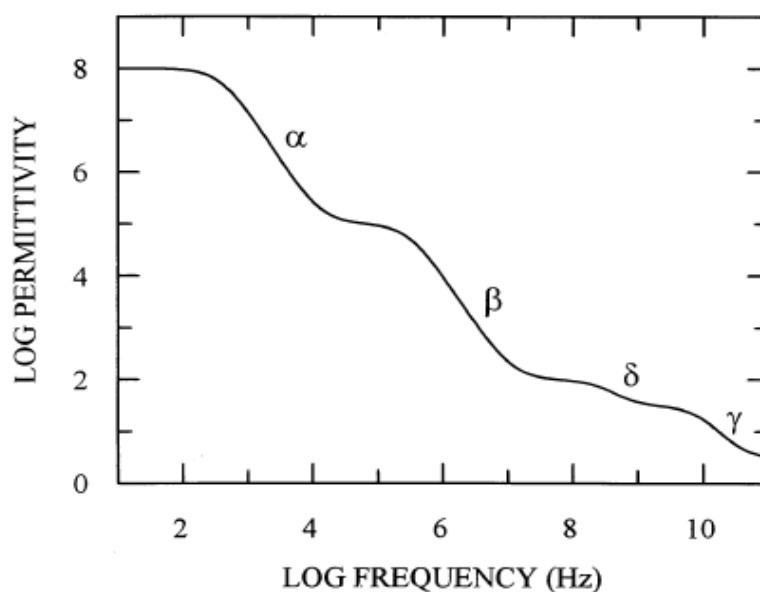


Figure 2.2 Simulated dispersion regions of relative permittivity and conductivity (Markx and Davey, 1999).

## 2.5 Electrical model for cells and cell suspension

The development of the cell's electrical model can be traced to early 1910 when Hober measured the electrical impedance of suspensions of erythrocytes up to frequencies of 10 MHz and found that their impedance decreased with increasing frequency. He concluded that the cells were composed of a poor conducting membrane surrounding a cytoplasm of relatively low resistivity (Hober, 1910; McAdams and Jossinet, 1995). Fricke developed a shell model in which a spherical cell was surrounded by a thin shell of low conductivity and gave the first indication of the capacitance of cell membrane to be about  $0.81 \text{ pF/cm}^2$  and deduced the membrane thickness, which was very close to the value determined by electron microscopy three decades later (Fricke and Morse, 1925; Robertson, 1981; Coster, Chilcott et al., 1996).

Since a cell is composed of intracellular cytoplasm and cell membrane, the electrical properties of cell are dependent on the electrical properties of the components. The simple model of a cell is an electrolytic solution surrounded by a cell membrane. In cell suspensions, the extracellular medium consists primarily of ionic solutions. The intracellular material is an ionic solution with charged ions and proteins, which is treated as a resistor. The cellular membrane is primarily considered as a capacitor due to the structure of the membrane. When taking ion channels into consideration, the conductance of membrane should be added into the cell model due to the influence of ion channels on the permeability of the membrane.

In this way, the model for a membrane is described as a combination of a resistor and capacitor. However, the resistance of membrane is much larger than the resistance of the intracellular medium, thus the cell membrane is assumed to be non-conducting in many cases (Figure 2.3) (Foster and Schwan, 1989). The model shown in Figure 2.3 represents one Debye type relaxation process with a single dispersion, which is the dielectric relaxation response of an ideal, non-interacting population of dipoles to an AC electric field. This model is able to describe qualitatively the observed main dispersion in the  $\beta$  dispersion region as defined by Schwan. This simple model is a good approach not only for most cells suspension but also tissues over the frequency range between 10 kHz and several MHz (Pliquett, 2008).

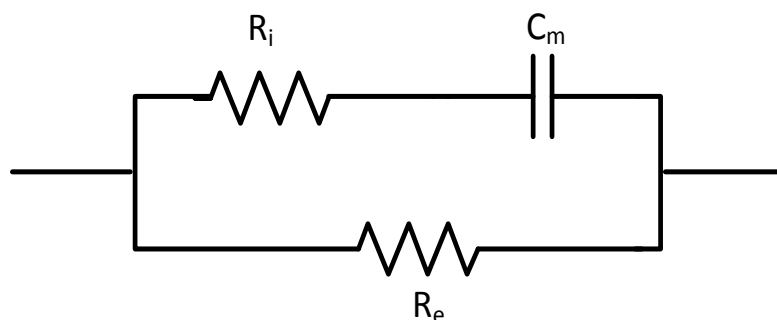


Figure 2.3 Three-component circuit model of the cell. It consists of a resistance for the extra-cellular electrolytic medium ( $R_e$ ) in parallel with the series combination of a resistance for the intra-cellular electrolytic medium ( $R_i$ ) and a capacitance for the cell membrane ( $C_m$ ).

For cell suspension, the impedance contributions from all cells are combined, therefore the same electrical model can be employed to characterize the impedance behaviour of cell suspension as seen from the measurement electrodes. The principle for impedance measurement of cell suspensions is shown in Figure 2.4.

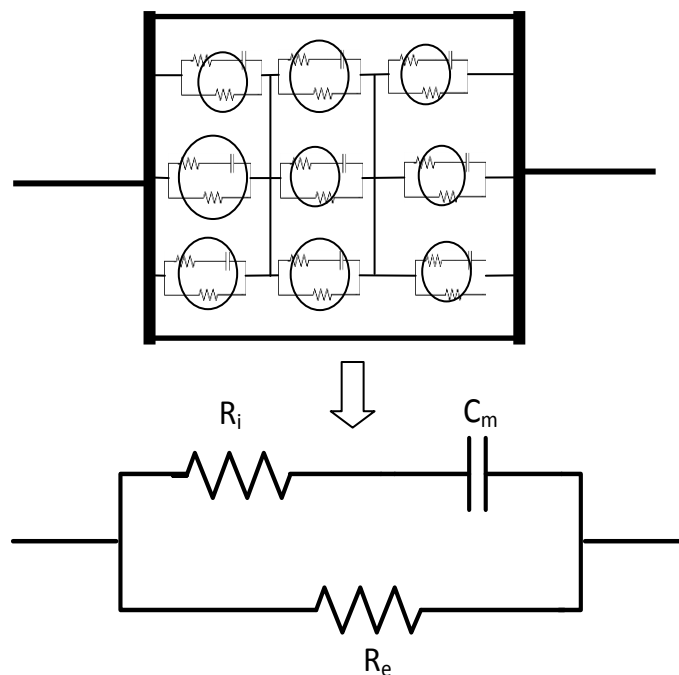


Figure 2.4 Electrical models for cell suspension. Each cell in suspension is regarded as a three-component model. All of the cells are combined and contribute to the general impedance of the suspension. Therefore, the three-component model can also be applied to cell suspension as well (The figure has been adapted and slightly modified from the figure at <https://sites.google.com/site/antonivorra/home/electrical-bioimpedance>)

At low frequencies, currents cannot penetrate into the cell due to the high impedance of the cell membrane. Therefore, the impedance at low frequency mainly indicates the electrical property of extracellular fluid,  $R_e$ . As the frequency increases and the membrane become more conducting, the current flow is related to the ratio of conductivity of the suspension to that of bulk solution (Coster, Chilcott et al., 1996). Therefore at extremely high frequency it represents a combination of intracellular and extracellular fluid, which in the idealized situation is equal to the parallel resistances of

intracellular and extracellular fluid. The reduction in impedance in the frequency range is called  $\beta$  dispersion. A schematic diagram of the current routes at different frequencies is given as follows.

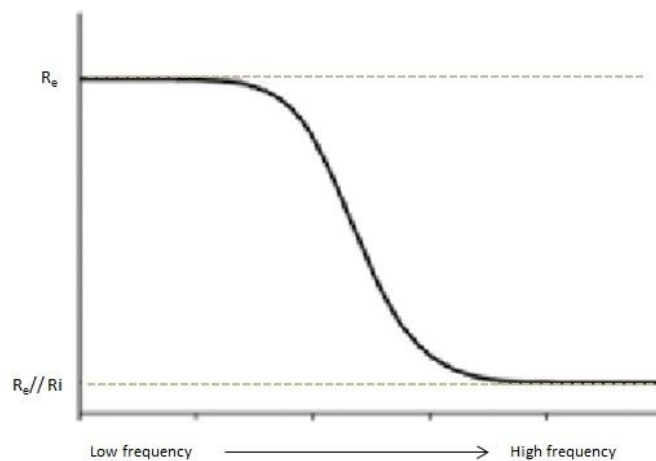
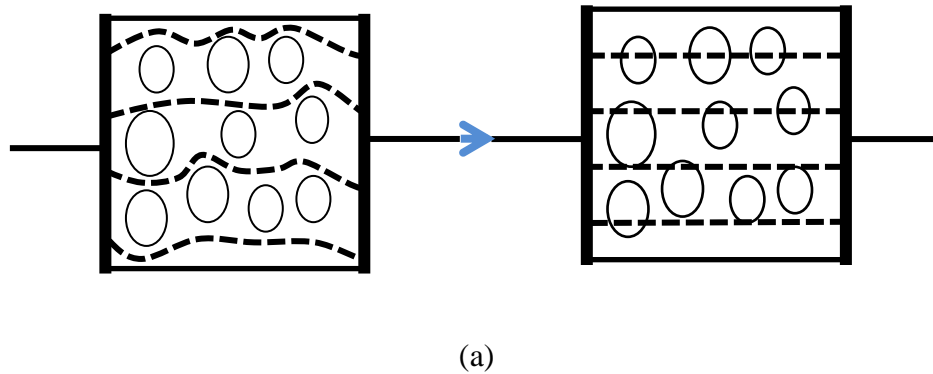


Figure 2.5 Current route and impedance behaviour of cell suspension at different frequencies. (a) Schematic figure of current route in cell suspension at different frequencies. The current is restricted to extracellular spaces at low frequency whereas high frequency currents can flow freely through cells. (b) Idealized graph of impedance trend versus frequency in cell suspension. The idealized impedance at very low frequency is the resistance of the medium and the idealized impedance at very high frequency is the parallel resistance of intracellular resistance and medium resistance.

In 1940 Cole introduced the first mathematical expression to describe the frequency dependent phenomenon as suggested by Fricke (Cole, 1940), which is known as the Cole equation.

$$Z = R_{\infty} + \frac{R_0 - R_{\infty}}{1 + (j\omega/f_c)^{\alpha}} \quad (2.7)$$

where  $Z$  is the impedance value at frequency  $\omega$ ,  $j$  is the imaginary number  $\sqrt{-1}$ , The exponent parameter  $\alpha$  takes a value between 0 and 1, which allows the description of different spectral shapes.  $R_0$  is the low frequency impedance, simply given by the extracellular resistance,  $R_e$ .  $R_{\infty}$  is the high frequency impedance, given by:

$$R_{\infty} = \frac{R_i \times R_e}{R_i + R_e} \quad (2.8)$$

and  $f_c$  is the characteristic frequency of the dispersion, which is usually defined as the frequency where the gradient of real part curve is at its maximum value, and the value of the imaginary part is at its maximum value. The characteristic frequency can be calculated according to equation 2.9:

$$f_c = \frac{1}{2\pi(R_i + R_e) \times C} \quad (2.9)$$

A cell suspension basically consists of a cell population surrounded by an extracellular fluid, which contains proteins and electrolytes. Dielectric properties of biological cell suspensions have been studied since the beginning of the last century and in the last few years a number of comprehensive reviews have been published (Hanai and Sekine, 1986; Asami, 2002; Asami, 2002). Thus biological cell suspensions have served as a good model for exploring the electrical properties of cells.

Models of cell suspension systems were first developed by Maxwell for the direct current (DC) case and Wagner for the alternating current (AC) case. Cell suspension will exhibit a  $\beta$  dispersion in the radio frequency range, which is due to the interfacial polarization between the intracellular and extracellular solution and the cell membrane (Pethig and Kell, 1987).

## 2.6 Introduction of cancer and its biological properties

Cancer has become the second leading cause of death worldwide, only behind the cardiovascular disease. According to the latest WHO report, about 12.7 million cancer cases and 7.6 million cancer deaths are estimated to have occurred in 2008 (Jemal, Bray et al., 2011). Moreover, the number keeps on increasing worldwide as a result of population ageing and growth as well as an increasing adoption of cancer-causing behaviours, such as smoking. Over the last few decades significant progress has been achieved in understanding the mechanisms involved in cancer development and its treatment. Many physiological differences have been found between cancer and normal tissue and cells.

In this section, a general introduction of mechanisms for carcinogenesis and its relationship with the cell cycle and checkpoint are summarized. In addition, features of carcinoma compared to those of the normal tissue are provided in this part. Based on this information, the characteristics of cancer cells from a biological aspect are presented, which provides the foundation for our study. At the end of this chapter a brief review of the current progress in cancer research by impedance-based techniques will be presented.

### 2.6.1 Cancer and cell cycle

Proliferation of cells is a complex process based on many subroutines, which require stringent control mechanisms in the cell cycle for the normal growth of the body. Regulation of the cell cycle consists of a series of checks and balances that monitor the state of all factors involved in cell proliferation, including cell genome integrity, the presence of growth factors, the nutritional status etc. In normal cells, cell division is divided into four phases,  $G_1$ , S,  $G_2$  and M (Figure 2.6). As to adult cell, they do not experience cell division, therefore a quiescent inactive phase  $G_0$ , which is outside the cell cycle is introduced for cells stopping division. In  $G_1$  (Gap one), the first phase within the interphase, although it is the related quiescent phase, significant biosynthetic activities happen. This phase is marked by the synthesis of 20 amino acids, which is the

basis for the synthesis of proteins and enzymes required in the S phase. The ensuing S phase starts when DNA synthesis commences. In the S phase the amount of DNA in the cell has effectively doubled, though the ploidy of the cell remains the same. When the cell enters into the G<sub>2</sub> phase, significant biosynthesis occurs involving the production of proteins required in mitosis. After processing the G<sub>2</sub> phase, cells move forward to the mitosis stage, in which the doubled chromosomes in the cell nucleus are separated into two identical nuclei sets. Followed by cytokinesis, the mother cell divides into two identical daughter cells (Pecorino, 2008).

For normal cells, once they enter the replicative phase of the cell cycle, they will follow the cell cycle step by step strictly due to the check of one G<sub>1</sub> restriction point and several checkpoints within the cell cycle. As to the restriction point (R point), the cumulative exposure to specific signals, such as growth factors, is assessed and if the sum of these signals satisfies the conditions required by the R point, proliferation ensues (Martinez, Parker et al., 2003). And those checkpoints are actually a series of biochemical signalling pathways that could sense DNA damage and induce a cellular response to it. Hence they are of great significance in maintaining the genome integrity. Moreover, when DNA damage is detected by several signalling proteins in cells, such as p53, ataxia telangiectasia mutated (ATM) and CHK2, the cell mitosis will be terminated. Lack of these functional proteins, or any protein mutation causes cell division to occur in the presence of DNA damage, leading to further genetic changes of the daughter cells and progression towards malignancy (Souhami and Tobias, 2005; Souhami and Tobias, 2007).

Carcinogenesis is the process that gets the genetic mutations leading to cancer. As to normal cells the process of acquisition of a single mutation or accumulation of mutations is definitely under the monitor and repair system of the cells themselves. As to cancer cells, they are not precisely following the cell cycles shown in Figure 2.6. Disruption of a checkpoint function could lead to mutations; as a result, a single mutated gene is produced due to external stimulation factor, which is irreversible. Cells with initiated mutations will proliferate with increasing population. The accumulation of genetic mutations will finally lead to cancer.

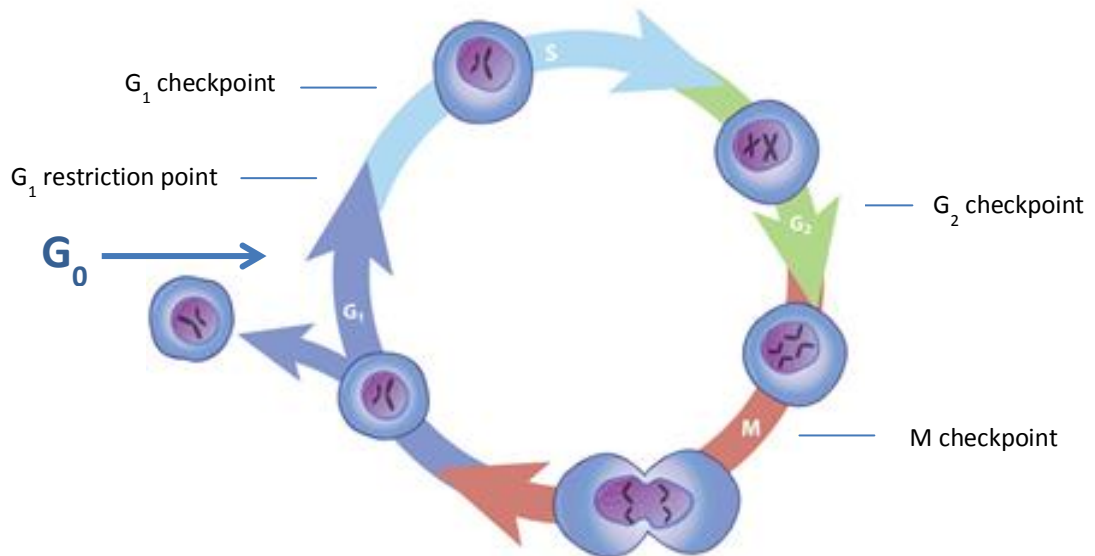


Figure 2.6 The cell cycle. The full cell cycle is divided into four phases,  $G_1$ , S,  $G_2$  and M, and a quiescent phase  $G_0$ , which is outside the cell cycle is introduced for cells stopping division. The  $G_1$  restriction point and checkpoints at different stages of cell play critical roles in cell cycle controlling. (Note: the adapted figure is from Scitable by Nature education with minor modification [<http://www.nature.com/scitable/topicpage/eukaryotes-and-cell-cycle-14046014>]).

### 2.6.2 Features of cancer cells

Cancer is a process of accumulation of many genetic mutations from a single cell. The neoplastic cell shows many features that differ from a normal cell. A significant amount of research has been conducted to differentiate cancer cell/tissue from normal cell/tissue. The difference between cancer cell/tissue and normal cell/tissue might help to explore the mechanism involved in carcinogenesis and understand the behaviour of cancer cell. Ultimately this will lead to progress in cancer treatment (Hanahan and Weinberg, 2000; Souhami and Tobias, 2007; Marte, Eccleston et al., 2008). A list of characteristics of distinguishing the cancer cell from normal cell is summarized based on the research carried out so far, which is shown in Table 2.1.

Table 2.1 Comparison of cancer cell and normal cell

	Cancer cell	Normal cell
1	Immortality	Sensitivity to apoptotic cell death
2	Loss of cell cycle control	Strictly follows the cell cycle
3	Uncontrolled growth rate	Stable growth rate
4	Increased genetic instability	Genetic stability
5	Loss of contact inhibition	Contact inhibition
6	Capacity to invade and destroy normal tissue	-

As stated above, remarkable changes in cancer cells are found in the structure of organelles, expression of essential proteins, especially lots of enzymes etc. Thus the neoplastic cells show significant difference from normal cells in their growth process. Meanwhile, those changes are closely related to the response of electrical properties in cells. For example, the variation of the expression of proteins that constitute ion channels on cell membrane will directly lead to the changes of ion concentration in both intracellular plasma and extracellular fluid. Due to the changes of different ions concentrations in the process of cancer transformation, the permeability of cell membrane has become an indicator for our study of its electrical properties.

Many studies have focused on the detection of the changes to explore the new methods for cancer detection. For our study, it is those structural changes that provide the basic evidence and foundation for the detection of electrical changes. Therefore, at the end of this chapter, a brief summary of the structural features of cells in the neoplastic process is given and the related changes in electrical properties are provided as well.

### 2.6.3 Cell components changes in carcinogenesis

#### **Nucleus**

Nucleus changes during the neoplastic process are of great significance for the reason

that they are the origin of all consequent changes. Morphological changes in the structure of the nucleus and abnormalities of chromosomes are found in cancer cells (Zink, Fischer et al., 2004). In the aspect of abnormalities in chromosomes, a gain or loss, deletion, inversion, translocation and selective amplification of a certain region of chromosomes have been found according to the previous research, which directly leads to the regulation of the expression of many proteins involved in the cancer transformation process.

The alterations of nucleus structure include enlarged nucleus size and irregular nucleus shape and changes in numbers and sizes of nucleoli, chromatin pattern, and perinucleolar space (Dey, 2010). Nucleus margin irregularity is common in cancer, which may be seen as nucleus grooving, moulding, and nucleus convolutions (Rajesh, Dey et al., 2003). All those alterations might be related to the altered functional properties of cancer cells. However, the relationship between nucleus morphology alterations and their functional changes is still unclear.

### **Cell membrane**

Remarkable changes occur in the structure of cell membrane during the process of cancer transformation due to its important role in the uptake of metabolites. Cancer cells have cell membranes that exhibit different content in lipids or sterols compared to normal cells (Koizumi, Tamiya-Koizumi et al., 1980; Meng, Riordan et al., 2004). Many proteins that are involved in the transport in ion channels are regulated in their quantity. As a result, the alterations in both membrane composition and protein content increase the permeability of the cell membrane, which results in the movement of ions and water content on both sides of the cell membrane (Anghileri, Crone-Escanye et al., 1988; Dobrzyńska, Szachowicz-Petelska et al., 2005). It has been reported that due to the changes of membrane permeability, the intracellular concentration of sodium and water is increasing while the extracellular concentrations of potassium, calcium and magnesium is increasing. Therefore, cancer cells have lower potassium concentrations and higher sodium and water content than normal cells (Cone, 1970; Cone, 1974). The

changes in the ion concentrations, especially the increased intracellular concentration of sodium, and an increase in negative charges on the cell coat (glycocalyx) result in the decrease of membrane potential. Besides ion movements, membrane composition changes, the energy abnormalities, and membrane charge distribution abnormalities may also lead to a drop in membrane capacitance.

### **Cytoskeleton**

The cytoskeleton is closely related to the morphology of cells. The cytoskeleton in the cancer cell becomes disintegrated and irregular compared to that of the normal cell. Moreover, the proteins of the cytoskeleton are altered and the contact and connections with the extracellular matrix (ECM) and neighbouring cells are broken in a cancer cell, which consequently reduces the cell stiffness and accordingly increases their deformability (Guck, Schinkinger et al., 2005; Suresh, 2007).

When it comes to the tissue level, there are some other alterations in the extracellular region of cancer besides the cell membrane and intracellular plasma. The types of extracellular matrix receptors expressed are switched to facilitate the transmission of growth signals, which could influence cell behaviours including cell mobility, resistance to apoptosis and entrance to the cancer cell cycle. An increase of vascularisation is found in cancers, which supply the nutrition and oxygen for their growth of cancer. Meanwhile, a loss in cell contact between cells is found, which directly leads to the reduction of the cell packing density (Hanahan and Weinberg, 2000). There are remarkable changes in the expression of the proteins, especially many proteases involved in the invasion of normal tissue. Cancer cells characteristically display higher external proteolytic (protease) activity than normal cells (Edwards and Murphy, 1998).

#### **2.6.4 Biological methods for cancer research**

The physiological properties of cells differ significantly depending on their structures and the cell processes involved in these cell functions could be monitored by various

biological assays. Many researchers have focused on the detection of those biological changes and as a result, a great number of biomarkers are found to be indicators for cancer detection and many biological assays have been developed to investigate the biological properties of cells (Marte, Eccleston et al., 2008; Abeel, Helleputte et al., 2010). Many techniques have been developed for the investigation of cell structures and cell functions.

Electron microscopy serves as a vital instrument to detect the morphological changes of cells. The main advantage of electron microscopy lies in its high spatial resolution. With environmental scanning electron microscopy, cell morphology is better preserved. However, cells cannot be left viable after analysis, which makes electron microscopy an end-point detection. Moreover, a great deal of time and a high level of skill are needed in order to prepare and measure cells using electron microscopy.

Genomic and proteomic assays have now been widely adopted in cancer research since those assays offer increased chemical information at the expense of high resolution. For example, DNA ladder assays are adopted to investigate DNA content and fragments. Despite their high sensitivity, most of them are invasive so that they cannot preserve cell viability.

Flow cytometry is one of the most commonly used methods in research into cell biological properties, which is often used in conjunction with many other techniques in cell function detection due to its high efficiency and multi-parameter detection. Flow cytometry can provide information of both single cell and cell populations on the DNA and protein, viability dyes, membrane dynamics at one time, which makes it an indispensable technology in cell research (Rieseberg, Kasper et al., 2001). However, flow cytometry can only measure a single point at one time for a particular group of cells, thus it cannot provide continuous information on a biological process with dynamic detection. Its high cost of both detection and maintenance also hinders its use for wider application.

Therefore, most conventional cell assays cannot provide information of the dynamic response to cellular changes due to labelling or dye-based end-point detection. These assays are not able to provide continuous monitoring of a sample, and in consequence the information achieved will not reflect the real changes of cell activities at a specific time to a specific agent.

### **2.6.5 Impedance measurement for cancer research**

As stated above, all the biophysical changes in cancer cells induce specific characteristics of their electrical properties, which can be detected by impedance spectroscopy. The research into the electrical properties of normal and cancerous tissue can be tracked back as early as 1926 when Fricke and Morse found a marked difference in capacitance of breast tumours compared to normal breast tissue (Fricke and Morse, 1925). With respect to the bioimpedance of cancer, it has been revealed that overall cancer has lower impedivity than normal tissue (Smith, Foster et al., 1986; Jossinet, 1998; Wang, Tang et al., 2001; Brown, Milnes et al., 2005). Impedivity is the equivalent for AC current of the resistivity for DC current (Jossinet, 1998). The alteration in impedance of cancer might be attributed to increased cellular water, ion content, increased cell membrane permeability and packing density. All these changes may exert influence on the overall impedance changes.

Most of impedance research on cancer tissue has supported the conclusion that the capacitance of cancer is lower than normal tissue. The reasons for this are the ion movements, membrane composition changes that stem from the increased permeability of the cell membrane. Meanwhile, the energy abnormalities, and membrane charge distribution abnormalities also lead to a drop in membrane capacitance (Morimoto, Kimura et al., 1993; Han, Yang et al., 2007). The change in the extra-cellular electrical properties of cancer can be observed from the impedance at low frequencies, while the changes in the intracellular electrical properties of cancer can be observed at high frequency. So far there is no consensus arrived at as to the impedance changes in both extracellular and intracellular parts of cancer cells. However, results from much

research have revealed that the electrical properties of the extracellular part is related to the changes in cell arrangement and the ion content change due to the increased cell membrane permeability mentioned above. The changes in intra-cellular resistance are due to the disintegration of the cytoskeleton and changes in ion concentration and water content. Factors influencing the electrical parameters of the tissue are summarized in Table 2.2.

Table 2.2 Relationship between the biological changes and parameters calculated in tissue

Parameters	Intracellular resistance	Extracellular resistance	Membrane capacitance
Related factors	Intracellular water content; Enlarged nucleus size ; Intracellular volume ; Proteins content; Ion changes.	Cell arrangement; Stiffness of ECM; Vascularization; Ion content.	Cell volume; Membrane permeability.
Reference	(Jossinet, 1998) (Brown, Tidy et al., 2000) (Zou and Guo, 2003) (Suresh, 2007)	(Brown, Tidy et al., 2000) (Malich, Scholz et al., 2007) (Suresh, 2007)	(Anghileri, Crone-Escanye et al., 1988) (Brown, Tidy et al., 2000) (Dobrzyńska, Szachowicz-Petelska et al., 2005)

## ***Chapter 3***

# ***IMPEDANCE MEASUREMENT OF SALINE SOLUTION***

---

### **3.1 Introduction**

Dielectric studies of biological materials are of significant importance in revealing electrical properties of biological materials. The two-electrode and four-electrode techniques are classical methods used in impedance measurement of biological systems. The two-electrode method is widely used in the measurement of the dielectric properties due to its simple system set up and ease of application. It has been widely adopted in the measurement of cells over many decades (Mazzeo and Flewitt, 2007). However, electrode polarization is a remarkable problem in impedance and dielectric measurement of conductive materials, especially conductive biological systems. The four-electrode measurement is proposed to overcome the limitations existing in two-electrode measurement, and has achieved good outcomes since 1963 (Schwan, 1968; Grimnes and Martinsen, 2008).

In this study we focus on investigating the dispersion in cell suspensions using our measurement system. Therefore, requirements of the bandwidth of the system and the accuracy of data should be taken into consideration. The two-electrode experiment requires a simple experimental setup but produce a more complex result and corresponding data analysis, while the four-electrode experiment requires a more complex setup but leads to a simple process of data acquisition and analysis.

This chapter describes how two-electrode and four-electrode measurements were implemented and evaluated for accuracy over the required frequency range. The

purpose of this study is to review and compare these two traditional methods to choose the better method for further study of cell suspensions based on the current bioimpedance system. A brief literature review on electrode polarization is provided at the beginning of this chapter. To interpret the measurement results, a suitable model is adopted to represent the effects of electrode polarization on the results from the two-electrode measurement. A detailed discussion of the parameters of the model is presented. At the end of this chapter, a comparison of two-electrode and four-electrode techniques will be presented.

### 3.2 Principles of two-electrode and four-electrode measurements

Figure 3.1 illustrates the principles of the two-electrode and four-electrode measurements. In four-electrode measurement the voltage of the sample is detected by the inner electrodes instead of the outer electrodes. When using the four-electrode technique, it is possible to measure the impedance of the biological sample without being affected by the electrode polarization (Feder, 1968).

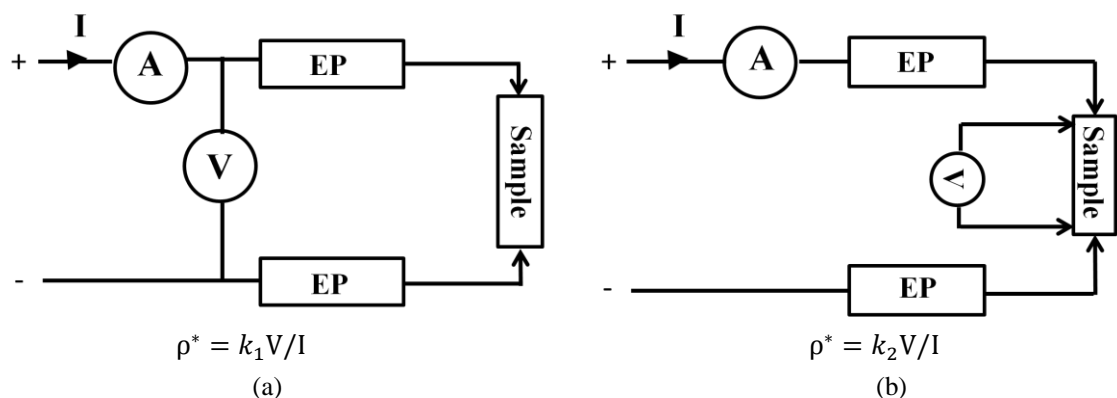


Figure 3.1 The principle of the two-electrode (a) and four-electrode (b) impedance method. EP in the figure represents the effect of the electrode polarization. In (a), both the current and the voltage are measured by the same two electrodes; in (b) the current is passed through the sample via the two outer electrodes and a potential drop across the sample is measured by the inner electrodes. The effect of electrode polarization on the results is eliminated in the four-electrode measurement. The  $k_1$  and  $k_2$  are the geometric factors relating  $V/I$  to the complex impedance.

### 3.3 Electrode polarization

#### 3.3.1 Electrode polarization and its effects in bioimpedance measurement

Electrode polarization was firstly proposed by Kohlrausch in 1898 (Kohlrausch and Holborn, 1898). This common phenomenon is observed at low frequencies and is due to the formation of charge at the interface between the electrode and electrolyte. It is the result of an unequal distribution of ions between different phases. When the metal electrode is immersed in a solution, charges will diffuse from the electrode into the solution, which produces a net charge at the surface of the electrode. As a result, ions in solution are absorbed onto the surface of the electrode and a layer forms on the surface, which is called a 'Stern' layer. Further from this layer, another diffuse layer, a Gouy-Chapman layer, forms with the ions in the solution. This model is called the Gouy-Chapman-Stern model (GCS) (Sawan, Laaziri et al., 2007). Both the layer at the surface and the diffuse layer constitute the 'double layer' (Grimnes and Martinsen, 2008).

Electrode polarization has been reported to be related to the conductivity of the electrolyte in the measurement, the properties of electrodes (Kalvoy, Johnsen et al., 2011) and frequency. Meanwhile, electrode polarization is closely dependent on the sample and current density. The study by Mirtaheri *et al* has shown that electrode polarization becomes more pronounced in highly conductive media since the ratio of electrode polarization impedance to the bulk resistance is increasing as the conductivity of the bulk increases at low frequency ( $< 10^3$  Hz) (Mirtaheri, Grimnes et al., 2005). Electrode polarization becomes more pronounced when using small electrodes (Kalvoy, Johnsen et al., 2011). In addition, electrode polarization has been reported to be related to contact area, alloy composition, surface structure, and treatment of the active electrode at low frequency, while at high frequency it relates to the electrode area geometry, and the resistivity of saline (Liu, 1985; Schwan, 1992).

The impact of electrode polarization is generally so significant that the correction for it is one of the most important steps towards successful interpretation of results from

conductive samples, especially from the most aqueous biological systems. As to measurement of cells, this common artifact would be likely to completely overshadow any contribution from  $\alpha$ -dispersion and  $\beta$ -dispersion, which has been observed in certain systems at low frequencies and is due to the presence of counter ions for  $\alpha$ - dispersion and membrane polarization for  $\beta$ -dispersion (Schwan, 1957; Raicu, Saibara et al., 1998; Raicu, Saibara et al., 1998; Peters, Hendriks et al., 2001). This leads to an overlap between contributions from electrode polarization and the biological sample, making it very difficult to distinguish between useful and spurious signals. Consequently, raw data of impedance measurements must be conveniently corrected for the electrode polarization artifacts before the dielectric parameters can be extracted.

### **3.3.2 Methods to reduce the effect of electrode polarization**

To reduce the effect of electrode polarization on the measurement of conductive samples, especially at low frequencies, a great deal of work has been proposed to alleviate or reduce the electrode polarization influence on impedance measurement. Schwan has pioneered in this field since 1950 and many papers have been published in this area (Schwan, 1966; Jaron, Schwan et al., 1968; Schwan, 1968; Schwan, 1992). Kalvoy *et al* has done a detailed summary on the efforts made by Schwan on electrode polarization (Kalvoy, Johnsen et al., 2011). The methods that have been adopted to reduce the influence of electrode polarization in different systems are summarized as follows.

First of all, the influence of electrode polarization on measurement can be alleviated by the design of the electrodes. The first principle is to use chemically inert electrodes. Platinum has been widely chosen for impedance measurement due to its chemical inertness (Schwan, 1968), and it can be processed by applying platinum black to increase the surface area, which will contribute to reducing the electrode polarization by 2-4 orders of magnitude (Schwan, 1966). Another effective and most commonly used method to reduce the effect of electrode polarisation is to measure the sample by using

the four-electrode technique (Schwan and Ferris, 1968). Alternating current passed through the sample via the two outer current electrodes and a voltage from sample is measured via two inner electrodes. More detailed information will be discussed in the comparison of the two methods later in this chapter. Some other methods are proposed to correct the results after the experimental data have been acquired, these include the distance variation technique first proposed by Fricke and Curtis (Fricke and Curtis, 1937), the substitution method proposed by Schwan (Schwan, 1963), the frequency-derivative method proposed by Raicu (Raicu, Saibara et al., 1998), increased current density by Schwan (Schwan, 1968) and theoretical modelling of electrode polarization together with data processing (Schwan, 1963).

Among these methods, both the four-electrode measurement and mathematical interpretation of electrode polarization and then subtraction of electrode polarization from the measurement are two widely adopted methods. Therefore, in this study, we adopted both the four-electrode technique and two-electrode technique combined with modelling the electrode polarization effect using an equivalent circuit and data processing. So far several electrical models have been proposed over the years to interpret the characteristics of electrode polarization in the frequency domain. More information on the development of equivalent circuit models for electrode polarization can be found in the following reviews (McAdams, Lackermeier et al., 1995; Franks, Schenker et al., 2005; Chang, Park et al., 2007).

### **Electrode polarization model**

Constant phase angle (CPA) is a non-intuitive circuit element that was discovered (or invented) while looking at the response of real-world systems. It has been applied to describe the frequency response of the electrode-electrolyte interface since it could represent the effect of electrode polarization well to the change of frequency (McAdams, Lackermeier et al., 1995; Bordi, Cametti et al., 2001; Stoneman, Kosempa et al., 2007).

This can be written as

$$Z_{CPA} = K \times (j\omega)^{-\beta} \quad (3.1)$$

where  $K$  is a constant and  $0 < \beta < 1$ .  $\beta$  is a parameter related to the nature of the electrode and the properties of its interface, it is a direct measure of the degree of the irregularity of the electrode surface. For a perfectly smooth surface,  $\beta = 1$  (pure capacitive behaviour).  $K$  depends on several factors, such as the electrical properties of the sample.

Meanwhile some charge does manage to leak across the double layer due to electrochemical reactions taking place at the interface during the measurement. Such charge leakage experiences a 'charge transfer' resistance,  $R_{ct}$  (McAdams and Jossinet, 1994; Franks, Schenker et al., 2005). Briefly, the model in this study consists of an interface capacitance represented by a constant phase angle (CPA), shunted by a charge transfer resistance,  $R_{ct}$ , in series with the solution resistance and the sample.  $Z_{CPA}$  represents the double-layer capacitance that is distorted by surface roughness effects and the parallel resistance represents faradaic charge transfer. The electrode circuit model for electrode polarization is given in Figure 3.2.

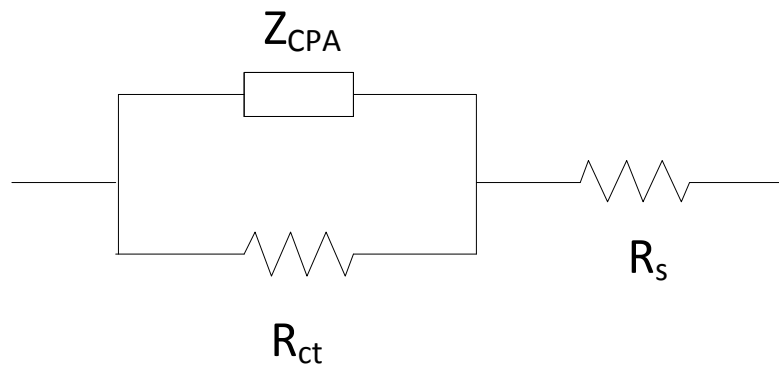


Figure 3.2 Electrical circuit model for electrode polarization.

### 3.4 Objective of this study

As introduced above, electrode polarization exerts a strong influence on the measurement results, especially for highly conductive biological materials. The

dispersion of cells might get overshadowed due to the effect of electrode polarization. In order to choose the suitable method for cell suspension, both two-electrode and four-electrode methods are adopted and analysed for further comparison to choose the most suitable method for the study. Moreover, in order to better interpret the results of the two-electrode measurement, an equivalent electrical circuit model is provided to represent the effect of electrode polarization. Thus, we measured the impedance of various saline solutions at 20 °C from 10 Hz to 10 MHz using a Solartron 1260 impedance analyser. Finally, the results of two measurement methods are compared in this study. The work is the foundation for the further study of impedance measurement and analysis of cell suspensions.

### **3.5 Material and method**

#### **3.5.1 Preparation of the electrolyte**

NaCl solution was chosen in this study since NaCl is a strong electrolyte, thus relatively stable over the period of measurement in a small volume. NaCl solutions with different conductivity were required for impedance measurement. The conductivities of solutions were measured using a conductivity meter (Hanna Instruments).

#### **3.5.2 Instrumentation setup**

In this study, a Solartron 1260 Impedance Analyser was chosen for impedance measurement of saline solutions and cell suspension. A PC was connected to the impedance analyser via a GPIB-USB cable to serve as the DAQ module; a LabVIEW programme was used to control the measurement procedures and set functional parameters. An illustration of how the system components function together is shown in Figure 3.3.

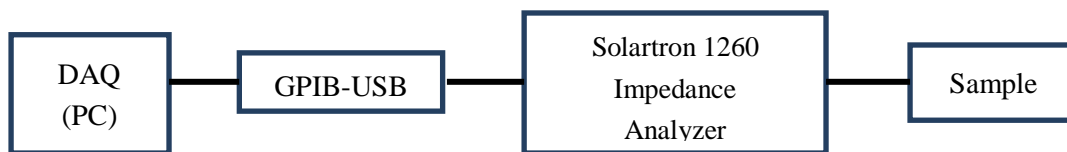
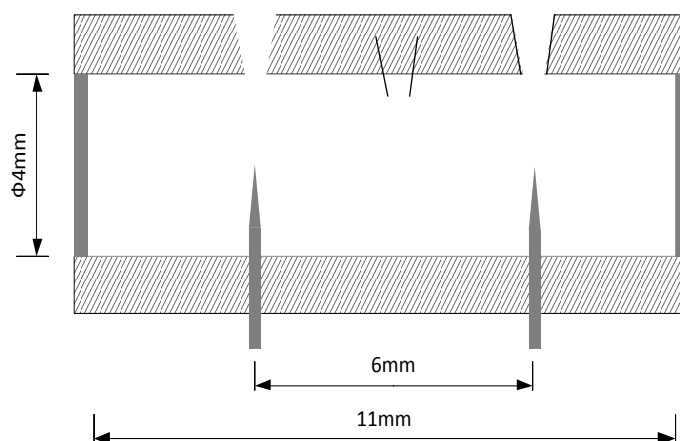
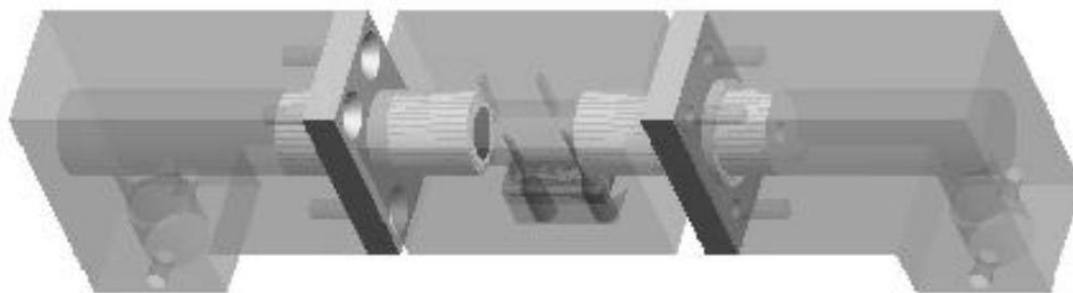


Figure 3.3 Illustration of the system components.

An impedance measurement chamber was designed and adopted for the measurement of saline and cell suspension. The structure of the chamber is shown in Figure 3.4 (Qiao, Wang et al., 2012). The prepared saline solution was injected into the chamber. To ensure the accuracy of the result, bubbles in the chambers were eliminated before the measurement. The chamber was then attached to a base unit that helped to connect the chamber to the impedance analyser. Each measurement swept between 10 Hz and 1 MHz within a period of approximately 60 seconds. Results of 30 frequencies were recorded for further analysis.



(A)



(B)

Figure 3.4 Illustration of the adopted chamber in the measurement. (A) Cross-section profile of the chamber. The chamber is 4 mm in diameter and 11 mm in length. Two stainless steel plated disc electrodes were positioned at the ends of the chamber. Another two needle electrodes were positioned 6mm apart on the bottom of chamber for voltage measurement. There are two open holes (diameter around 1 mm) on the top that were used for adding samples. (B) 3-D view of the chamber. This chamber was designed and provided by Dr. Qiao, the figures were adapted from (Qiao, 2012).

### 3.5.3 Measurement and data analysis

Both two-electrode measurement and four-electrode measurement of saline solutions were carried out on the basis of this system. An amplitude of 10 mV was chosen for the impedance measurements. Since the electrode polarization could influence the result from several Hz to MHz, therefore, the analysed frequency range was chosen from 10 Hz to 10 MHz for the comparison between the two-electrode and four-electrode technique. Frequencies below 10 Hz were not favoured since it took quite a long time to get a stable value. The solutions were measured following the same procedure. The measurement of each solution was performed 3 times to verify the repeatability of the tests. Saline solutions with conductivity detected using a conductivity meter were prepared and measured in the system introduced above. All the measurements were conducted at  $20 \pm 0.5$  °C.

In order to extract the parameters involved in electrode polarization in two-electrode measurement, the raw data of resistance and reactance for saline solutions of different conductivities were fitted to the equation derived from the electrical model (Figure 2.3) by MATLAB (Mathworks Inc.). The best-fit parameters were estimated by automatically comparing the theoretical simulations to the real data. In order to fit both the real part and imaginary part simultaneously, the real part and imaginary part of impedance were merged into a matrix. The Mean Squared Error (MSE), as given in equation 3.2, was employed to evaluate the quality of fitting. The smaller the MSE, the better the fitting quality will be. In equation 3.2,  $N$  is the number of frequency points,  $D$  is the observed data and  $D_{\text{cal}}$  is the output data after function fitting. To fit measurement results into models,  $Z_{\text{real}}$  and  $\sigma_{\text{real}}$  were used, instead of  $D$  in equation 3.2, to fit into the electrical circuit model and physical model, respectively.

$$\text{MSE} = \frac{\sum_{i=1}^N (D - D_{\text{cal}})^2}{N} \quad (3.2)$$

### **Equivalent circuit model**

To illuminate the electrode polarization effect on the measurement result, an equivalent circuit model was used for analysis (Figure 3.2). The equivalent circuit model for electrode polarization adopted in this study comprised a constant phase angle (CPA) impedance  $Z_{\text{CPA}}$  in parallel with  $R_{\text{ct}}$ . The CPA impedance is a measure of the non-faradaic impedance arising from the interface polarization, and is given by empirical equation 3.3.  $R_{\text{ct}}$  represents the charge transfer resistance. The resistance of the NaCl solution was in series with the electrode polarization model.

The corresponding equation for this circuit model is given in equation 3.4 and 3.5. The two equations could be converted to each other due to the relationship of parameter  $K$  and the capacitance of double layer,  $C_{\text{dl}}$ . Parameters involved in this model were derived by applying curve fitting with MATLAB (Mathworks Inc).

The model for electrode polarization is represented by a CPA impedance  $Z_{CPA}$  in parallel with  $R_{ct}$ . The saline solution is considered to be a pure resistance, which is shown as  $R_s$  in this figure.

$$Z_{CPA} = K \times (j\omega)^{-\beta} \quad (3.3)$$

Therefore, the impedance for the equivalent circuit model was

$$Z = \frac{K \times R_{ct}}{(j\omega)^{\beta} \times R_{ct} + K} + R_s \quad (3.4)$$

$$Z = \frac{R_{ct}}{1 + R_{ct} \times (j\omega C_{dl})^{\beta}} + R_s \quad (3.5)$$

where  $C_{dl}$  is the capacitance of the double layer and  $K = 1/(C_{dl})^{\beta}$ , which is a size dependent constant and  $0 < \beta < 1$ .  $R_{ct}$  is the resistance with that due to faradaic charge transfer and  $R_s$  represents the resistance of the saline.

## 3.6 Result and Discussion

### 3.6.1 System calibration

Before the impedance measurement of electrolyte, the system was tested with two standard resistors to check the accuracy of the system. The resistance of the two resistors was 100  $\Omega$  and 500  $\Omega$  respectively. The results presented from the impedance analyser are close to the original resistance, which indicated the accurate performance of the system, which is shown in Figure 3.5.

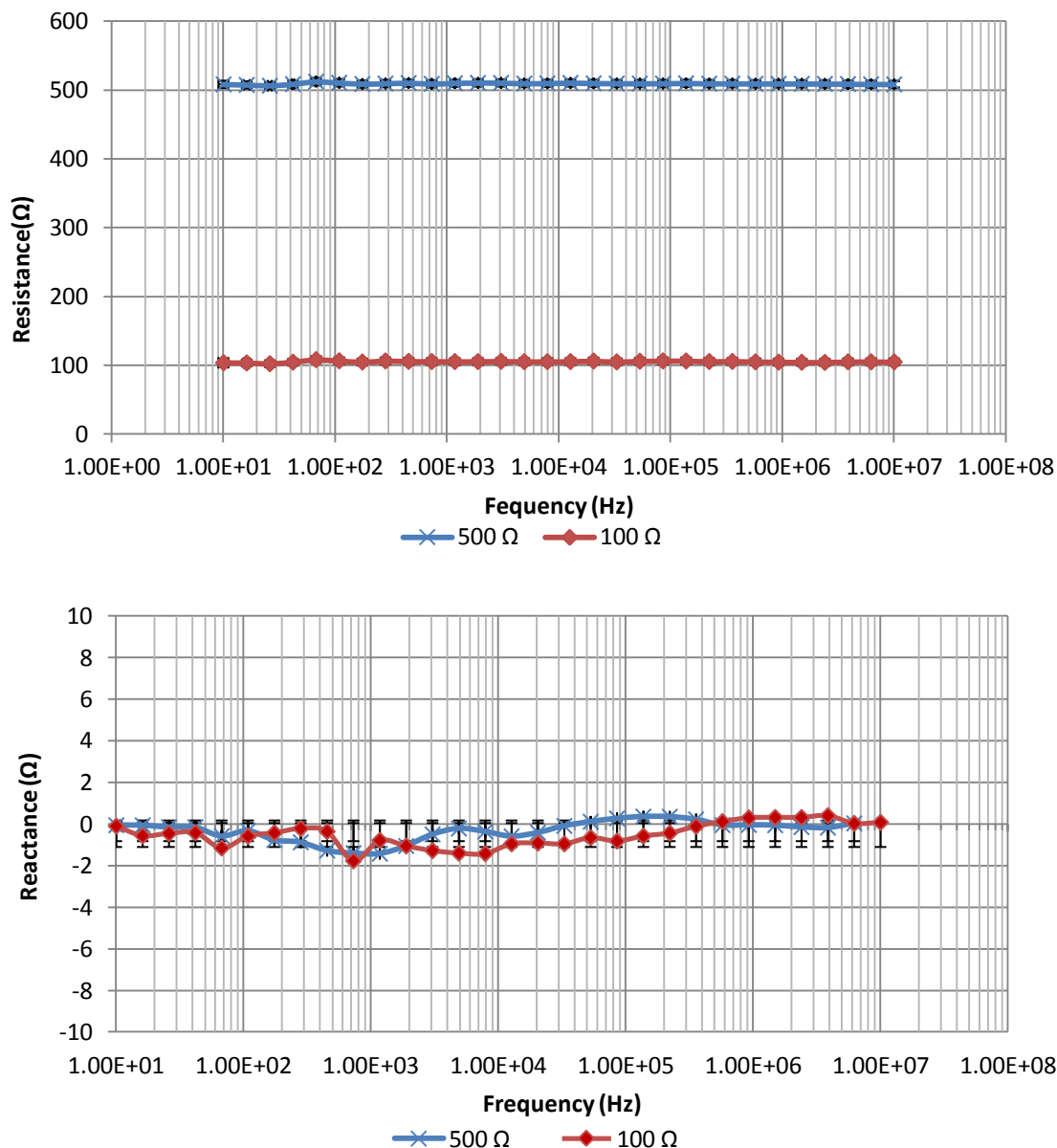


Figure 3.5 Impedance results of pure resistance. The measured impedance of two standard resistors, which were 100  $\Omega$  and 500  $\Omega$  respectively, was close to their real values. The real part of the impedance representing resistance was stable and close to 100  $\Omega$  and 500  $\Omega$  respectively along with the frequency, and the imaginary part of impedance fluctuated around 0  $\Omega$ . The results indicated the stable and accurate performance of the system.

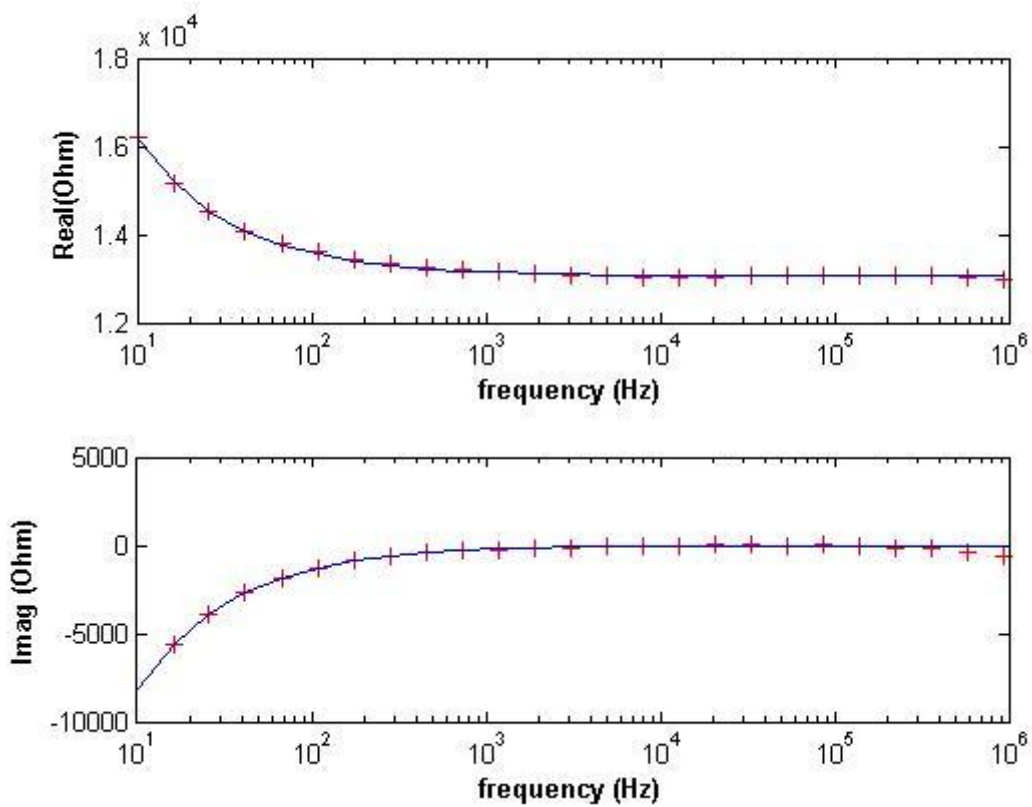
### 3.6.2 Electrical polarization

In order to investigate the electrode polarization effect on the two-electrode measurement, saline solutions with different conductivities were measured using the

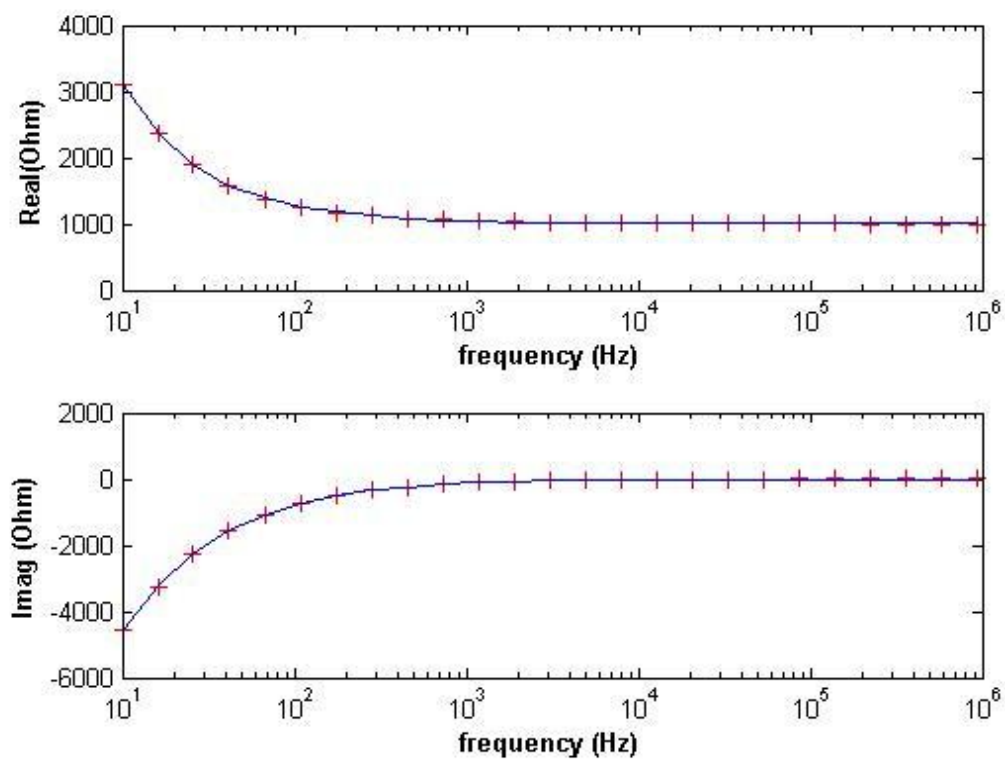
two-electrode technique. Consistent with other research, there is an apparent electrode polarization in the frequency range from 10 Hz to several kHz. Moreover, as we can see from Table 3.1, the ratio of the maximum real value to the average value of saline solution is increasing as the conductivity of saline solution increases, which verified that the effect of electrode polarization became more potent as the ion concentration of the saline solution increases. An equivalent circuit (Figure 3.2), as discussed in the review, was adopted to represent the effect of electrode polarization and the results of curve fitting are shown in Figure 3.6. It can be seen from the fitting result that the model with  $Z_{CPA}$  parallel with  $R_{ct}$  turned out to fit the data well. Parts of the fitting result of the saline in different conductivity were shown in Figure 3.6 and four parameters in the model were extracted and summarized in Table 3.2.

Table 3.1 Effect of electrode polarization on electrolyte of different conductivity

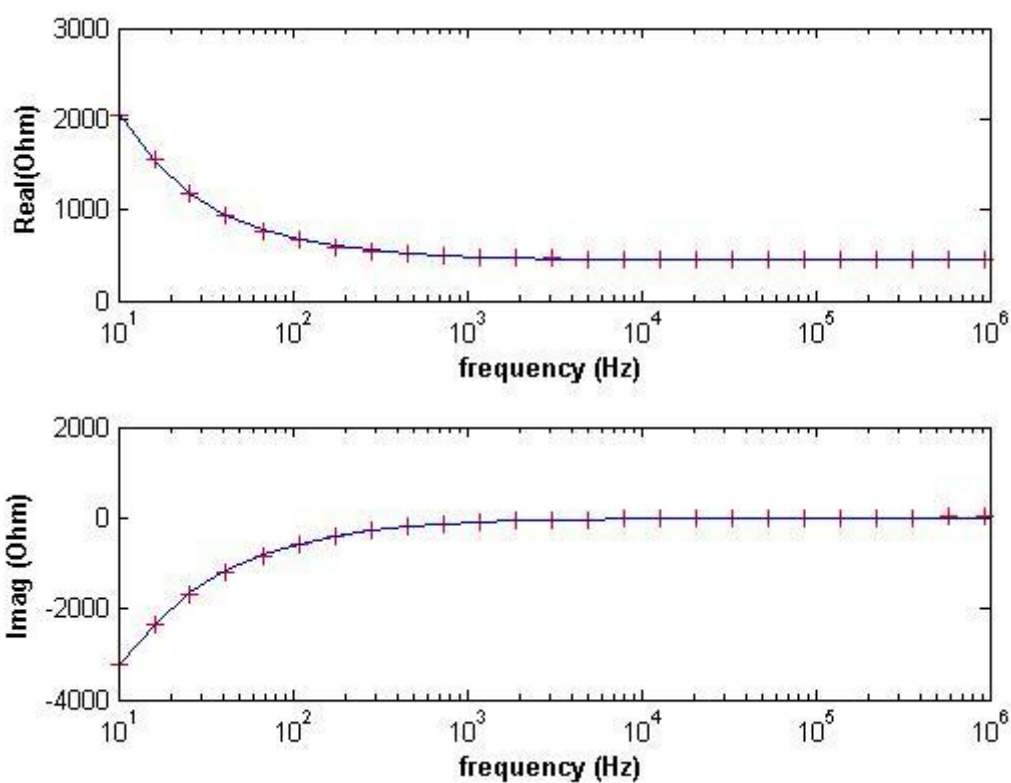
Conductivity (mS/cm)	Ratio of max resistance to average resistance
0.65	1.242
1.31	1.304
2.64	1.680
4.70	2.159
5.40	2.985
8.79	2.985
15.80	3.413
20.01	4.372



(A) 0.65 mS/cm



(B) 8.79 mS/cm



(C) 20.01 mS/cm

Figure 3.6 Part of fitting results of the saline solution with the electrical circuit model. The conductivity is 0.65 mS/cm, 8.79 mS/cm and 20.01 mS/cm respectively for (A), (B) and (C).

Table 3.2 The fitting results of parameters involved in equivalent circuit model

Conductivity (mS/cm)	Two-electrode measurement				Four-electrode measurement
	$K$ ( $\Omega$ /s)	$\beta$	$R_{ct}$ ( $\Omega$ )	$R_s$ ( $\Omega$ )	$R_s$ ( $\Omega$ )
0.65	2.15e+05	0.773	9.40e+05	1.31e+04	7.12e+03
1.31	1.09e+05	0.732	6.26e+05	6.70e+03	3.59e+03
2.64	1.33e+05	0.741	9.40e+05	3.20e+03	1.72e+03
4.70	1.31e+05	0.773	4.06e+04	1.79e+03	980
5.41	1.16e+05	0.712	1.68e+05	1.32e+03	884
8.79	1.42e+05	0.795	4.26e+04	999	556
15.80	8.64e+04	0.767	4.69e+04	578	312

In order to evaluate the fitting result with the real value, a comparison between the conductivity derived from the fitted  $R_s$  value and the measured conductivity by conductivity meter is given in Figure 3.7. The theoretical resistivity was deduced from the measured conductivity according to equation 3.6, and the fitting resistivity was deduced from the fitting result of  $R_s$  based on equation 3.7. The result from Figure 3.7 demonstrated a good agreement.

$$\rho = \frac{1}{\sigma} \quad (3.6)$$

$$\rho = \frac{R_s \times S}{L} \quad (3.7)$$

where  $S$  and  $L$  are the cross-sectional area and length of the samples.

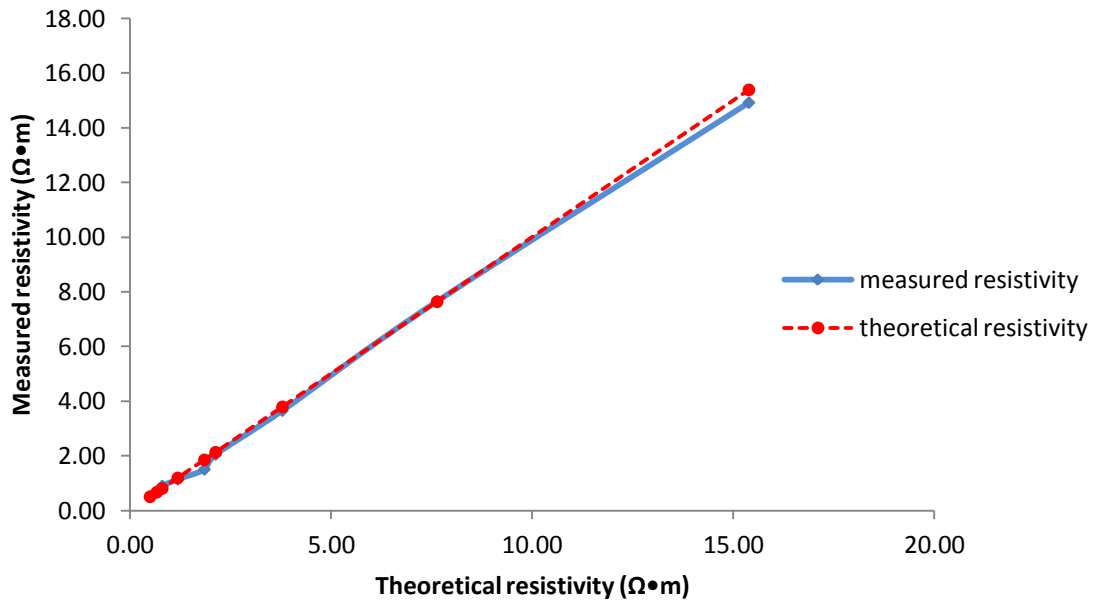


Figure 3.7 Comparison between the measured resistivity derived from the fitted  $R_s$  value and the theoretical resistivity measured using the two-electrode measurement method.

As can be observed from Table 3.2,  $\beta$  did not change very much with the conductivity; conversely in the measurement of NaCl. A similar conclusion has been derived by Stoneman (Stoneman, Kosempa et al., 2007). In the paper a method of correction for

contributions of electrode polarization to the dielectric properties of tissues is proposed. In the study, he observed that one of the parameters  $\eta$ , which is equal to  $\beta$  in our study, is only dependent on electrode properties and can thus be determined separately. While  $K$  changed significantly for different distances between the probe and the sample and from sample to sample, the exponent  $\eta$  only changed by about 2% for the gel/KCl solution system and by about 35% for the Teflon slab. Therefore, when the sample investigated contains the same electrolyte as the thin layer between the sample and electrodes, the values of  $\beta$  with respect to different samples will be the same.

Bordi *et al* (Bordi, Cametti et al., 2001) observed a similar result after the correction of electrode polarization by a constant phase angle  $Z_{CPA}$  in series with the sample admittance. The electrode polarization parameters  $\alpha$  was found to be the function of the electrolyte concentration. It was observed that parameter  $(1-\alpha)$  is independent of the ion concentration of the saline solution but related to the valence of the ions in the solution. The value of  $\alpha$ , the counterpart of  $\beta$  in this study, was approximately 0.75 for univalent ions; while for the divalent ions the value was 0.68 when stainless steel electrodes were used for the measurement.

In our study, as we can see from Table 3.2,  $\beta$  fluctuated around a constant as the conductivity of NaCl changes, which is approximately 0.76 (Figure 3.8). The result is consistent with both groups mentioned above. For our system, the steel electrode was adopted for the measurement, which is the same in the study by Bordi (Bordi, Cametti et al., 2001). The result was further confirmed since the exponent  $\beta$  we got with the NaCl solution is almost the same as that in the study by Bordi, which was approximately 0.75.

It was observed that  $K$  changed significantly for samples with different conductivities. The result was consistent with the study by Stoneman *et al* (Stoneman, Kosempa et al., 2007).  $K$  represents the magnitude of the capacitance of the electrical double layer existing at the interface of the electrode and electrolyte, which is dependent on the

property of the electrode and sample, ion concentrations of the buffer according to Gouy-Chapman-Stern model (GCS). Therefore the value of  $K$  varied from sample to sample even under the same system.

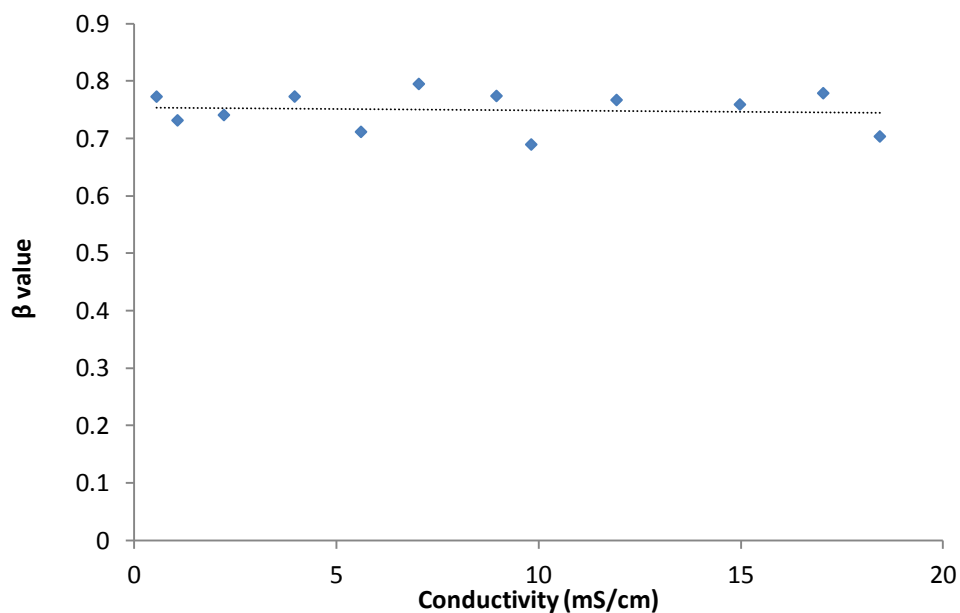


Figure 3.8 Variation of parameter  $\beta$  with the changes of saline conductivity.

As to four-electrode measurement, the theoretical resistivity  $\rho$  is calculated from the measured conductivity  $\sigma$  according to equation 3.6, and the resistivity is calculated from fitting result of  $R_s$  according to equation 3.7. The result from Figure 3.9 verified the good fitting result, which indicated that the four-electrode measurement adopted in this study could reflect the accurate impedance of samples.

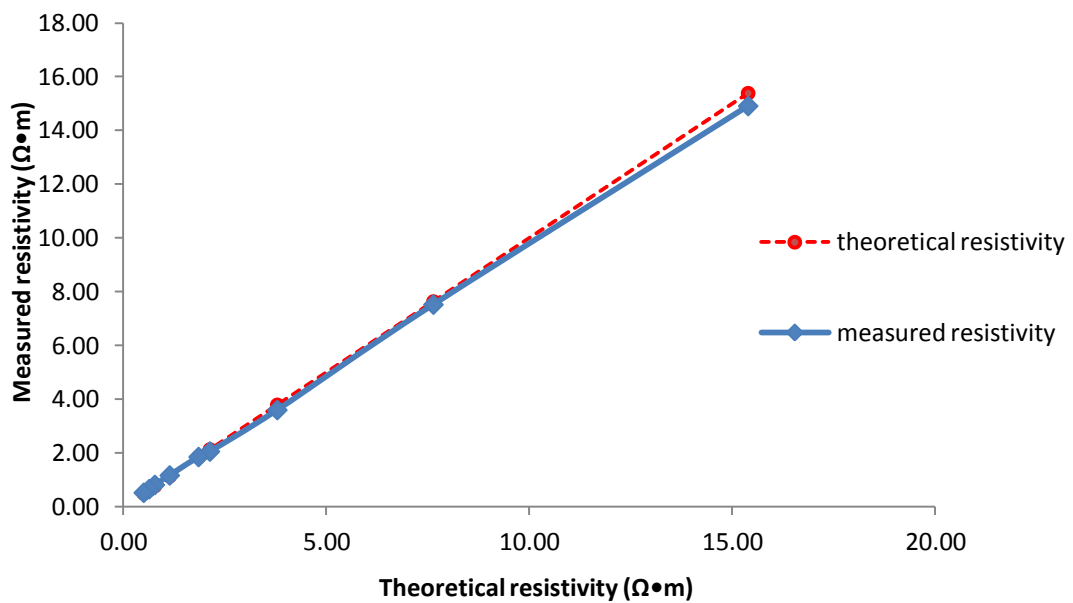


Figure 3.9 Comparison between the measured resistivity derived from fitted  $R_s$  value and the resistivity measured using the four-electrode measurement method.

### 3.6.4 Comparison of two-electrode and four-electrode measurement

#### Frequency range of measurement

In order to explore the impedance performance of cells with this system, a comparison between the performance of the two-electrode measurement and four-electrode measurement was carried out as a basic experiment for further research. As seen from Figure 3.10 and Figure 3.11, the bandwidth changes with different loadings. The higher the loading is, the narrower the bandwidth is. It is observed that the bandwidth of the four-electrode measurement was around 100 kHz when the saline with a conductivity of 0.65 mS/cm was measured by the two-electrode method. While for the four-electrode measurement, the bandwidth is around 1 MHz. For the saline solution with a conductivity of 8.96 mS/cm, the conductivity of which is similar to the buffer adopted for cell suspension measurement, the bandwidth of four-electrode measurement of the system arrives at around 1 MHz compared to the 5 MHz of two-electrode measurement.

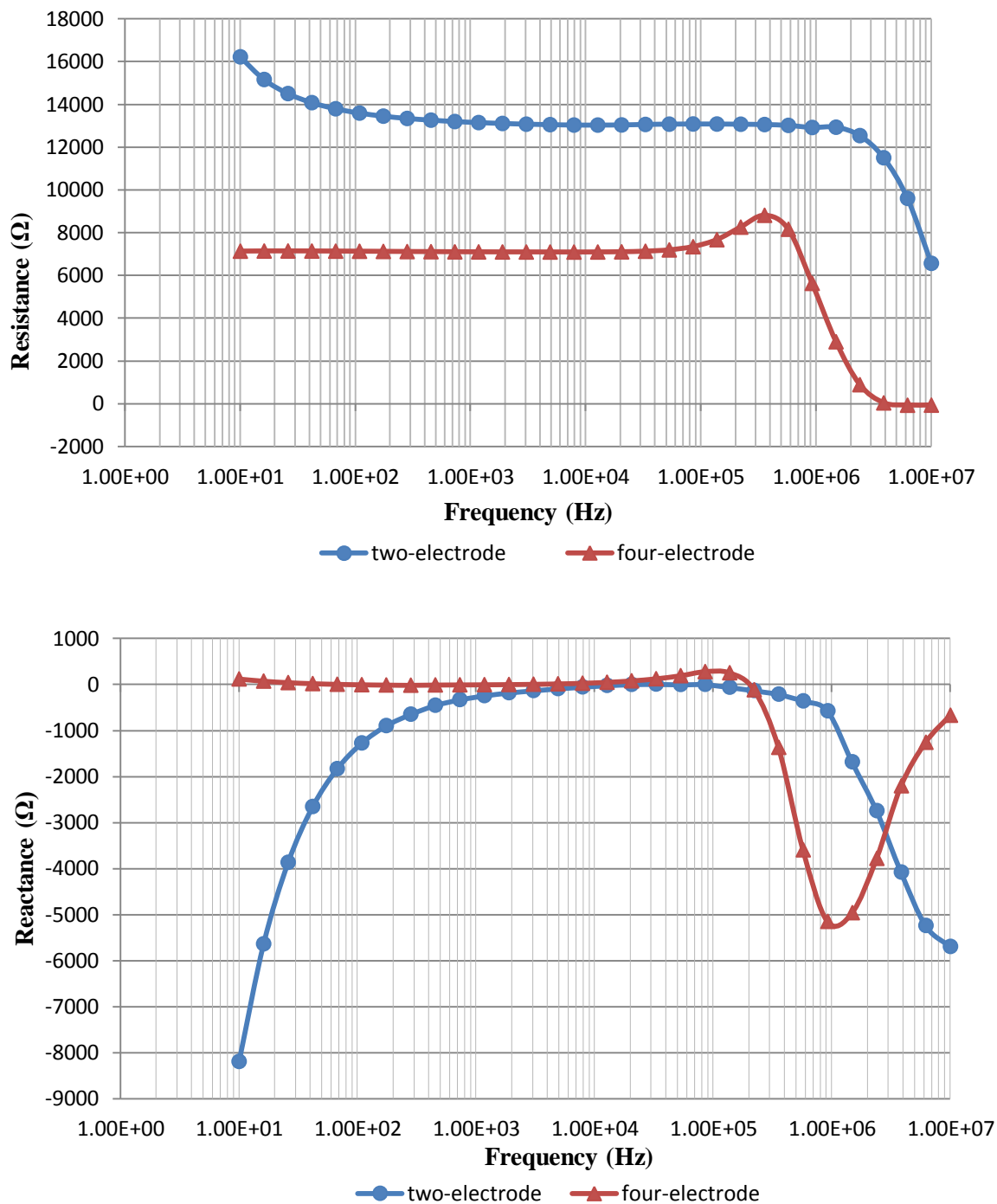


Figure 3.10 Comparison of frequency ranges of two-electrode and four-electrode measurements in conductivity of 0.65 mS/cm.

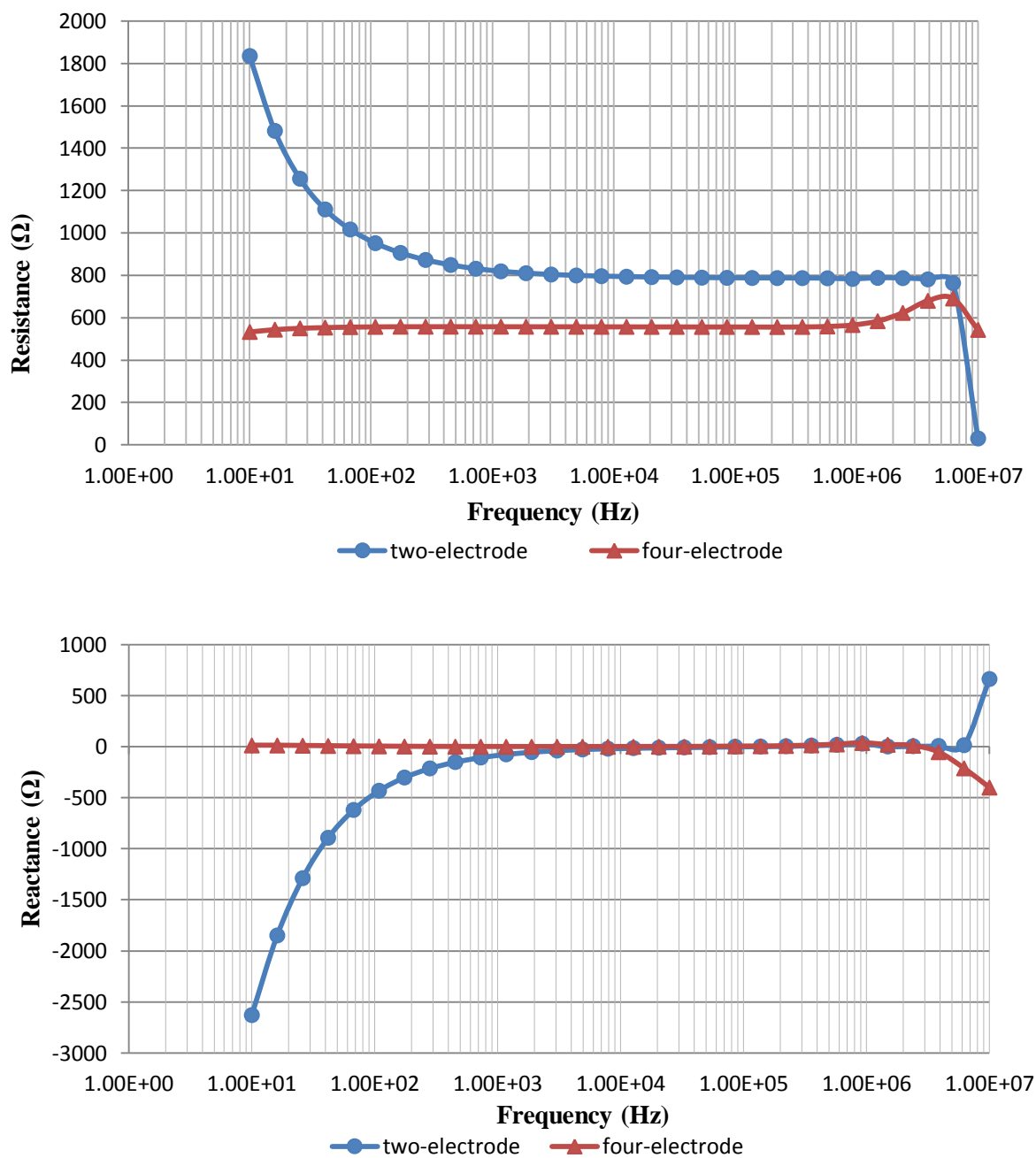


Figure 3.11 Comparison of frequency ranges of two-electrode and four-electrode measurements in conductivity of 8.79 mS/cm.

As shown in Figure 3.1, in the four-electrode measurement the potential difference on the samples are measured by different electrodes from the current stimulation electrodes. Due to the typical “stray capacitance” effect in the measurement system, the cable connected to the voltage measurement electrode and voltmeter in the four-electrode

measurement exhibits stray capacitance and thus leads to decreasing impedance and finally results in the narrower bandwidth when compared to the two-electrode measurement.

Based on the comparison provided above, it was found that both methods stand out for different reasons. The two-electrode measurement showed advantages in providing a wider bandwidth and a relatively simple setup for the system. The investigation of electrode polarization also indicated that the effect of electrode polarization could be reduced by decreasing the conductivity of the buffer. Our analysis of the electrode polarization showed that the influence of electrode polarization could be reduced to some extent by modelling its effect with CPA. However, the parameters involved were related to many factors that may lead to inaccurate interpretation of the results. Therefore, more studies on the effects of different factors affecting CPA need be conducted before yielding an accurate result.

For the four-electrode measurement, the bandwidth is comparatively narrow due to the effect of stray capacitance existing in the measurement system. Moreover, the system was relatively complicated. But the four-electrode measurement showed great advantage in the reduction of electrode polarization, thus the complicated interpretation of derived data was not required. As the previous feasibility study indicated, the characteristic frequency from the study of cell suspensions was less than 1 MHz. Moreover it was difficult for us to decrease the conductivity of the buffer solution in cell suspension due to the resolution of the current system. Therefore, the bandwidth of the system using either two-electrodes or four-electrodes could meet the requirement for the impedance measurements of cell suspensions. Due to the significant benefit of the four-electrode measurement in eliminating electrode polarization, the four-electrode measurement was adopted in this study for the further investigation of cell suspensions described in the following chapters.

### 3.7 Summary

Two-electrode and four-electrode measurements were performed and compared in order to choose the more suitable method for impedance measurement of cell suspension. The results indicated that both the two-electrode measurement and four-electrode measurement produced accurate data. The two-electrode measurement was significantly affected by electrode polarization, especially at low frequencies. A CPA model was proposed in this study to interpret the effect of electrode polarization. The results indicated this model could represent the effect of electrode polarization in this system. The investigation on the parameters involved in the model indicated that  $\beta$  was completely dependent on the nature of the electrodes, while  $K$  and  $R_{ct}$  not only depend on the properties of the electrodes, but also relate to the electrical properties of different samples and other factors.

For the valid frequency range, two-electrode measurement showed a remarkable advantage over four-electrode measurement, especially for saline of low conductivity. However, as to the saline solution of high conductivity, the valid frequency ranges for two-electrode and four-electrode measurements were similar. Based on the evaluation from data accuracy and frequency range, four-electrode measurement was chosen for further analysis of cell suspension.

## ***Chapter 4***

# ***DIFFERENTIATION OF CANCER CELLS FROM NORMAL CELLS BY BIOIMPEDANCE SPECTROSCOPY***

### **4.1 Introduction**

In Chapter 3 both two-electrode and four-electrode impedance measurements were compared in bandwidth, accuracy of performance and electrode polarization was taken into consideration in the two-electrode method of measurement. Finally, the four-electrode method was chosen in this study for cell suspension measurement. This chapter explains how the normal cell line and cancer/malignant cell line were measured using the impedance analyser, and the electrical parameters of different cells are extracted using the equivalent circuit model and the physical models respectively. The results from the two models are analysed and provide the information from different points of view. The properties of the impedance performance and parameters are compared between the normal cells and cancer cells.

This chapter investigates the differentiation of cancer cell in suspension by impedance spectroscopy. In the first part, a brief research review of the cell suspension and models adopted for the study of the dielectric properties of cell suspensions is presented. In this study both the electric circuit model and the physical model are adopted to analyse the result. Detailed discussion of impedance parameters is given based on the results of the two models. The comparison of the electrical properties of normal cell suspensions and cancer cell suspensions provides the foundation for the construction of the relationship between the biological properties and electrical properties.

## 4.2 Background of study

As stated in Chapter 2, many studies have been carried out in investigating the impedance of different biological materials with impedance spectroscopy (Pauly, Packer et al., 1960; Schwan, 1968; Pethig and Kell, 1987; Gabriel, Gabriel et al., 1996; Schwan and Takashima, 2003). Impedance spectroscopy is a promising technique delivering real-time and non-invasive cancer detection. Electrical impedance based techniques have been developed to detect cancer from the surrounding tissue by investigating the relationship between the impedance performance of tissues and their physiological status. Impedance studies on tissues have shown that the measurement of impedance and the dielectric properties of tissue can indicate the pathological status of cancer in tissues. There are many papers working on different tissues (Surowiec, Stuchly et al., 1988; Swarup, Stuchly et al., 1991; Gabriel, Lau et al., 1996; Jossinet and Schmitt, 1999; Stoneman, Kosempa et al., 2007). Although valuable information can be derived from the impedance measurement of tissues, there are many factors that may lead to inaccurate interpretation of results, including the heterogeneity of tissue and the complex composition and structure of tissues. Therefore, much attention has been given to the measurement of cells instead of tissues. It is expected to get more accurate and in-depth results from the impedance measurement of cell populations. At the cellular level, impedance spectroscopy also shows promising advantages and has been applied in many fields, including cell culture monitoring and cell differentiation (Gheorghiu and Asami, 1998; Ron, Shur et al., 2010). Most of the current applications focus on the detection of changes in the quantity of cells and the change of impedance is attributed to the changes of cell numbers in these applications. Also a few studies focus on the impedance changes due to the difference in cell nature (Han and Frazier, 2006; Han, Yang et al., 2007).

### 4.2.1 Dielectric properties of cell suspensions

Cell suspension has always been one of the most important subjects for impedance research in the past few decades and a large number of studies have been presented by

researchers. As addressed in Chapter 2, cell membrane is a lipid bilayer containing a variety of proteins and is regarded as a non- or low- conducting shell. A biological cell is considered to be a heterogeneous system since it consists of cell membrane and cytoplasm. If the cytoplasm is assumed to be a homogeneous phase, the ‘single-shell’ model could be used to represent the electrical model of the cell that contains a conducting sphere covered by an insulating thin shell (Asami, 2002). When cells are diluted with a medium of different conductivity, there are interfaces where materials of different properties contact each other in this heterogeneous system. Therefore interfacial polarization occurs due to the build-up of charges on the different interfaces (Grimnes and Martinsen, 2008). As stated in Chapter 2, at least three dispersions occur in biological systems over a wide range of frequencies, which are characterised as  $\alpha$ -,  $\beta$ -,  $\gamma$ - dispersion respectively. The cell suspensions show dielectric relaxation in the radio frequency range due to the interfacial polarization. The dielectric relaxation due to interfacial polarization provides information on the heterogeneous structure and the electrical properties of the constituent components using an appropriate theory.

The equivalent, homogeneous complex permittivity for a dielectric model consisting of spheres covered with shells was first proposed by Maxwell (Maxwell, 1873) who laid an important foundation for the development of the later theories for a heterogeneous systems. There are two major models that are widely accepted and adopted in the analysis of the electrical properties of cell suspensions. In 1960 Pauly and Schwan (Pauly, Packer et al., 1960) derived a complete expression to calculate the dielectric constant and the conductivity of the suspensions based on the basic theory proposed by Maxwell, which is termed the Pauly–Schwan (P-S) theory. The research investigated the electrical properties of the mitochondrial membrane in the suspension system containing mitochondria separated from rat liver and with the theory and equations established by Pauly and Schwan, the membrane capacitance of the cell was established to be  $0.5 \mu\text{F}/\text{cm}^2$  to  $0.6 \mu\text{F}/\text{cm}^2$ . Based on the P-S theory, in 1979 Hanai *et al* presented a theoretical formula for analysis of the dielectric behaviour of the concentrated suspensions of spherical particles covered with a shell phase. This theory is termed the

Hanai-Asami- Koizumi (H-A-K) theory. Both of the equations have been widely adopted to evaluate the parameters of cells including the capacitance of the cell membrane, the conductivity of the intracellular plasma and the volume fraction of the cell suspension.

The models are based on the Maxwell mixture theory of inhomogeneous dielectrics and Cole-Cole models. (Cole and Cole, 1941; Pauly, Packer et al., 1960). The Maxwell mixture theory describes the dielectric behaviour of colloidal particles in suspension that relates the complex permittivity of the suspension to the complex permittivity of the particle, the suspending medium and the volume fraction (Sun and Morgan). The Cole-Cole model is a relaxation model that was used to represent the dispersion and absorption of a considerable number of liquid and dielectrics. The equations for two theories are given as follows from equation 4.1 to 4.4. Both theories are given in the forms of permittivity and conductivity respectively (Qiao, 2012).

The suspension system was treated as a tri-phase system and analysed as a mathematic situation in which a suspension of spherical particles with permittivity  $\epsilon_i$  and conductivity  $\sigma_i$  surrounded by a membrane shell suspended in a medium with permittivity  $\epsilon_2$  and conductivity  $\sigma_2$ . The cell membrane conductance was negligible compared to that of the intracellular and extracellular fluids.

$$\epsilon^* = \epsilon_2 \frac{1+2pf_{CM}}{1-pf_{CM}} \quad (4.1)$$

$$f_{CM} = \frac{\epsilon_c - \epsilon_2}{\epsilon_c + 2\epsilon_2} \quad (4.2)$$

$$\sigma^*(\omega) = \sigma_\infty + \frac{(\sigma_0 - \sigma_\infty)}{1 + (-j\omega\tau)^{1-\alpha}} \quad (4.3)$$

$$\varepsilon^*(\omega) = \varepsilon_\infty + \frac{\varepsilon_0 - \varepsilon_\infty}{1 + (j\omega\tau)^{1-\alpha}} \quad (4.4)$$

where

$\varepsilon^*$  = permittivity of suspension;

$\varepsilon_2$  = permittivity of medium;

$\varepsilon_c$  = permittivity of cells;

$p$  = the volume fraction;

$\tau$  = relaxation time (s); which is related to the characteristic frequency  $f_c$  according to the relationship  $\tau = 1/2\pi f_c$ .

$\sigma_0$  = conductivity of cell suspension at low frequency;

$\sigma_\infty$  = conductivity of cell suspension at high frequency;

$\sigma$  = conductivity of the suspension;

$\varepsilon_0$  = permittivity of cell suspension at low frequency;

$\varepsilon_\infty$  = permittivity of cell suspension at high frequency;

$\alpha$  = dispersion coefficient,  $0 < \alpha < 1$ ;

$\omega = 2\pi f$ .

#### Pauly-Schwan's model

The relationship between the electrical parameters of cell suspensions is described by the P-S theory and parameters from the dispersion equations are presented by the following equations 4.5 to 4.8 according to the results derived from equation 4.1 to 4.4 (Schwan, 1957; Pauly, Packer et al., 1960; Qiao, Wang et al., 2012). The cells in suspension were assumed to be spheroid. At high frequency,  $\sigma_c(\omega)$  could be assumed to be  $\sigma_i$ , therefore, equation 4.5 can be converted into equation 4.7, while at low frequency,  $\sigma_c(\omega)$  could be assumed to be 0 due to the high resistance of cell membrane, therefore, equation 4.5 can be converted into equation 4.6.

$$\frac{\sigma(\omega) - \sigma_2}{\sigma(\omega) + 2\sigma_2} = \frac{p(\sigma_c(\omega) - \sigma_2)}{\sigma_c(\omega) + 2\sigma_2} \quad (4.5)$$

$$\sigma_0 = \sigma_2 \frac{1-p}{1+\frac{p}{2}} \quad (4.6)$$

$$\sigma_\infty = \sigma_2 \frac{1+2p \frac{\sigma_i - \sigma_2}{\sigma_i + 2\sigma_2}}{1-p \frac{\sigma_i - \sigma_2}{\sigma_i + 2\sigma_2}} \quad (4.7)$$

$$\tau = rC \frac{\sigma_i + 2\sigma_2}{2\sigma_i \sigma_2} \quad (4.8)$$

where

$\sigma_i$  = intracellular conductivity of cell suspension;

$\sigma_2$  = conductivity of outside medium;

$\sigma_c$  = conductivity of cells;

$p$  = volume fraction of cell in suspension;

$C$  = capacitance of cell suspension;

$r$  = radius of cells in suspension.

Pauly-Schwan theory provides a method to obtain the electrical parameters of cell suspensions including  $\sigma_c$ ,  $\sigma_i$ ,  $C$ ,  $f_c$ . The limitation of this model is that the membrane conductance is neglected and the volume fraction of the cell suspension is limited to 0.3 since a nonlinear response was predicted by this theory once the cell volume fraction goes beyond this limit (Pauly, Packer et al., 1960).

#### Hanai-Asami-Koizumi's model

The Hanai-Asami-Koizumi model is proposed to overcome the calculation of the system with higher volume fraction. A second set of expressions describing the electrical performance of cell suspension, especially in high concentration suspensions was proposed by Hanai *et al* in 1979 (Hanai, Asami et al., 1979). The cells in suspension were assumed to be spheroid. The relation of dielectric properties of the

cells with those measured parameters from suspension is given as follows from equation 4.9 to 4.12 (Hanai, Asami et al., 1979; Qiao, 2012). At high frequency,  $\sigma_c(\omega)$  could be assumed to be  $\sigma_i$ , therefore, equation 4.9 can be converted into equation 4.10 while at low frequency,  $\sigma_c(\omega)$  could be assumed to be 0, therefore, equation 4.9 can be converted into equation 4.11.

$$1 - p = \left( \frac{\sigma(\omega) - \sigma_c(\omega)}{\sigma_2 - \sigma_c(\omega)} \right) \left( \frac{\sigma_2}{\sigma(\omega)} \right)^{1/3} \quad (4.9)$$

$$1 - p = \left( \frac{\sigma_\infty - \sigma_i}{\sigma_2 - \sigma_i} \right) \left( \frac{\sigma_2}{\sigma_\infty} \right)^{1/3} \quad (4.10)$$

$$p = 1 - (\sigma_0 / \sigma_2)^{2/3} \quad (4.11)$$

$$C = \frac{2\varepsilon_v \varepsilon_0 \sigma_2 - \sigma_0 \varepsilon_2}{3r \sigma_2 - \sigma_0} \quad (4.12)$$

where

$\sigma_i$  = intracellular conductivity of cell suspension;

$\sigma_2$  = conductivity of outside medium;

$\sigma_c$  = conductivity of cells;

$C$  = capacitance of cell suspension;

$\sigma_0$  = conductivity of cell suspension at low frequency;

$\sigma_\infty$  = conductivity of cell suspension at high frequency;

$p$  = volume fraction of cell in suspension;

$r$  = radius of cells in suspension.

$\varepsilon_i$  = permittivity of intracellular fluid;

$\varepsilon_v$  = permittivity of vacuum.

$\varepsilon_0$  = permittivity of cell suspension at low frequency;

$\varepsilon_2$  = permittivity of outside medium.

When the volume fraction of cell suspension is higher than 0.3, the cell suspension system can be analysed with Hanai-Asami-Koizumi model as shown from equations 4.9

to 4.12. All parameters including cell volume fraction  $p$ ,  $\sigma_c$ ,  $C$ ,  $\varepsilon_i$  can be calculated with the above equations.

Although both two theories could be used for extracting electrical parameters of cell suspension system, the applicability of the equations should be well examined before the application. The P-S theory is restricted by the volume fraction and used in the case of a single dispersion. Only when the volume fraction is less than 0.3 does the result from the theoretical calculation match the real value well. The H-A-K theory is suitable for a high volume fraction up to 0.8 and it can be applied to a system with several dispersions. Irimajiri *et al.* adopted the Pauly-Schwann and Hanai-Asami-Koizumi models to investigate the electrical properties of rat leukemia cell suspensions from 10 kHz to 500 MHz (Irimajiri, Asami et al., 1987). The result demonstrated that the overall value derived from the Pauly-Schwann model is higher than that from the other model. The volume fraction calculated was 0.668 from the Pauly-Schwann model compared to 0.604 from the Hanai-Asami-Koizumi model. Kaneko examined the applicability of mixture equations in the study of dielectric analysis of sheep erythrocyte ghost (Kaneko, Asami et al., 1991). The two models were compared in different volume fraction systems. Since the capacitance of cell suspensions is the intrinsic parameter of ghosts and is not related to the change in volume fraction, the comparison of capacitance derived from the two models confirmed that the H-A-K equation is applicable to a wider range of volume fraction than the P-S equation. The internal conductivity was in good agreement with external conductivity at a volume fraction up to 0.7 when the H-A-K equations are employed, while the P-S equation can support a good match when the volume fraction is less than 0.3. Therefore, the volume fraction is a key factor requiring consideration when choosing the theory in the study. When the volume fraction is less than 0.3, both P-S and H-A-K theories can be adopted while the H-A-K will give results closer to the real values when the volume fraction is more than 0.3.

Since it was first introduced by Fricke who calculated the membrane capacitance of red blood cells (Fricke and Morse, 1925), the physical model has been widely applied in the

dielectric study of biological materials. More attention has been drawn in this field after the proposal of the classic Pauly-Schwan theory and the improved theory of the Hanai-Asami-Koizumi model. So far the physical models have been applied in studies of the electrical properties of erythrocyte suspensions (Bordi, Cametti et al., 2002), cell cycle monitoring (Gheorghiu and Asami, 1998), dielectric dispersions of lymphocytes and erythrocytes (Asami, Takahashi et al., 1989), electrical properties of protoplast suspensions (Zhao, Bai et al., 2006).

### **4.3 Objectives of this study**

As introduced above, the physical model for analysing dielectric properties of biological materials has been adopted by many researchers. In this study, the cell suspensions of normal cells and cancer cells are investigated using an impedance analyser. The physical model is proposed for the identification of cancerous cells in cell suspensions for the first time. The parameters involved in the physical model are extracted by mathematically fitting the data to equations with MATLAB. By comparing the results of various parameters, we expect to identify the cancerous cells from the normal cells in cell suspensions. Another model applied in this study is the electrical model that represents the cell as different electrical components. The various parameters of the electrical model are derived from the data fitting. By comparing the results from two models, a feasible means used to discriminate the cancer cell from normal cells is expected to be achieved.

## **4.4 Materials and Methods**

### **4.4.1 Cell culture**

Human breast cancer cell line MCF-7 (CLS-Cell lines service, Germany) and human breast tissue cell line MCF-10A (American Type Culture Collection, USA) were cultured in DMEM/F12 media (Invitrogen, UK) supplemented with 10% heat-

inactivated fetal bovine serum, 100 IU/mL penicillin, 100 µg/mL streptomycin, 2 mM L-glutamine (Invitrogen, UK), 20 ng/mL epidermal growth factor (Invitrogen, UK), 500 ng/mL hydrocortisone (Sigma, UK), 100 ng/mL cholera toxin (Sigma, UK) and 10 µg/mL bovine insulin (Sigma, UK). The cells were cultured in an incubator at 37 °C with 5% CO<sub>2</sub>. The cell culture and cell viability measurements were carried out in The School of Life Sciences of the University of Sussex by Wei Duan. The protocols for cell culture and cell viability measurements were provided by Wei Duan with slight modifications.

#### **4.4.2 Cell suspension preparation and viability measurement**

To keep the osmotic pressure of cells in suspension, the cell suspension was diluted with an isotonic medium that was composed of 8.5% (w/v) sucrose (Fisher, UK) and 0.3% (w/v) dextrose (Fisher, UK) (Gascoyne, Wang et al., 1997). In order to adjust the conductivity of the isotonic medium to 9 mS/cm, phosphate buffered saline (PBS) (Invitrogen, UK) was adopted (Labeed, Coley et al., 2006) in the sample preparation. All the operations were conducted at 37 °C.

To prepare the cell suspensions, cells were digested and suspended with cell culture medium. Then the cell samples were washed twice with isotonic medium. The viability was calculated according to the results of Trypan Blue (Sigma, UK) staining. A haemocytometer was adopted for cell counting. To compare the viability changes before and after the impedance measurement, cell count was recorded.

#### **4.4.3 Volume fraction measurement**

The volume fraction of cells suspension was measured using Packed Cell Volume counting tubes (PCV tubes) (Sigma-Aldrich, UK). The tube was centrifuged at 5000 rpm for 1 minute. The protocol for volume fraction measurements was provided by Wei Duan with slight modifications.

## 4.5 Impedance measurement system

Both the chamber and the impedance system are the same as that used in the electrode polarization study of Chapter 3. The cell suspension was added to the chamber and air bubbles were eliminated. The chamber was vibrated to ensure an even distribution of cells within the suspension. Then the chamber was connected to the impedance analyser for impedance measurement. The measurement swept between 1 kHz and 25 MHz. There were 20 points of frequencies recorded within a period of approximately 50 seconds.

The two cell lines (MCF-10A, MCF-7) were measured according to the same procedure. To avoid the influence from temperature on the measured impedance all measurements were undertaken in an incubator with a controlled temperature of 37 °C. The measurement of each cell line was performed three times to ensure the repeatability of the tests.

### 4.5.1 Data analysis

Both the real (resistance,  $R$ ) and imaginary (reactance,  $X$ ) components of the cell suspension shown in equation 4.13 were calibrated with the results of the buffer solution that is the buffer adopted to suspend the cells. The resistance was calibrated according to equation 4.14 and the reactance was calibrated by equation 4.15. From these measurements the conductivity ( $\sigma$ ) was evaluated using equation 4.16 (Qiao, 2012).

$$Z(\omega) = R(\omega) + j \cdot X(\omega) \quad (4.13)$$

$$R_{cal}(\omega) = R_{mea}(\omega) \times \frac{R_{ref}}{R_{ref}(\omega)} \quad (4.14)$$

$$X_{cal}(\omega) = X_{mea}(\omega) - (0 - X_{ref}(\omega)) \quad (4.15)$$

$$\sigma(\omega) = \frac{1}{R_{cal}(\omega) \times S} \quad (4.16)$$

where  $R_{cal}$  is the resistance after calibration and  $R_{mea}$  is the measured resistance.  $X_{cal}$  is the reactance after calibration and  $X_{mea}$  is the measured reactance.

In order to extract the electrical parameters of cells, the results from cell suspensions were extracted and analysed from equivalent circuit models and physical models using MATLAB (Mathworks Inc.). The same fitting principle as in Chapter 3 was employed to evaluate the quality of fitting in this study. The smaller MSE, the better the fitting quality will be.

### **Physical model**

In both the P-S and H-A-K models, the suspension system was assumed to obey the Cole-Cole equation (Cole and Cole, 1941). The conductivity form of Cole-Cole equation is shown in equation 4.17. According to the relationship in equation 4.18 (Cole and Cole, 1941), and the relationship between  $\omega$ ,  $\tau$  and  $f$ :  $\omega = 2\pi f$  and  $\tau = \frac{1}{2\pi f_c}$ , the real part of  $\sigma^*(\omega)$  is shown in equation 4.19, which was derived from equation 4.18 (Qiao, 2012).

$$\sigma^*(\omega) = \sigma_{\infty} + \frac{(\sigma_0 - \sigma_{\infty})}{1 + (-j\omega\tau)^{1-\alpha}} + j\omega\epsilon_0\epsilon_{\infty} \quad (4.17)$$

$$j^{\alpha} = \cos\left(\frac{\alpha\pi}{2}\right) + j\sin\left(\frac{\alpha\pi}{2}\right) \quad (4.18)$$

$$\sigma'(\omega) = \sigma_{\infty} + (\sigma_0 - \sigma_{\infty}) \frac{1 + (f/f_c)^{1-\alpha} \sin(\alpha\pi/2)}{1 + (f/f_c)^{2(1-\alpha)} + 2(f/f_c)^{1-\alpha} \sin(\alpha\pi/2)} \quad (4.19)$$

where

$\sigma^*$  = the complex conductivity of the suspension;

$\sigma_{\infty}$  = the conductivity of the suspension at high frequency;

$\sigma_0$  = conductivity of the suspension at low frequency;

$\sigma'$  = the real part of  $\sigma^*$ ;

$\alpha$  = the dispersion coefficient ( $0 < \alpha < 1$ );

$\epsilon_0$  = the permittivity of vacuum;

$\epsilon_\infty$  = the permittivity of the suspension at high frequency.

According to the Pauly- Schwan model (1960), the conductivity of suspension at low and high conductivity can be referred to equation 4.6 and 4.7. According to equation 4.20, the conductivity of the suspension in high frequency range is related to the buffer conductivity,  $\sigma_2$ , cytoplasm conductivity,  $\sigma_i$ , and cell volume fraction,  $p$ . Finally, the membrane capacitance,  $C^*$ , can be derived from equation 4.8 (Qiao, Wang et al., 2012).

$$\sigma_\infty = \sigma_2 \left( 1 + 3p \frac{\sigma_i - \sigma_2}{\sigma_i + 2\sigma_2} \right) \quad (4.20)$$

where

$\sigma_\infty$  = the conductivity of the suspension at high frequency;

$p$  = the volume fraction;

$\sigma_2$  = the conductivity of buffer;

$\sigma_i$  = the intracellular conductivity.

### **Electrical circuit**

As stated in Chapter 2, an equivalent circuit was proposed to illustrate the electrical properties of the cell suspension (Figure 2.3). It consists of the resistance of the buffer,  $R_e$ , and the membrane capacitance,  $C_m$  in series with the intracellular resistance,  $R_i$ .

In general, at low frequencies, the current is prevented from flowing through the intracellular space due to the high resistance of the cell membrane. Therefore, the impedance of the cell suspension in the ideal case equals the extracellular resistance,  $R_e$ . In the high frequency range, the membrane becomes more conducting, thus the current can pass through the intracellular resistance. As a result, the impedance of cell suspension is decreasing and approaching to the parallel value of  $R_e$  and  $R_i$ .

## 4.6 Result and discussion

### 4.6.1 System errors

Before the measurement of cell suspension, the system was tested with two standard electrolytes (Hanna Instruments, USA). Both electrolytes of high conductivity and low conductivity were used for conductivity meter calibration to check the stability and accuracy of the system. The conductivities of the standard solutions were 1.413 mS/cm and 12.88 mS/cm at 25 °C respectively and the corresponding conductivities from 16 °C to 37 °C were also provided.

In this study, the experiment was conducted at 37°C, the conductivities of both electrolyte solutions at 37°C are provided by Hanna Instruments, which are 13.62 mS/cm and 1.494 mS/cm respectively. The measured conductivity was calculated from the average resistance measured by the impedance analyser according to equation 4.17. As shown in Figure 4.1, the calculated conductivities for both solutions were 14.28 mS/cm and 1.554 mS/cm respectively. According to equation 4.21, the systematic error for both the high conductivity solution and low conductivity solution was calculated to be 4.85% and 4.02% respectively. Since the conductivities of medium and cell suspension in this study fall into the prescribed conductivity range, the average error of the system in the impedance measurement of cell suspension was assumed to fall into the range of 4.02% to 4.90%.

$$\text{system error} = \frac{|\sigma_{\text{measured}} - \sigma_{\text{real}}|}{\sigma_{\text{real}}} \times 100\% \quad (4.21)$$

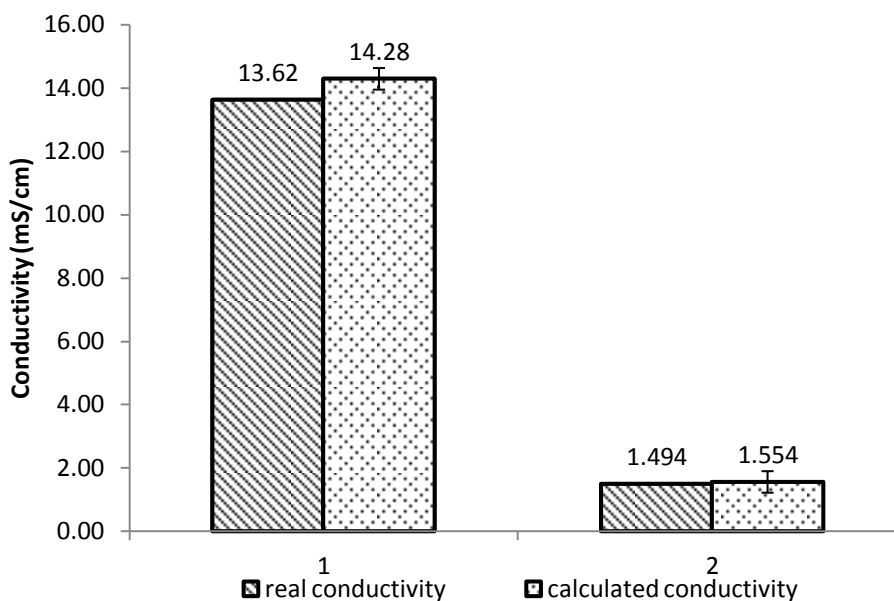


Figure 4.1 Accuracy performance of the measurement system. Both the standard conductivities and measured conductivities of two standard solutions were shown. Observed from the left columns, the calculated conductivity was 14.28 mS/cm compared to the real conductivity 13.62 mS/cm. For the solution of low conductivity, the calculated conductivity was 1.494 mS/cm compared to the real conductivity 1.554 mS/cm.

#### 4.6.2 Environmental parameters control and their effects on measurement results

Since the cell parameters could be affected by the variations of the outside environment, it was critical for us to control the conditions of the experiment to maintain the normal status of the cells. In this study, the cell suspensions were diluted with an isotonic solution, which will keep equal the osmotic pressure of the cells. Moreover, all the experiments were conducted at 37 °C, which was the same as the culture temperature of the two cell lines. The similarity of the environment to the culture system helps to provide more accurate information on the electrical properties of the cell suspension. To certify that the cells could survive for the period of preparation and measurement, the cell viability in suspension was assessed continuously for 3 hours in the isotonic buffer used for impedance measurement. The results indicated that both cell lines showed a minor drop in the viability for this period (less than 10%) (data not shown). In addition,

the volume fractions of two cell suspensions were kept at 0.20 (Table 4.2), which located in the valid range of both P-S and H-A-K models. All those parameters were controlled in the measurement to maintain the normal status for cells in suspension.

To verify that the cells could survive the measurement process, the viability of the cells was tested before and after impedance measurements. As shown in Table 4.1, the viability of MCF-10A and MCF-7 before the measurement was similar: 96.60% and 99.42% respectively. However, there were minor decreases of the cell viability of both MCF-10A and MCF-7 after the measurement. The rate of the cell viability changes was calculated to be 8.24% and 6.62% to MCF-10A and MCF-7 respectively. All the measurements for each cell line took less than 1 min. Since the voltage adopted in the measurements was 10 mV, the heat arising from electric current to the cell suspension system amounted to  $5.46 \times 10^{-6}$  J according to the Joule's law. This physical law expressed the relationship between the heat generated by the current flowing through a conductor,  $Q=V^2t/R$ , where  $Q$  is the heat generated by a constant voltage  $V$  flowing through a conductor of electrical resistance  $R$ , for a time  $t$ . Therefore we assume that the heat derived from current is negligible in the study.

Knowledge of the cell size distribution is necessary to interpret the experimental results. The measurement of the cell diameter in suspension showed that the cell diameter was symmetrically distributed and their average diameters were calculated to be  $17.71 \mu\text{m}$  and  $17.09 \mu\text{m}$  for MCF-10A and MCF-7 respectively (Qiao, Wang et al., 2012). The diameters of most cells are located close to the average diameter.

Table 4.1 Viability of cells before and after impedance measurement

	MCF-10A	MCF-7
Before measurement (%)	96.60 $\pm$ 1.12	99.42 $\pm$ 0.67
After measurement (%)	88.64 $\pm$ 0.85	92.84 $\pm$ 1.06
Changes after measurement (%)	8.24	6.62

Table 4.2 Volume fraction of cell suspension and diameter of cells

	Volume fraction
MCF-10A	0.20
MCF-7	0.20

(Acknowledge to Wei Duan for her support in cell diameter measurement.)

### 4.6.3 Impedance of cell suspension

To reduce the system error, the impedance of MCF-10A and MCF-7 was calibrated with the impedance result of phosphate buffered saline (PBS). The calibrated result is shown in Figure 4.2. As shown in the figure, the two cell suspensions showed a similar trend with the increase of frequency. At low frequency ( $< 10$  kHz), the impedance of MCF-10A and MCF-7 was relatively stable with resistance around  $650 \Omega$  and  $600 \Omega$  and reactance close to  $0 \Omega$  respectively. The impedance experienced a decline along with the rise of frequency, which is due to the increasing susceptance of the cell membrane. At high frequency ( $>1$  MHz) the impedance of both cell suspensions tends to reach another stable level for the reason that cell membrane was fully conducting at high frequency. It can be seen that the dielectric dispersion occurred over the frequency range of 10 kHz to 2 MHz, which is the so-called  $\beta$ -dispersion resulting from the polarization of the cell membrane.

It was observed that the impedances of the two cell lines were stable for three repeated measurements, which was confirmed by the low standard deviation evaluated. The difference between the two cell lines amounted to approximately 8% over the frequencies, which was more significant than the system errors. Therefore, it was reasonable to claim that normal cells and cancer cells in suspension could be differentiated by impedance spectroscopy. Although MCF-10A and MCF-7 shared a similar trend over the frequency range, it is observed that the overall impedance of MCF-10A is higher than that of MCF-7. This conclusion is consistent with results

from many other studies of the impedance of cancer cell/tissue; it is lower than the normal cell/tissue (Surowiec, Stuchly et al., 1988; Chauveau, Hamzaoui et al., 1999; Zou and Guo, 2003). The result indicates that it is feasible to differentiate MCF-10A and MCF-7 suspensions with impedance spectroscopy.

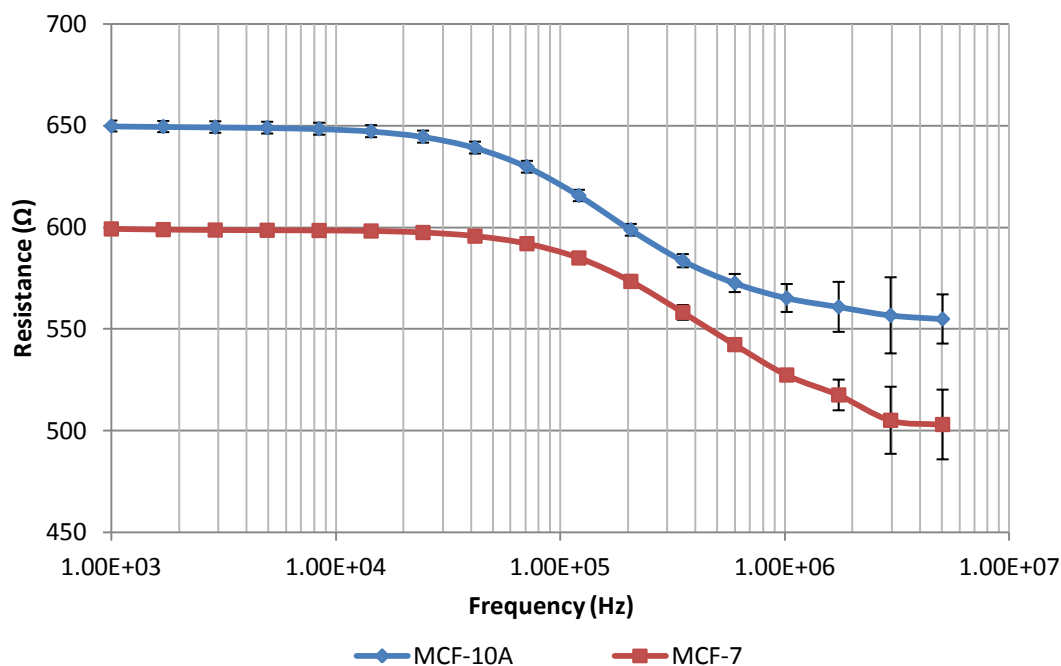


Figure 4.2 The resistance of MCF-10A and MCF-7 cell suspensions.

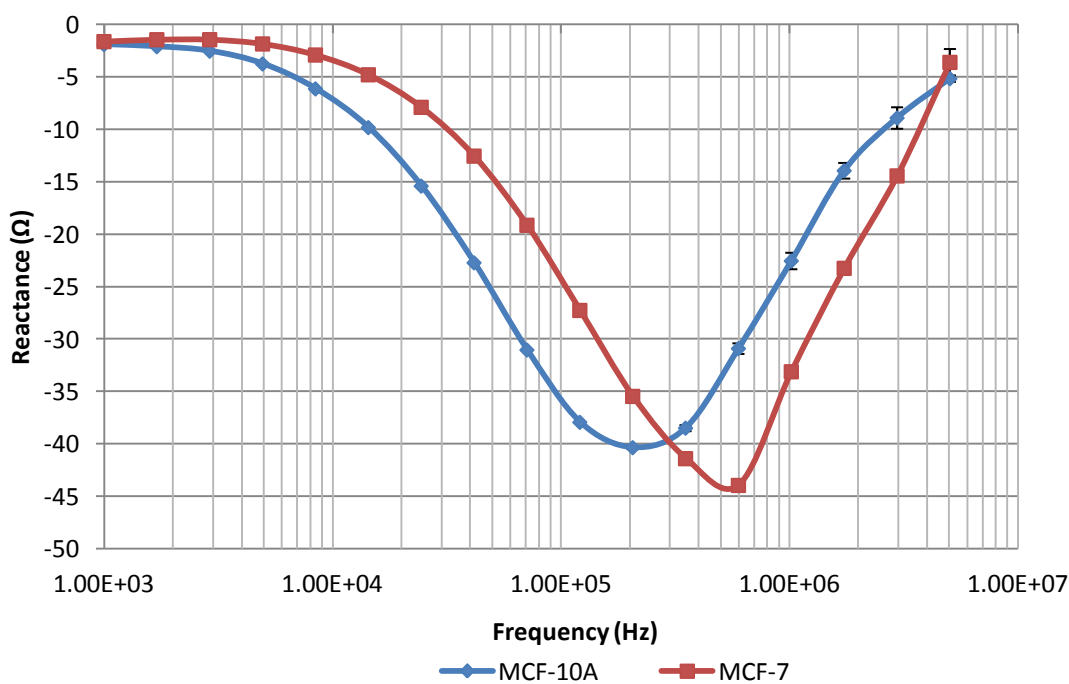


Figure 4.3 The reactance of MCF-10A and MCF-7 cell suspensions.

#### 4.6.4 Electric equivalent model

According to the result in Chapter 3, the four-electrode measurement was adopted to reduce the influence of electrode polarization. The equivalent model presented in this study comprises a resistor,  $R_i$ , in series with a capacitor,  $C_m$ , that represents the intracellular plasma and membrane respectively, in parallel with another resistance,  $R_e$ , for extracellular fluid, see Figure 2.3. The overall impedance of this system  $Z$  of the model is given in equation 4.22 and the converted form of it is shown in equation 4.23. The minimum value and the characteristic frequency corresponding to minimum reactance can be deduced from the imaginary part of  $Z$  and the result of it is shown in equation 4.24 and 4.25.

$$Z = \frac{1}{\frac{1}{R_e} + \frac{1}{R_i + \frac{1}{j\omega C_m}}} \quad (4.22)$$

$$Z = \frac{R_e \times (j\omega C_m \times R_i + 1)}{j\omega C_m \times (R_i + R_e) + 1} \quad (4.23)$$

$$Z_{img\_min} = -\frac{R_e^2}{2(R_e + R_i)} \quad (4.24)$$

$$f_c = \frac{1}{2\pi C_m (R_e + R_i)} \quad (4.25)$$

The parameters in this model were extracted by mathematical fitting with equation 4.23. As shown in Figure 4.4 and Figure 4.5, both MCF-7 and MCF-10A cell suspensions fit well with the proposed model. The fitting result of both cell suspensions was shown in Table 4.3. It can be seen that MCF-7 has lower extracellular resistance, intracellular resistance and membrane capacitance compared to MCF-10A. The extracellular resistance of MCF-10A and MCF-7 are 647  $\Omega$  and 597  $\Omega$  respectively, which is lower than the buffer resistance 973  $\Omega$ . The reason might be because the decreasing cross-section area due to the cells in the suspension when the current passed through the sample.

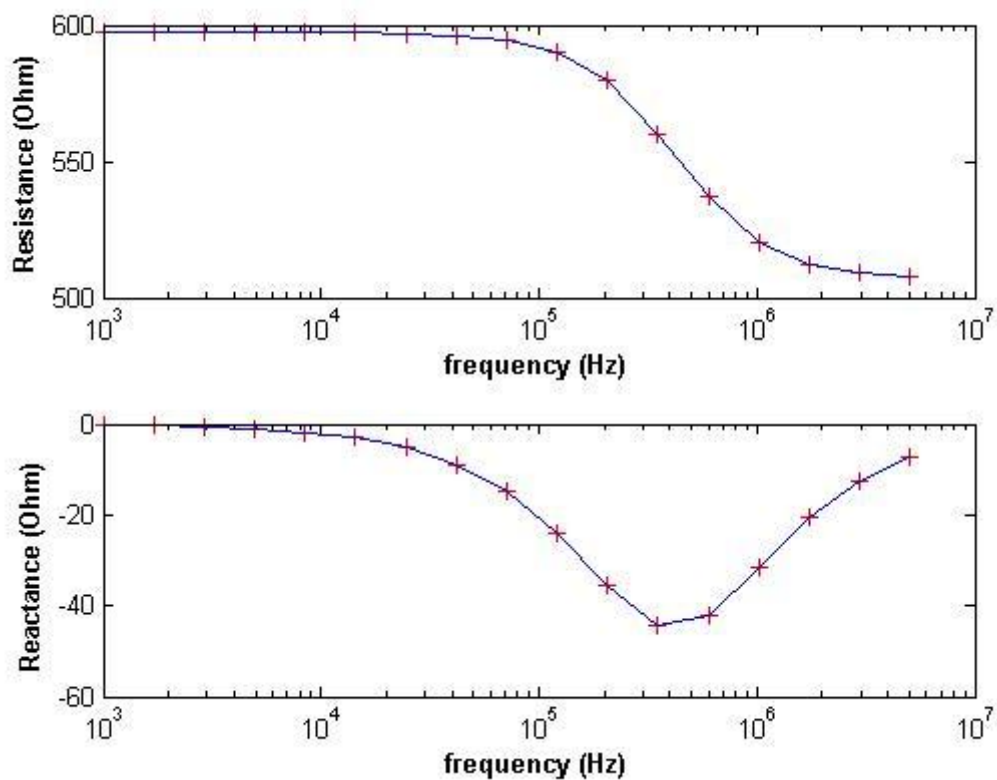


Figure 4.4 Fitting result of MCF-7 cell suspension with equivalent circuit model. The original values of the parameters were calculated from equation 4.24 and 4.25 with the assumption that the electrical currents are restricted to the extracellular fluid at low frequency.

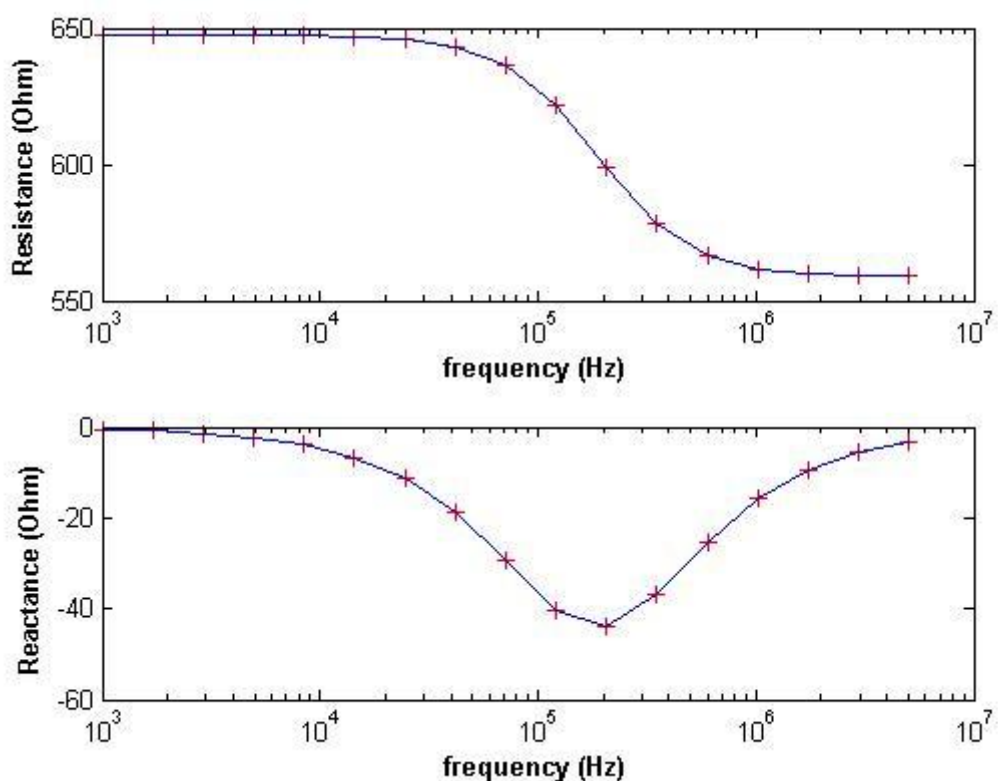


Figure 4.5 Fitting result of MCF-10A cell suspension with equivalent circuit model. The original values of the parameters were calculated from equation 4.24 and 4.25 with the assumption that the electrical currents are restricted in extracellular fluid at low frequency.

Table 4.3 Electrical parameters of cell suspensions from equivalent circuit model

	$R_e$ ( $\Omega$ )	$R_i$ ( $\Omega$ )	$C_m$ (nF)	MSE
MCF-10A	647	4.09e+03	0.18	23.449
MCF-7	597	3.38e+03	0.096	19.94

#### 4.6.5 Results from the physical model

Figure 4.6 and Figure 4.7 illustrate the fitting results of MCF-10A and MCF-7 by MATLAB. The low MSE values demonstrate the good quality of data fitting with equation 4.19. As seen from the figures, the conductivity of the both suspensions shares a similar trend as the frequency increases. At low frequency, the conductivity stays at a

low level and tends to be stable. As the frequency increases, the conductivity increase gradually and reaches another stable high value. The conductivity of MCF-10A at low frequency amounts to around 7.35 mS/cm. It is lower than that of MCF-7 which is around 8 mS/cm at low frequency. It is observed that the overall conductivity of MCF-7 is higher than that of MCF-10A. Apparently the two cell suspensions can be differentiated from their conductivity performance.

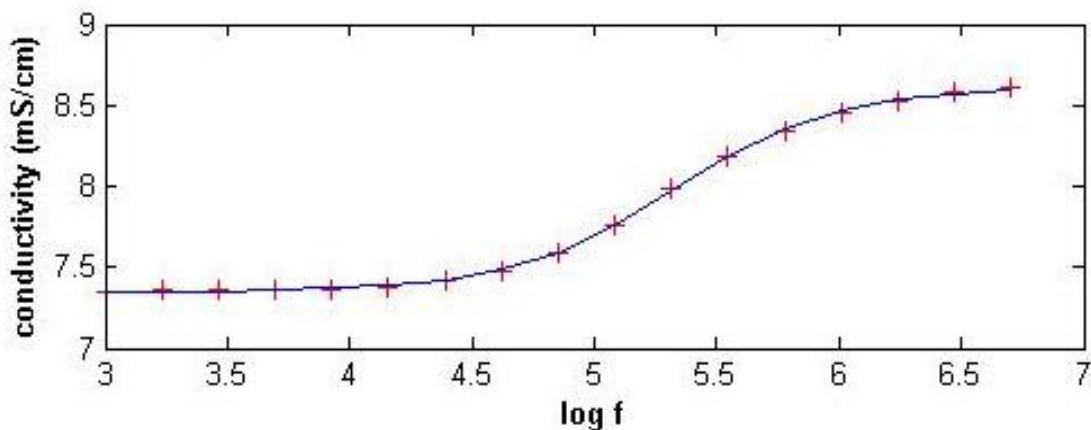


Figure 4.6 Physical model fitting of MCF-10A cells. Note: the conductivity of cell suspension is calculated from the corresponding resistance of suspension with the equation:  $\sigma = l/(R \times S)$ .

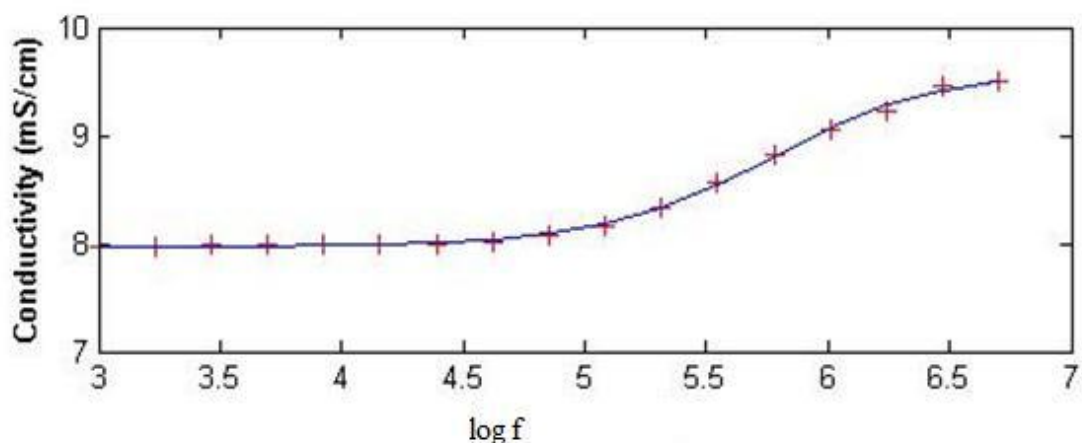


Figure 4.7 Physical model fitting of MCF-7 cells. Note: the conductivity of cell suspension is calculated from the corresponding resistance of suspension with the equation:  $\sigma = l/(R \times S)$ .

Four parameters involved in equation 4.19 are extracted from the fitting and the results are summarized in Table 4.4. As shown in the table, there are substantial differences

between the two cell lines. The conductivity at low frequency of MCF-7, which amounts to 9.63 mS/cm is higher than that of MCF-10A, which is 8.62 mS/cm. It is also observed that the characteristic frequency fitted from the physical model is quite close to the value read from Figure 4.2 and 4.3 which is around 200 kHz and 555 kHz respectively.

Table 4.4 Fitting result of electrical parameters of cell suspension

	$\sigma_{\infty}$ (mS/cm)	$\sigma_0$ (mS/cm)	$f_c$ (kHz)	$\alpha$	MSE
MCF-10A	8.62	7.34	214.6	0.173	9.75e-05
MCF-7	9.63	7.96	589.0	0.194	3.37e-04

According to the Pauly-Schwan model, other parameters including intracellular conductivity  $\sigma_i$  and cell membrane capacitance  $C_m$  could be derived from equation 4.8 and 4.20 based on the parameters derived from mathematic fitting. The summary of the results is shown in Table 4.5. As seen from the table, the intracellular conductivity of MCF-7 arrives at 12.55 mS/cm, which is substantially higher when compared to MCF-10A. While the capacitance of the cell membrane of MCF-7 is lower than that of MCF-10A. The value of capacitance is of the same order of magnitude as many published results. In 1925 the capacitance of red blood cell membrane was first estimated by Fricke to be 0.81 nF/cm<sup>2</sup>, which is the first publication on the membrane capacitance (Fricke and Morse, 1925). Evidence could be found in the study by Han who also revealed the capacitance of MCF-10A and MCF-7, which were 1.94  $\mu$ F/cm<sup>2</sup> and 1.63  $\mu$ F/cm<sup>2</sup> respectively (Han, Yang et al., 2007).

Table 4.5 Other electrical parameters of cells derived from physical model

	d (μm)	σ <sub>i</sub> (mS/cm)	C <sub>m</sub> (μF/cm <sup>2</sup> )
MCF-10A	17.71	7.24	2.16
MCF-7	17.09	12.55	1.13

Note: d is the average diameter of cell of interest.

The total volume fraction can be calculated with equation 4.6 after  $\sigma_0$  has been derived. The calculated volume fraction was 0.131 for MCF-10A and 0.08 for MCF-7 respectively, which is significantly lower than the measured volume fraction evaluated from Packed Cell Volume counting tubes. The possible reason for this might be the incomplete packing degree, which is related to both external medium and the centrifugal speed applied.

Another related point to consider is that the conductivity of cells  $\sigma_c$  at low frequency is regarded to be approximately equal to 0. However, it is possible that the cell might be not completely insulated at low frequency. According to equation 4.26, which is converted from equation 4.5, the volume fraction  $p$  could be derived from the equation below. If  $\sigma_c > 0$  in this equation, the value of  $\frac{\sigma_c(\omega)+2\sigma_2}{\sigma_2-\sigma_c(\omega)}$  will increase as  $\sigma_c$  increases (Qiao, Wang et al., 2012).

$$p = \frac{(\sigma(\omega)-\sigma_2) \times (\sigma_c(\omega)+2\sigma_2)}{(\sigma(\omega)+2\sigma_2) \times (\sigma_c(\omega)-\sigma_2)} \quad (4.26)$$

#### 4.6.6 Applications of two models

The electric circuit model was used to interpret the overall electrical properties of a cell suspension. As shown in the result, there is an apparent difference between MCF-10A and MCF-7 in intracellular resistance and membrane capacitance, which indicates that the electrical model can be used as a method to differentiate different cell lines.

However, the variations of electrical parameters involved in the circuit are related to the parameters of the cell suspension itself, such as the cell size, the cell number in suspension. Therefore, the parameters derived from the electrical circuit could be regarded as an absolute value for the cell suspension, thus only the electrical properties of cell suspensions other than cell itself could be evaluated with this method. However, the electric circuit model has no restrictions on the cell morphology. The model will take effect if the cell could be treated as a combination of electrical components.

As to the physical model, the cell suspension is treated as a two-phase system in this study, which includes cells and buffer. The parameters derived from the physical model give the information on the cell itself since both the cell size and the volume fraction are taken into consideration in the study. As shown in the result, both the intracellular conductivity and membrane capacitance could be derived from the physical model. Apparent differences found between the parameters of MCF-10A and MCF-7 also indicates that the physical model could be a feasible method for cell differentiation.

Moreover, the results from the physical model could serve as cell constant since the parameters derived from the physical model are not dependent on the dimensions of the cell itself, such as cell size and cell numbers. In this study, cell membrane capacitance was  $2.16 \mu\text{F}/\text{cm}^2$  for MCF-10A and  $1.13 \mu\text{F}/\text{cm}^2$  for MCF-7. The cell membrane capacitance of the red cell was reported to be  $0.81 \mu\text{F}/\text{cm}^2$  (Fricke and Morse, 1925) and the membrane capacitance of rat basophilic leukemia was reported to be approximately  $1 \mu\text{F}/\text{cm}^2$  up to  $5 \mu\text{F}/\text{cm}^2$  (Irimajiri, Asami et al., 1987). Results on cell membrane capacitance in this study are of the same order of magnitude as the previous studies. Another study by Han reported the cell membrane capacitance of MCF-10A and MCF-7 to be  $1.94 \pm 0.14$  and  $1.86 \pm 0.11 \mu\text{F}/\text{cm}^2$  respectively with the single-cell impedance spectroscopy. The capacitances of MCF-10 from the two studies are close to each other while the capacitance of MCF-7 in cell suspension is lower than that of the single cell impedance study. The reason for this might be that the membrane value in the cell suspensions used gives general information on cell populations, which will mask

the individual difference between cells. However, the value evaluated from single cells might relate to the properties of each cell.

#### 4.7 Summary

In this study, breast cancer cells and normal breast cells in suspension were investigated by impedance spectroscopy. The results indicated there were significant differences between cancer cell and normal cell. It is verified that two cell lines in suspension can be distinguished by impedance spectroscopy. The overall impedance of breast cancer cell line MCF-7 is lower than normal cell line MCF-10A.

Both an electrical model and a physical model were adopted for further analysis of impedance parameters. Differences in the electrical parameters were observed from the two models. The results from the physical model provided the differences between cells themselves, including the intracellular conductivity and cell membrane capacitance, while the results from electrical model provided general information including intracellular resistance and cell capacitance, which are dependent on cell numbers, cell size and other parameters.

## **Chapter 5**

# **RELATIONSHIP BETWEEN ELECTRICAL AND BIOLOGICAL PROPERTIES OF CELLS**

### **5.1 Introduction**

In Chapter 4 the electrical parameters of normal cells (MCF-10A) and cancer cells (MCF-7) were derived from both an electrical circuit model and a physical model. Both the quantity-related parameters (extracellular resistance  $R_e$ , intracellular resistance  $R_i$  and membrane capacitance  $C_m$ ) and the cell constant (intracellular conductivity,  $\sigma_i$  and membrane capacitance,  $C$ ) were extracted from two models. In this chapter we focus on an investigation into the biological properties of two cell lines. By analysing and comparing the features of MCF-10A and MCF-7 we expect to build the relationship between electrical parameters from models and biological properties existing in the cells themselves. The results will help to provide evidence for the applications in cancer identification and cell differentiation by impedance spectroscopy.

#### **5.1.1 Changes of the electrical parameters in normal cells and cancer cells**

The comparison of cancer and normal tissue electrical properties was made as early as 1926 in which significant differences in capacitance were found between malignant tissue and normal tissue. The potential for these electrical differences to be used in cancer detection was subsequently investigated, many studies *in vitro* and *in vivo* have been completed (Surowiec, Stuchly et al., 1988; Morimoto, Kimura et al., 1993; Jossinet, 1996; Chauveau, Hamzaoui et al., 1999). In 1988 Surowiec *et al* studied the conductive and dielectric properties of freshly-excised ductal and lobular carcinomas *in vitro* over the frequency range from 20 kHz to 100 MHz (Surowiec, Stuchly et al.,

1988). The result demonstrated that tumour had increased capacitance and conductance and thus decreased impedance compared to normal tissue. The comparison of the dielectric properties of MCA1 fibrosarcoma by Swarup indicated there was a significant difference at various stages of development as measured at frequencies below 10 MHz (Swarup, Stuchly et al., 1991). Jossinet studied the impedance of six groups of breast tissue over a frequency range of 488 Hz to 1 MHz (Jossinet, 1996; Jossinet and Schmitt, 1999). The impedance spectra were obtained for 120 samples obtained from 64 patients, with the sample groups divided into three types of normal breast tissue, two types of benign tissue, and carcinoma. Obvious differences were observed in the shape and location of the various impedance loci in the resistance and reactance plane. Several parameters were found to distinguish the carcinoma samples from the rest of the samples. Chauveau *et al* have also investigated the bioimpedance parameters of normal and pathological tissues *ex vivo* over the frequency range from 10 kHz to 10 MHz (Chauveau, Hamzaoui et al., 1999). An electrical circuit model that includes a constant phase element, the extracellular resistance, the intracellular resistance, and the membrane capacitance was adopted and all parameters were calculated from the measurements. The author attempted to find two parameters that allow cancerous tissues to be differentiated from normal tissues and those with fibrocystic changes.

Several research groups have reported *in vivo* breast tumor diagnosis systems based on electrical impedance measurements (Morimoto, Kimura et al., 1993; Osterman, Kerner et al., 2000). Morimoto *et al* measured the electrical impedance of breast tumors *in vivo* (Morimoto, Kimura et al., 1993). Parameters including extracellular resistance, the intracellular resistance, and the membrane capacitance were calculated based on the measured complex impedance and a model circuit. Their studies concluded that there are statistically significant differences between pathological and normal tissue. Moreover, the study claimed that both intracellular resistance and extracellular resistance of malignant tissue were higher than those of normal tissue while the membrane capacitance of cancer tissue was lower than that of normal tissue.

There is no consensus established on the difference of electrical parameters in cancer tissue and normal tissue, including intracellular conductivity and membrane capacitance. However, agreement has been achieved as to the changes of the impedance. The impedance of cancer tissue is significantly lower than that of normal tissue.

As to the electrical parameters at the cell level, significant changes could be found between the normal cells and cancer cells in suspension in our study (Table 5.1). Compared to MCF-10A, the impedance of MCF-7 is lower, which is in agreement with the conclusion from other studies. As seen from table 5.1, the intracellular conductivity is significantly lower in normal cells than in cancer cells while the membrane capacitance is substantially higher in normal cells than in cancer cells. The parameters of intracellular resistance and capacitance show the same trend. Moreover, the results from our study are in agreement with the membrane capacitance calculated from impedance derived from single cell measurement of breast cells in different stages by Han (Han, Yang et al., 2007). The capacitance was  $1.94 \pm 0.14$ ,  $1.86 \pm 0.11$   $\mu\text{F}/\text{cm}^2$  for MCF-10A and MCF-7 respectively.

Table 5.1 Electrical parameters comparison of MCF-10A and MCF-7 in this study

	Intracellular conductivity $\sigma_i$ (mS/cm)	Membrane capacitance $C$ ( $\mu\text{F}/\text{cm}^2$ )	Extracellular resistance $R_e$ ( $\Omega$ )	Intracellular resistance $R_i$ ( $\Omega$ )	Membrane capacitance $C_m$ (nF)
Normal cell (MCF-10A)	7.24	2.16	647	4.09e+03	0.18
Cancer cell (MCF-7)	12.55	1.13	597	3.38e+03	0.096

## 5.2 Objectives of this study

In this chapter the biological properties of the two cell lines are investigated from various aspects. Based on the conclusion derived from impedance measurement and

analysis of electrical parameters, the possible relationships between biological and electrical properties are proposed. Together with the conclusions from other studies, the possible factors related to the electrical parameters are summarized. The conclusion of this chapter will help to provide evidence for future work in cancer detection of impedance based techniques.

### **5.3 Material and method**

#### **5.3.1 Transmission electron microscopy (TEM) observation of cells**

In order to get the biological features of different cells, two cell suspensions before and after impedance measurement were observed. The TEM experiments were carried out in School of Life Sciences with guidance from Dr. Julian R. Thorpe.

The samples experienced five preparation procedures before the observation including fixation, dehydration, embedding, block trimming and sectioning, and uranyl acetate staining. The samples were primarily fixed for 4 hours at 4 °C in 25% glutaraldehyde in 0.1 M buffer (pH 7.4) and gently mixed. After primary fixation the cells were washed repeatedly with culture medium and subjected to secondary fixation with 1% osmium tetroxide in the dark at room temperature for two hours followed by repeated washing with distilled water. After fixation, the samples were dehydrated in ethanol in 50%, 75% and 100% for 20min each time. The dehydrated samples were suspended in propylene oxide for 2×20 minutes at 4 °C, followed by treatment with a 1:1 mixture of propylene oxide (PO) and TAAB for one hour at 60 °C. The resin blocks were carefully trimmed to expose the underlying agar blocks.

Sections of various thicknesses (200 nm, 300 nm, and 500 nm) were cut using a Leica Ultracut UCT microtome and transferred to 300 mesh copper grids. A 10% alcoholic solution of uranyl acetate was prepared and centrifuged to remove any precipitate therein. The sections on copper grids were stained for 1 hour with uranyl acetate in a

dark room temperature and then washed with distilled water thoroughly. Finally sections on grids were observed using a Jeol (JEM 2000 FX) electron microscope at 160 kV. The steps including section, staining and observation were conducted by Dr. Julian R. Thorpe in the School of Life Sciences of the University of Sussex.

## **5.4 Results and discussion**

### **5.4.1 Biological feature analysis from electrode microscopy**

Electron microscopy was used to investigate the difference between the two cell lines in cell morphology and some other features. Figure 5.1 and Figure 5.2 demonstrate the difference of the two cell lines. It is observed from Figure 5.1 and Figure 5.2 that the morphology of MCF-10A and MCF-7 in suspension is relatively regular and circular in suspension, and the nucleus of the cell in MCF-10A is apparently smaller than that of MCF-7. It is apparent that the chromatin is more condensed in MCF-7 than in MCF-10A, which is consistent with the results derived from some other studies (Chow, Factor et al., 2012; Nandakumar, Kelbauskas et al., 2012). Nandakumar *et al* adopted isotropic 3D nucleus morphometry and attempted to quantitatively characterize nucleus structure in 3D and to assess its variation with malignancy (Nandakumar, Kelbauskas et al., 2012). The study led to the conclusion that cell and nucleus volumes increased from normal cell to metastatic cell. Moreover, the abnormal cell nuclei had markedly higher density and clumpier chromatin organization compared to that of the normal one. Both of these results are the same as those derived from the electron microscopy in this study. The study also proposed that there was little difference in the volume ratio of the nucleus to cytoplasm between the normal cell line and the cancer cell line. Although a similar conclusion has been derived in both studies regarding the change in nucleus size, no significant change has been found in the cell size in this study. It is observed that the average diameter of both cell lines is around 17  $\mu\text{m}$  in this study.

Several studies have shown interest in the biomechanics of cancer cells and related

studies have been conducted on the investigation of breast cancer cells (Suresh, 2007; Li, Lee et al., 2008). It is observed that the cancerous cells MCF-7 are more deformable than the normal MCF-10A cells. The reasons accounting for this have been found to be the reduction of the proteins involved in the cytoskeleton. It is found that the F-actin in MCF-7 is 30% less when compared to MCF-10A (Suresh, 2007). Studies by Li *et al* adopted AFM imaging and confocal fluorescence imaging to investigate the cytoskeletal structures of both MCF-7 and MCF-10A. It is observed that malignant (MCF-7) breast cells have an apparent lower Young's modulus than that of non-malignant (MCF-10A) counterparts at physiological temperature, which means MCF-10A is more mechanically stiff than MCF-7. The reason for this was investigated in a further study with confocal and atomic force microscopy (AFM) images, which showed a significant difference in the organization of actin structures. It was found that MCF-10A possesses a more pronounced network of actin filaments than MCF-7. The actin structures in MCF-7 form a more disorganized and cross-linked network with no striations and there are fewer actin filaments existing at the basal plane of the cell. The reduced organized actin filament in MCF-7 is one contributing factor in making it is softer than MCF-10A (Li, Lee et al., 2008).

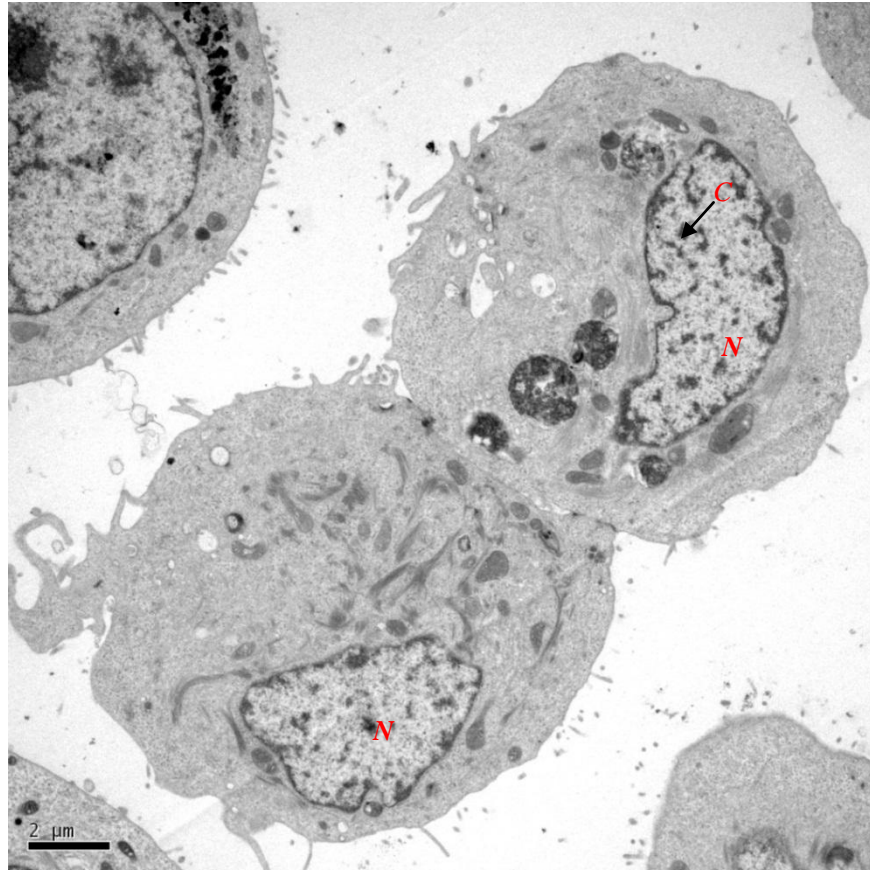


Figure 5.1 Transmission electron micrograph of MCF-10A. *N* indicates the area of the nucleus. *C* indicates the chromatin in the nucleus.

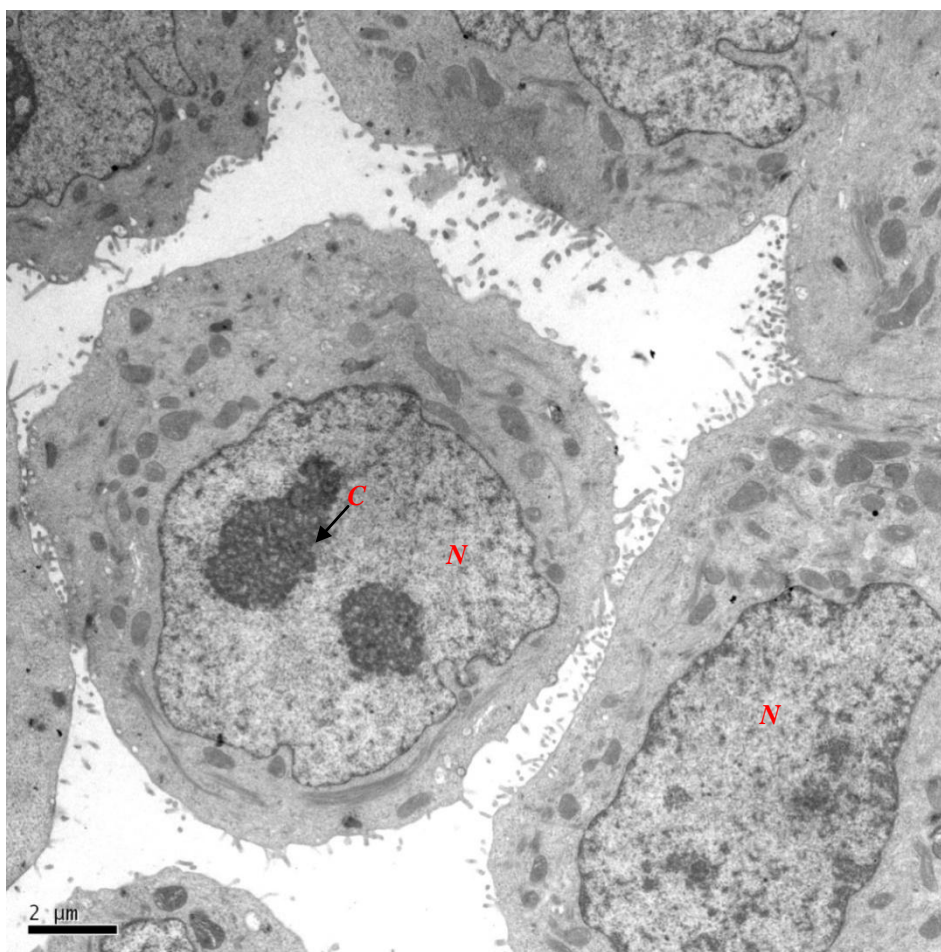


Figure 5.2 Transmission electron micrographs of MCF-7. *N* indicates the area of the nucleus. *C* indicates the chromatin in nucleus.

#### 5.4.2 Relationship between electrical properties and biological properties of cells

Attempts have been made by many researchers in the last few decades in the investigation on the biological properties of cancer cells. In this section, some basic information and conclusions of the previous research will be summarized and analysed in order to relate those conclusions to the results in our study.

As stated in Chapter 2, cell membrane plays a critical role in the transport of ion charges across cell membrane due to its special membrane structure. In normal cells, cell membrane is selectively permeable to sodium and potassium ions, which leads to a different concentration on the two sides of the membrane. A study by Reilly revealed

that the inner membrane is slightly negative compared to the outer membrane (Reilly, Antoni et al., 1998). As a result, an electrical potential is created across the cell membrane, which is called the membrane potential. In normal cells the membrane potential is around -60 to -100mV. The electrical force arising from the electrical potential across the membrane in turn helps to control the permeability of membrane to many nutrients related to energy production and molecular synthesis. Normal healthy cells tend to keep a lower sodium concentration and a higher potassium concentration inside the cell, which is regulated by the ion channels located on the cell membrane. However, significant changes occur in the cell membrane when the cell becomes cancerous. One of the most remarkable changes is the altered cell permeability, which results in the increased permeability of the membrane to water soluble materials, which leads to significant changes in the ion distribution across the cell membrane (Abercrombie, 1980). Studies have found that the sodium and water flow into the intracellular region and potassium, calcium and zinc ion flow out to the outer space of cell. As a result, the sodium concentration is kept at a higher level while there is a lower level of potassium, magnesium and calcium in cancer cells when compared to normal cells. Another characteristic of the cell membrane in cancer cells is the increased content of glycocalyx on the outer cell membrane, which is the major negatively charged molecular on the outer membrane of cells. The general effect of these changes is that the membrane potential is lower in cancer cells than in normal cells (Cone, 1970; Cone, 1974; Hazlewo, Chang et al., 1974; Cope, 1978).

Studies also revealed that mitochondria are another critical organelle involved in the course of carcinogenesis. As addressed in Chapter 2, mitochondria are one of the most important organelles that act as the 'powerhouse of the cell' by aerobic metabolism and anaerobic metabolism. In normal cells, the positively charged hydrogen ions derived from oxidative phosphorylation create a strong membrane potential across the mitochondrial membrane. Hydrogen ions are maintained in a high concentration on the outside of the mitochondrial membrane by the action of the electron transport chain (Haltiwanger). However, due to the degenerative changes in the inner membrane of the

mitochondria, critical enzymes related to mitochondrial functions are reduced. The degeneration of mitochondria leads to the high dependence of glycolysis in cancer cells even in the presence of oxygen in the system, which was observed by Otto Warburg in the 1930s (Warburg, 1956). Moreover, a close connection between the abnormalities in mitochondrial structure and function (Modica-Napolitano, Steele et al., 1989) and a general elevation in the mitochondrial membrane potential ( $\Delta\Psi_m$ ) (Summerhayes, Lampidis et al., 1982) (Davis, Weiss et al., 1985; Chen, 1988) with malignant transformation has been verified by many studies (Houston, Augenlicht et al., 2011).

In summary, cancer cells differ from normal cells not only in the morphology of the cells but also in the structure and metabolism inside the cell. Cancer cells have altered membrane characteristics, which are manifested in the changed lipid and sterol content on the cell membrane and the increased membrane permeability of the cells. As a result, the intracellular and extracellular ion contents are different in cancer cells due to the altered membrane permeability. Cancer cells have a higher concentration of sodium and unstructured water and lower content of potassium compared to normal cells. Therefore, cancer cells exhibit a lower membrane potential than normal cells. The difference in protein expression, especially of many critical enzymes involved in energy production impair aerobic metabolism causing cancer cells to depend on anaerobic metabolism even in the presence of oxygen. Moreover, the cytoskeleton becomes disorganized and simplified in cancer cells.

### **Capacitance of cell membrane**

Changes affecting the composition of the cell membranes and their associated ions will finally affect and alter cellular capacitance. In cancer cells, because of the increased permeability of the cell membrane, the membrane potential is significantly lower than that of normal cell due to the changed distribution of ions. The most basic reason for the ion distribution is the structural changes in the ion channels. Studies have been reported that ion channels of different ions including sodium, potassium, chloride and calcium have been involved in the process of carcinogenesis due to their significance in the

maintenance of membrane potential and cancer development (Prevarskaya, Skryma et al., 2010). Therefore, it has been confirmed that the increased expression of those ion channels in cancer cells is an indicator of cancer.

A study on ion channel characterization by impedance spectroscopy has been carried out by Han *et al* in which changes in bovine chromaffin cells are detected by impedance spectroscopy; when the potassium and calcium ion channels are blocked individually and together (Han and Frazier, 2006). The capacitance variation when the ion channels were blocked was investigated in the study. Compared to normal cells, the capacitance of cancer cells increased by 21%, 77% and 163% respectively when  $K^+$  channels,  $Ca^{2+}$  channels were blocked respectively and together. The result in this study provides indirect evidence to support the decrease of capacitance in cancer cells due to the increased expression of ion channels of the cell membrane. In addition, the cell membrane could be treated as a capacitor, thus the changed distribution of ions on both sides of the cells can affect the membrane capacitance. A point necessary to mention is that there are some other membrane systems in the cell. One of them is the mitochondrial membrane, which might be another factor related to the change of membrane capacitance. Therefore, the principle reason for the change of electrical properties of the cell membrane is its altered permeability.

### **Intracellular conductivity**

The change of intracellular conductivity is related to many factors due to the complicated intracellular environment. A general conclusion is that the intracellular conductivity of cells is related to the ion concentration in intracellular plasma, the content of unstructured water, the size of the nucleus and the structure of the cytoskeleton in the cell (Haltiwanger). The major charge carriers involved in the biological systems include the positive charged  $K^+$ ,  $Na^+$ ,  $Ca^{2+}$  ions and the negative charged  $Cl^-$ , negatively charged electrons and positively charged  $H^+$  and some other charged groups involved in metabolism. As analysed above, there are significant changes occurring in cancer cells compared to normal cells. The concentration of  $Na^+$  is

maintained at a high level and the  $K^+$ ,  $Ca^{2+}$ , and  $Cl^-$  are pumped out of the cell. Moreover, there are more unstructured water flows into the cell that help to increase the mobility of ions in the intracellular plasma. Moreover the reduction of cytoskeletal proteins in cancer cells is likely to influence the intracellular conductivity.

Mitochondria play an important role in the changes of electrical properties in cancer cells since the mitochondria are hyperpolarized due to the increased rate of aerobic glycolysis (Weinberg and Chandel, 2009). Therefore, protons are still moved out from the oxidation of NADH while the coupled production of ATP from ADP and  $P_i$  is significantly reduced in mitochondria. The increased amount of  $H^+$  might contribute to the intracellular conductivity in cancer cells (Houston, Augenlicht et al., 2011).

The factors that might influence the membrane capacitance and intracellular conductivity are summarized above. Although the result from some factors is still unclear, the analysis of the reasons for different changes will provide a more clear direction for the in-depth research into the electrical properties of cancer cells and their corresponding biological changes.

## 5.5 Summary

The biological differences between MCF-10A and MCF-7 were investigated by electron microscopy. Significant difference in chromatin and nucleus was observed from the EM results. Meanwhile the comparisons of two cell lines from other papers were summarized. Based on these, the relationships between of biological properties and electrical properties were analysed. Moreover, the factors that might be responsible for the intracellular conductivity and membrane capacitance were analysed as well. This will provide a foundation for future research.

## ***Chapter 6***

### ***LIMITATIONS, CONCLUSION AND FUTURE WORK***

#### **6.1 Limitations**

As shown in the thesis, a normal breast cell line MCF-10A and cancerous breast cancer line MCF-7 were adopted to represent normal cells and cancer cells. Although reasonable results have been derived from this study, cell lines from different origins could be applied for further study in order to get more persuasive results on the comparison of cancer cells and normal cells and to verify if the results from this study also apply to other cell lines.

In this work, only two breast cell lines were studied, which provided relatively limited information on the carcinogenesis development of breast cancer. As to breast cancer cell lines, besides MCF-10A and MCF-7, there are some other breast cancer cell lines such as MBA-MD-231. More complete information would be obtained if a series of breast cell lines at different stages are studied.

The electrodes adopted in the measurement were made of stainless steel which has a relatively strong electrical polarization effect on the result and thus exerted a significant effect on the two-electrode measurement. However, the phenomenon will be improved if electrodes made of platinum were employed.

As seen from Chapter 4, the Pauly-Schwan model was applied in analysing the impedance results. The applicability of this model has been found to be quite effective at low concentrations ( $\leq 0.2$ ) but it is usually inadequate for high concentrations. In this

study, a volume fraction of 0.2 is used, which is on the edge of the conditions required for the Pauly-Schwan model due to the measurement resolution of the system applied. Dilution of cell suspensions with a lower volume fraction (0.05-0.1) did not lead to any clear difference between cancer cell lines and normal cell lines. Therefore, an improvement in the resolution of measurement system could provide a result with a lower volume fraction.

## 6.2 Conclusions

In this study, the application of impedance spectroscopy to distinguish cancer cells from normal cells in suspension was elaborated and implemented. In order to choose the suitable measurement technique for cell suspension, two-electrode and four-electrode measurements of NaCl solution with different conductivities were conducted and compared in this study. The results indicated that the two-electrode measurement was significantly affected by electrode polarization, especially at low frequency. The parameters involved in the electrode polarization model were found to be related to many factors including the electrode properties and samples and manipulation procedures. After the evaluation from data interpretation and frequency range, the four-electrode measurement was chosen for the impedance measurement of cell suspension.

The suspensions of MCF-10A and MCF-7, which represented normal breast cells and breast cancer cells, were investigated by impedance spectroscopy from 10 HZ to 25 MHz. Measurements were carried out at 37 °C and an isotonic buffer was used in the measurement to keep the normal state of cells in suspension. It was observed that the overall impedance of MCF-7 was lower than MCF-10A, which was consistent with the conclusions in other studies. Further analysis by electrical model and physical model showed significant differences in the electrical parameters involved between MCF-10A and MCF-7. Results implied that both models were capable of providing detailed information for the differentiation of normal and cancerous cells. Furthermore, the relationship between the electrical properties of the cell and its biological properties was

discussed. Electron microscopy presented the morphology difference between the two cell lines adopted in the study. Combined with the results from other studies, it was concluded that the capacitance of cell membrane is related to the permeability of cells and the intracellular conductivity is related to the ion changes in intracellular plasma, the unstructured water, the size of nucleus and the structure of cytoskeleton. The switch of metabolism in mitochondria in cancer cell might also influence the changes of membrane capacitance and intracellular conductivity.

In summary, it was concluded that impedance spectroscopy is a good technique to distinguish cancer cells from normal cells. The analysis based on the results from the measurements at the cell level can provide useful information in the relationship between the biological and electrical properties of cells, which will ultimately promote the further application of impedance based techniques to cancer research.

### **6.3 Future work**

Based on the limitations mentioned above, some future work could focus on the following issues.

- 1) The improvement of the system which will make it possible to measure the cell suspension with a lower volume fraction to produce a more valid result.
- 2) Different breast cancer cell lines could be studied in future in order to get more complete results, which could provide the impedance changes for cell lines at different stages. Moreover, cell lines other than breast cells could be investigated to verify the result in this study for different cell lines.
- 3) As to the investigations of the biological properties and electrical properties of cells, more detailed assays could be adopted for elucidation of different effects of biological factors on electrical results that could be called 'reference experiments'. For example, an experiment might be designed to change only the intracellular ion concentration and then relate this to the results from impedance measurement and electrical parameter analysis. In this way, the influence of the

ion concentration of cells on electrical response could be observed.

- 4) Single cell impedance spectroscopy is a promising method if the technological difficulties in single cell manipulation could be solved. Adoption of single cell impedance spectroscopy might be a new direction for differentiation of cancer cells and normal cells by impedance based techniques.

---

## References

- Abeel, T., T. Helleputte, et al. (2010). "Robust biomarker identification for cancer diagnosis with ensemble feature selection methods." Bioinformatics **26**(3): 392-398.
- Abercrombie, M. (1980). "Citation classic - the surface-properties of cancer-cells - a review." Current Contents/Life Sciences(27): 10-10.
- Aidley, D. J. and P. R. Stanfield (1996). Ion channels — Molecules in action. Cambridge, Cambridge University Press.
- Alberts, B., D. Bray, et al. (2007). Molecular Biology of the Cell. London, England, Taylor & Francis.
- Anghileri, L. J., M. C. Crone-Escanye, et al. (1988). "Mechanisms of gallium-67 accumulation by tumors: role of cell membrane permeability." Journal of Nuclear Medicine : Official publication, Society of Nuclear Medicine **29**(5): 663-668.
- Asami, K. (2002). "Characterization of biological cells by dielectric spectroscopy." Journal of Non-Crystalline Solids **305**(1-3): 268-277.
- Asami, K. (2002). "Characterization of heterogeneous systems by dielectric spectroscopy." Progress in Polymer Science **27**(8): 1617-1659.
- Asami, K., Y. Takahashi, et al. (1989). "Dielectric-Properties of Mouse Lymphocytes and Erythrocytes." Biochimica Et Biophysica Acta **1010**(1): 49-55.
- Bordi, F., C. Cametti, et al. (2001). "Reduction of the contribution of electrode polarization effects in the radiowave dielectric measurements of highly conductive biological cell suspensions." Bioelectrochemistry **54**(1): 53-61.
- Bordi, F., C. Cametti, et al. (2002). "Dielectric spectroscopy of erythrocyte cell suspensions. A comparison between Looyenga and Maxwell-Wagner-Hanai effective medium theory formulations." Journal of Non-Crystalline Solids **305**(1-3): 278-284.
- Brown, B. H., P. Milnes, et al. (2005). "Detection of cervical intraepithelial neoplasia using impedance spectroscopy: a prospective study." BJOG: An International Journal of Obstetrics & Gynaecology **112**(6): 802-806.
- Brown, B. H., J. A. Tidy, et al. (2000). "Relation between tissue structure and imposed electrical current flow in cervical neoplasia." The Lancet **355**(9207): 892-895.
- Chang, J., J. Park, et al. (2007). Fitting improvement using a new electrical circuit model for the electrode-electrolyte interface. Neural Engineering, 2007. CNE '07. 3rd International IEEE/EMBS Conference on.
- Charman, R. A. (1996). Electrical Properties of Cells and Tissues. London, UK, WB Saunders Company Ltd.
- Chauveau, N., L. Hamzaoui, et al. (1999). "Ex vivo discrimination between normal and pathological tissues in human breast surgical biopsies using bioimpedance spectroscopy." Electrical Bioimpedance Methods: Applications to Medicine and Biotechnology **873**: 42-50.
- Chen, L. B. (1988). "Mitochondrial membrane potential in living cells." Annual Review of Cell Biology **4**: 155-181.
- Chow, K.-H., R. E. Factor, et al. (2012). "The nuclear envelope environment and its cancer connections." Nature Reviews Cancer **12**(3): 196-209.
- Cole, K. S. (1940). "Permiability and impermeability of cell membranes for ions Sympos." Cold Spring Harbor Symposia on Quantitative Biology **8**: 110-122.

- Cole, K. S. and R. H. Cole (1941). "Dispersion and absorption in dielectrics I. Alternating current characteristics." The Journal of Chemical Physics **9**(4): 341-351.
- Cone, C. D. (1974). "The role of the surface electrical transmembrane potential in normal and malignant mitogenesis." Annals of the New York Academy of Sciences **238**(1): 420-435.
- Cone, J. C. D. (1970). "Variation of the Transmembrane Potential Level as a Basic Mechanism of Mitosis Control." Oncology **24**(6): 438-470.
- Cope, F. W. (1978). "A medical application of the Ling association-induction hypothesis: the high potassium, low sodium diet of the Gerson cancer therapy." Physical Chemistry Chemical Physics **10**(5): 465-468.
- Coster, H. G. L., T. C. Chilcott, et al. (1996). "Impedance spectroscopy of interfaces, membranes and ultrastructures." Bioelectrochemistry and Bioenergetics **40**(2): 79-98.
- Davis, S., M. J. Weiss, et al. (1985). "Mitochondrial and plasma membrane potentials cause unusual accumulation and retention of rhodamine 123 by human breast adenocarcinoma-derived MCF-7 cells." The Journal of Biological Chemistry **260**(25): 13844-13850.
- Dey, P. (2010). "Cancer nucleus: morphology and beyond." Diagnostic Cytopathology **38**(5): 382-90.
- Dijkstra, A., B. Brown, et al. (1993). "Clinical applications of electrical impedance tomography." Journal of Medical Engineering & Technology **17**(3): 89-98.
- Dobrzyńska, I., B. Szachowicz-Petelska, et al. (2005). "Changes in electric charge and phospholipids composition in human colorectal cancer cells." Molecular and Cellular Biochemistry **276**(1): 113-119.
- Edwards, D. R. and G. Murphy (1998). "Cancer: Proteases [mdash] invasion and more." Nature **394**(6693): 527-528.
- Feder, W. (1968). "Introduction to Bioelectrodes." Annals of the New York Academy of Sciences **148**(A1): 3-20.
- Foster, K. R. and H. P. Schwan (1989). "Dielectric properties of tissues and biological materials: a critical review." Critical Reviews™ in Biomedical Engineering **17**(1): 25-104.
- Franks, W., I. Schenker, et al. (2005). "Impedance characterization and modeling of electrodes for biomedical applications." Biomedical Engineering, IEEE Transactions on **52**(7): 1295-1302.
- Fricke, H. and H. J. Curtis (1937). "The dielectric properties of water–dielectric interphases." The Journal of Physical Chemistry **41**(5): 729-745.
- Fricke, H. and S. Morse (1925). "The electric resistance and capacity of blood for frequencies between 800 and 4 1/2 million cycles." Journal of General Physiology **9**(2): 153-167.
- Fricke, H. and S. Morse (1926). "The electrical capacity of tumors of the breast." Journal of Cancer Research **10**: 340–376.
- Gabriel, C., S. Gabriel, et al. (1996). "The dielectric properties of biological tissues: I. Literature survey." Physics in Medicine and Biology **41**(11): 2231.
- Gabriel, S., R. W. Lau, et al. (1996). "The dielectric properties of biological tissues: III. Parametric models for the dielectric spectrum of tissues." Physics in medicine and biology **41**(11): 2271.
- Gascoyne, P. R., X. B. Wang, et al. (1997). "Dielectrophoretic Separation of Cancer Cells from Blood." Industry Applications, IEEE Transactions on **33**(3): 670-678.
- Gheorghiu, E. and K. Asami (1998). "Monitoring cell cycle by impedance spectroscopy: experimental and theoretical aspects." Bioelectrochemistry and Bioenergetics **45**(2): 139-143.
- Grimnes, S. and Ø. G. Martinsen (2008). Chapter 1 - INTRODUCTION. Bioimpedance and Bioelectricity Basics (Second Edition). New York, Academic Press: 1-6.
- Guck, J., S. Schinkinger, et al. (2005). "Optical Deformability as an Inherent Cell Marker for Testing

- Malignant Transformation and Metastatic Competence." Biophysical Journal **88**(5): 3689-3698.
- Haltiwanger, S. "The electrical properties of cancer cells." <http://www.royalrife.com/haltiwanger1.pdf>.
- Han, A. and A. B. Frazier (2006). "Ion channel characterization using single cell impedance spectroscopy." Lab on a Chip **6**(11): 1412-1414.
- Han, A., L. Yang, et al. (2007). "Quantification of the Heterogeneity in Breast Cancer Cell Lines Using Whole-Cell Impedance Spectroscopy." Clinical Cancer Research **13**(1): 139-143.
- Hanahan, D. and R. A. Weinberg (2000). "The Hallmarks of Cancer." Cell **100**(1): 57-70.
- Hanai, T., K. Asami, et al. (1979). "Dielectric theory of concentrated suspensions of shell-spheres in particular referenc to the analysis of biological cell suspensions." Bulletin of the Institute for Chemical Research **57**(4): 279-305.
- Hanai, T. and K. Sekine (1986). "Theory of dielectric relaxations due to the interfacial polarization for two-component suspensions of spheres." Colloid & Polymer Science **264**(10): 888-895.
- Haque, R., J. Schottinger, et al. (2009). "Frequency of late-stage breast cancer diagnoses despite high mammography screening rates in an HMO." Journal of Clinical Oncology **27**(15): (suppl; abstr 1526).
- Hazlewoo, C., D. C. Chang, et al. (1974). "Nuclear Magnetic-Resonance Transverse Relaxation-Times of Water Protons in Skeletal-Muscle." Biophysical Journal **14**(8): 583-606.
- Hober, R. (1910). "A method to measure the electric conductability in the centre of cells." Pflugers Archiv Fur Die Gesamte Physiologie Des Menschen Und Der Tiere **133**(4/6): 237-253.
- Houston, M. A., L. H. Augenlicht, et al. (2011). "Stable differences in intrinsic mitochondrial membrane potential of tumor cell subpopulations reflect phenotypic heterogeneity." International Journal of Cell Biology **2011**: 978583.
- Irimajiri, A., K. Asami, et al. (1987). "Passive electrical-properties of the membrane and cytoplasm of cultured Rat Basophil Leukemia-cells .1. Dielectric behavior of cell-suspensions in 0.01-500 Mhz and its simulation with a single-shell model." Biochimica Et Biophysica Acta **896**(2): 203-213.
- Irimajiri, A., K. Asami, et al. (1987). "Passive electrical-properties of the membrane and cytoplasm of cultured Rat Basophil Leukemia-cells .2. effects of osmotic perturbation." Biochimica Et Biophysica Acta **896**(2): 214-223.
- Jaron, D., H. P. Schwan, et al. (1968). "A mathematical model for the polarization impedance of cardiac pacemaker electrodes." Medical & Biological Engineering & Computing **6**(6): 579-594.
- Jemal, A., F. Bray, et al. (2011). "Global cancer statistics." CA: A Cancer Journal for Clinicians **61**(2): 69-90.
- Jossinet, J. (1996). "Variability of impedivity in normal and pathological breast tissue." Medical & Biological Engineering & Computing **34**(5): 346-350.
- Jossinet, J. (1998). "The impedivity of freshly excised human breast tissue." Physiological Measurement **19**(1): 61-75.
- Jossinet, J. and M. Schmitt (1999). "A review of parameters for the bioelectrical characterization of breast tissue." Electrical Bioimpedance Methods: Applications to Medicine and Biotechnology **873**: 30-41.
- Kalvoy, H., G. K. Johnsen, et al. (2011). "New method for separation of electrode polarization impedance from measured tissue impedance." The Open Biomedical Engineering Journal **5**: 8-13.
- Kaneko, H., K. Asami, et al. (1991). "Dielectric analysis of aheep erythrocyte ghost - examination of applicability of dielectric mixture equations." Colloid and Polymer Science **269**(10): 1039-1044.
- Kohlrausch, F. and L. F. C. Holborn (1898). Das leitvermögen der elektrolyte, insbesondere der lösungen.

Methoden, resultate und chemische anwendungen. Leipzig, B.G. Teubner.

- Koizumi, K., K. Tamiya-Koizumi, et al. (1980). "Comparative study of the phospholipid composition of plasma membranes isolated from rat primary hepatomas induced by 3'-methyl-4-dimethylaminoazobenzene and from normal growing rat livers." Cancer Research **40**(3): 909-913.
- Labeed, F. H., H. M. Coley, et al. (2006). "Differences in the biophysical properties of membrane and cytoplasm of apoptotic cells revealed using dielectrophoresis." Biochimica et Biophysica Acta **1760**(6): 922-929.
- Li, Q. S., G. Y. H. Lee, et al. (2008). "AFM indentation study of breast cancer cells." Biochemical and Biophysical Research Communications **374**(4): 609-613.
- Liu, S. H. (1985). "Fractal model for the Ac response of a rough interface." Physical Review Letters **55**(5): 529-532.
- Malich, A., B. Scholz, et al. (2007). "The impact of lesion vascularisation on tumours detection by electrical impedance scanning at 200 Hz." Biomedical Imaging and Intervention Journal **3**(4): e33.
- Markx, G. H. and C. L. Davey (1999). "The dielectric properties of biological cells at radiofrequencies: applications in biotechnology." Enzyme and Microbial Technology **25**(3-5): 161-171.
- Marte, B., A. Eccleston, et al. (2008). "Molecular cancer diagnostics." Nature **452**(7187): 547-547.
- Martinez, J. D., M. T. Parker, et al. (2003). Burger's Medicinal Chemistry, Drug Discovery and Development, ©2003 John Wiley&Sons, Inc.
- Maxwell, J. C. (1873). A treatise on electricity and magnetism. U.K., Oxford : Clarendon Press.
- Mazzeo, B. A. and A. J. Flewitt (2007). "Two- and four-electrode, wide-bandwidth, dielectric spectrometer for conductive liquids: Theory, limitations, and experiment." Journal of Applied Physics **102**(10).
- McAdams, E. and J. Jossinet (1994). "Physical interpretation of Schwan's limit voltage of linearity." Medical and Biological Engineering and Computing **32**(2): 126-130.
- McAdams, E. T. and J. Jossinet (1995). "Tissue impedance: a historical overview." Physiological Measurement **16**(3 Suppl A): A1-13.
- McAdams, E. T., A. Lacknermeier, et al. (1995). "The linear and non-linear electrical properties of the electrode-electrolyte interface." Biosensors and Bioelectronics **10**(1-2): 67-74.
- Meng, X., N. H. Riordan, et al. (2004). "Cell membrane fatty acid composition differs between normal and malignant cell lines." Puerto Rico health sciences journal **23**(2): 103-106.
- Mirtaheri, P., S. Grimnes, et al. (2005). "Electrode polarization impedance in weak NaCl aqueous solutions." Biomedical Engineering, IEEE Transactions on **52**(12): 2093-2099.
- Modica-Napolitano, J. S., G. D. Steele, Jr., et al. (1989). "Aberrant mitochondria in two human colon carcinoma cell lines." Cancer research **49**(12): 3369-3373.
- Morimoto, T., S. Kimura, et al. (1993). "A Study of the Electrical Bio-impedance of Tumors." Journal of Investigative Surgery **6**(1): 25-32.
- Nandakumar, V., L. Kelbauskas, et al. (2012). "Isotropic 3D Nuclear Morphometry of Normal, Fibrocystic and Malignant Breast Epithelial Cells Reveals New Structural Alterations." PLoS ONE **7**(1): 29230.
- Oncley, J. L. (1940). "Electric Moments and Relaxation Times of Protein Molecules." The Journal of Physical Chemistry **44**(9): 1103-1113.
- Osterman, K. S., T. E. Kerner, et al. (2000). "Multifrequency electrical impedance imaging: preliminary in vivo experience in breast." Physiological Measurement **21**(1): 99-109.

- Pauly, H., L. Packer, et al. (1960). "Electrical Properties of Mitochondrial Membranes." Journal of Biophysical and Biochemical Cytology **7**(4): 589-601.
- Pecorino, L. (2008). Molecular biology of cancer: mechanisms, targets, and therapeutics New York, Oxford University Press.
- Peters, M. J., M. Hendriks, et al. (2001). "The passive DC conductivity of human tissues described by cells in solution." Bioelectrochemistry **53**(2): 155-160.
- Pethig, R. and D. B. Kell (1987). "The passive electrical properties of biological systems: their significance in physiology, biophysics and biotechnology." Physics in Medicine and Biology **32**(8): 933-970.
- Pietzsch, J. (2004). "Mind the membrane." Horizon Symposia: Living Frontier: 4.
- Pliquett, U. (2008). Electricity and biology. Electronics Conference, 2008. BEC 2008. 11th International Biennial Baltic.
- Pliquett, U., D. Frense, et al. (2010). "Testing miniaturized electrodes for impedance measurements within the beta-dispersion – a practical approach." Journal of Electrical Bioimpedance **1**: 41-55.
- Prevarskaya, N., R. Skryma, et al. (2010). "Ion channels and the hallmarks of cancer." Trends in molecular medicine **16**(3): 107-121.
- Qiao, G. (2012). In-vitro bioimpedance analysis techniques for malignant tissue identification. School of Engineering and Design. Brighton, University of Sussex. **Doctor of Philosophy**.
- Qiao, G., W. Wang, et al. (2012). "Bioimpedance analysis for the characterization of breast cancer cells in suspension." Biomedical Engineering, IEEE Transactions on, **59** (8): 2321-2329.
- Raicu, V., T. Saibara, et al. (1998). "Dielectric properties of rat liver in vivo: analysis by modeling hepatocytes in the tissue architecture." Bioelectrochemistry and Bioenergetics **47**(2): 333-342.
- Raicu, V., T. Saibara, et al. (1998). "Dielectric properties of rat liver in vivo: a noninvasive approach using an open-ended coaxial probe at audio/radio frequencies." Bioelectrochemistry and Bioenergetics **47**(2): 325-332.
- Rajesh, L., P. Dey, et al. (2003). "Fine needle aspiration cytology of lobular breast carcinoma. Comparison with other breast lesions." Acta cytologica **47**(2): 177-182.
- Reilly, J. P., H. Antoni, et al. (1998). Applied Bioelectricity: From Electrical Stimulation to Electropathology. New York, Springer: 239.
- Rieseberg, M., C. Kasper, et al. (2001). "Flow cytometry in biotechnology." Applied Microbiology and Biotechnology **56**(3): 350-360.
- Robertson, J. D. (1981). "Membrane-Structure." Journal of Cell Biology **91**(3): 189-204.
- Ron, A., I. Shur, et al. (2010). "Dielectric screening of early differentiation patterns in mesenchymal stem cells induced by steroid hormones." Bioelectrochemistry **78**(2): 161-172.
- Sawan, M., Y. Laaziri, et al. (2007). "Electrode-tissues interface: modeling and experimental validation." Biomedical Materials **2**(1): 7-15.
- Schwan, H. P. (1957). "Electrical properties of tissue and cell suspensions." Advances in Biological and Medical Physics **5**: 147-209.
- Schwan, H. P. (1963). Determination of biological impedances, New York: Academic.
- Schwan, H. P. (1966). "Alternating current electrode polarization." Biophysik **3**(2): 181-201.
- Schwan, H. P. (1968). "Electrode polarization impedance and measurements in biological materials." Annals of the New York Academy of Sciences **148**(1): 191-209.
- Schwan, H. P. (1992). "Linear and nonlinear electrode polarization and biological materials." Annals of Biomedical Engineering **20**(3): 269-288.
- Schwan, H. P. and C. D. Ferris (1968). "Four - electrode null techniques for impedance measurement with

- high resolution." Review of Scientific Instruments **39**(4): 481-485.
- Schwan, H. P. and S. Takashima (2003). Electrical Conduction and Dielectric Behavior in Biological Systems. digital Encyclopedia of Applied Physics, WILEY-VCH Verlag GmbH & Co KGaA.
- Singer, S. J. and G. L. Nicolson (1972). "The fluid mosaic model of the structure of cell membranes." Science **175**(4023): 720-731.
- Smith, S. R., K. R. Foster, et al. (1986). "Dielectric properties of VX-2 carcinoma versus normal liver tissue." Biomedical Engineering, IEEE Transactions on **33**(5): 522-524.
- Souhami, R. and J. Tobias (2007). Biology of Cancer. Cancer and its Management, Blackwell Science Ltd: 23-41.
- Souhami, R. L. and J. S. Tobias (2005). Cancer and its management. Oxford, Blackwell.
- Spreekens, K. J. A. and F. K. Stekelenburg (1986). "Rapid estimation of the bacteriological quality of fresh fish by impedance measurements." Applied Microbiology and Biotechnology **24**(1): 95-96.
- Stoneman, M. R., M. Kosempa, et al. (2007). "Correction of electrode polarization contributions to the dielectric properties of normal and cancerous breast tissues at audio/radiofrequencies." Physics in medicine and biology **52**(22): 6589-6604.
- Summerhayes, I. C., T. J. Lampidis, et al. (1982). "Unusual retention of rhodamine 123 by mitochondria in muscle and carcinoma cells." Proceedings of the National Academy of Sciences **79**(17): 5292-5296.
- Sun, T. and H. Morgan "Single-cell microfluidic impedance cytometry: a review." Microfluidics and Nanofluidics **8**(4): 423-443.
- Suresh, S. (2007). "Biomechanics and biophysics of cancer cells." Acta biomaterialia **3**(4): 413-38.
- Surowiec, A. J., S. S. Stuchly, et al. (1988). "Dielectric-Properties of Breast-Carcinoma and the Surrounding Tissues." Biomedical Engineering, IEEE Transactions on **35**(4): 257-263.
- Swarup, A., S. S. Stuchly, et al. (1991). "Dielectric-Properties of Mouse Mca1 Fibrosarcoma at Different Stages of Development." Bioelectromagnetics **12**(1): 1-8.
- Varshney, M. and Y. Li (2008). "Double interdigitated array microelectrode-based impedance biosensor for detection of viable Escherichia coli O157:H7 in growth medium." Talanta **74**(4): 518-525.
- Wang, W., M. Tang, et al. (2001). "Preliminary results from an EIT breast imaging simulation system." Physiological Measurement **22**(1): 39-48.
- Warburg, O. (1956). "On the origin of cancer cells." Science **123**(3191): 309-314.
- Weinberg, F. and N. S. Chandel (2009). "Mitochondrial Metabolism and Cancer." Hypoxia and Consequences from Molecule to Malady **1177**: 66-73.
- Zhao, K., W. Bai, et al. (2006). "Dielectric spectroscopy of Anabaena 7120 protoplast suspensions." Bioelectrochemistry **69**(1): 49-57.
- Zink, D., A. H. Fischer, et al. (2004). "Nuclear structure in cancer cells." Nature Reviews Cancer **4**(9): 677-687.
- Zou, Y. and Z. Guo (2003). "A review of electrical impedance techniques for breast cancer detection." Medical Engineering & Physics **25**(2): 79-90.